



Shippensburg University of Pennsylvania
School of Engineering
SENIOR DESIGN PROJECT

3D PEEK Printer

April 29, 2021

Josh Booth 600310453

Caleb Coldsmith 600305553

Dillon LaBonte 600302809

Supervised by: Dr. Joao P. Dias; Dr. Sangkook Lee

School of Engineering
Submitted in partial fulfillment of the requirements of B.S. Degree in
Engineering

Students Statement

We, the undersigned students, certify and confirm that the work submitted in this project report is entirely our own and has not been copied from any other source. Any material that has been used from other sources has been properly cited and acknowledged in the report.

We are fully aware that any copying or improper citation of references/sources used in this report will be considered plagiarism, which is a clear violation of the Code of Ethics of the Shippensburg University of Pennsylvania.

Josh Booth 600310453

Caleb Coldsmith 600305553

Dillon LaBonte 600302809

Supervisor Certification

This to certify that the work presented in this senior year project manuscript was carried out under my supervision, which is entitled:

“3D PEEK Printer”

Josh Booth 60031045301

Caleb Coldsmith 600305553

Dillon LaBonte 600302809

I certify that the students have successfully finished their senior year project and by submitting this report they have fulfilled in partial the requirements of B.S. Degree in Computer/Mechanical Engineering.

I also certify that I have **read, reviewed, and corrected the technical content** of this report and I believe that it is adequate in scope, quality and content and it is in alignment with the ABET requirements and the department guidelines.

[Dr. Joao P. Dias \(Civil and Mechanical Engineering Department\)](#)

[Dr. Sangkook Lee \(Computer, Electrical and Software Engineering Department\)](#)

ACKNOWLEDGMENT

We would like to thank our sponsor, Mark Booth, for hist funding, help, and advice during this project.

ABSTRACT

This report covers the design and manufacturing process of a large (300x280x1330mm), high-temperature 3D printer capable of printing engineering-grade plastics, such as PEEK at a price point well below comparable printers on the market (\$2,500.) The 3D printing market is expanding rapidly due to the low cost of a 3D printer, fast production time, and low cost per print. Most consumer-grade 3D printers are only capable of printing low-temperature materials, due to the drastically increased cost of printing engineering-grade, high-temperature plastics. As 3D printing parts and technologies progress, the market is slowly expanding to offering 3D printers that print stronger and higher temperature plastics, but with a very sharp increase in cost or a trade-off of a very small build volume, making these printers much less accessible to the non-enterprise consumer. The 3D PEEK Printer's (3DPP) design was built from the ground up with low cost in mind, countering the high cost and small build volume problems through a combination of traditional, cheap printer movement system with high-temperature parts while employing novel solutions to counter the thermal issues and other issues spurred from the verticality of the print volume.

TABLE OF CONTENTS

LIST OF FIGURES	8
LIST OF TABLES	11
LIST OF SYMBOLS AND ABBREVIATIONS	12
CHAPTER 1: INTRODUCTION	13
1.1 Problem Statement and Purpose	13
1.2 Project and Design Objectives	13
1.3 Intended Outcomes and Deliverables	14
1.4 Summary of Report Structure	15
CHAPTER 2: BACKGROUND	16
2.1 A Brief History of 3D Printing	16
2.2 FDM 3D Printing Process Overview	16
2.3 FDM Movement Systems	17
2.4 Filament Types	20
2.5 Heated Chamber	22
2.6 Existing Printer Solutions	22
2.7 Market Analysis	23
CHAPTER 3: METHODS AND MATERIALS	25
3.1 System Design and Components	25
3.1.1 Chamber Frame	25
3.1.2 X-Axis	28
3.1.2.1 X-Axis Movement	28
3.1.2.2 X-Axis Thermal Solution	35
3.1.3 Y-Axis	37
3.1.3.1 Y-Axis Movement	37
3.1.3.2 Y-Axis Thermal Solution	45
3.1.4 Z-Axis Movement	46
3.1.5 Extruder	58
3.1.6 Heated Chamber	64
3.1.7 Electrical System	70
3.1.8 Firmware	79
3.1.9 Software	90
3.1.10 Electronics Case	93
3.1.11 CAD Model	99
3.2 Design Alternatives	106
3.2.1 Belt/Counterweight Z-Axis Movement System	106
3.2.2 Top-Mounted Z-Axis Stepper Motors	108
3.2.3 Heated Bed Belt Mount	109
3.2.4 Alternative Power Cable Solution	110

3.3	System Analysis and Optimization	111
3.4	Simulation and/or Experimental Test	111
3.4.1	Fluid Velocity	113
3.4.2	Warm-Up Time Comparison	114
3.4.3	Surface Temperature Distribution	115
CHAPTER 4: RESULTS AND DISCUSSIONS		119
4.1	Results	119
4.2	Discussions	125
CHAPTER 5: PROJECT MANAGEMENT		127
5.1	Tasks, Schedule and Milestones	127
5.2	Resources and Cost Management	130
5.3	Lessons Learned	133
CHAPTER 6: IMPACT OF THE ENGINEERING SOLUTION		135
6.1	Economical, Societal and Global	135
6.2	Environmental and Ethical	136
CHAPTER 7: CONCLUSIONS AND RECOMMENDATIONS		137
7.1	Summary of Achievements of the Project Objectives	137
7.2	New Skills and Experiences Learnt	137
7.3	Recommendations for Future Work	138
REFERENCES		140

LIST OF FIGURES

<i>Figure</i>	<i>Page</i>
Fig. 1. Cartesian Movement System Diagram	18
Fig. 2. Delta Movement System Diagram	19
Fig. 3. CoreXY Movement System Diagram	19
Fig. 4. Nearly Empty Chamber Frame	26
Fig. 5. CAD Model of the Chamber Frame	27
Fig. 6. Simplified X-Axis Movement Diagram	28
Fig. 7. X-Axis Free Body Diagram	28
Fig. 8. Speed vs Torque Curve for 1A NEMA 17 Stepper Motor	30
Fig. 9. X-Gantry vs. X-Carriage	33
Fig. 10. X-Axis Tensioner	34
Fig. 11. X-Stop With 10nF Filter Capacitor	34
Fig. 12. Finished X-Gantry	35
Fig. 13. X-axis Stepper Motor with Peltier Plate, Aluminum Heat Sink, and Fan	36
Fig. 14. Installed POM V-Wheel	36
Fig. 15. Simplified Y-Axis Movement Diagram	37
Fig. 16. Y-Axis Free Body Diagram	37
Fig. 17. Speed vs. Torque Curve for 2A NEMA 17 Stepper Motor	39
Fig. 18. CR10S Pro V2 Y-Axis Tensioner Base	41
Fig. 19. CR10S Pro V2 Y-Axis Tensioner Screw	41
Fig. 20. CR10S Pro V2 Y-Axis Tensioner Nut	42
Fig. 21. Assembled Y-Axis Tensioning Mechanism	42
Fig. 22. Y-Axis Aluminum Extrusions	43
Fig. 23. Bed Base Plate	44
Fig. 24. Finished Y-Axis	45
Fig. 25. Ender 3 - Z Motor Mount	47

Fig. 26. Modified Z-Axis Motor Mount	48
Fig. 27. Assembled Z-Axis Mount	49
Fig. 28. X-Gantry Free Body Diagram	50
Fig. 29. Simplified Z-Axis Movement Diagram	53
Fig. 30. Z-Sync Tensioning Mechanism	55
Fig. 31. Lead Screw Guide	56
Fig. 32. BLTouch Stowed	57
Fig. 33. BLTouch Deployed	58
Fig. 34. E3D V6 Hotend Diagram	60
Fig. 35. Airflow Analysis from Petsfang Duct	61
Fig. 36. Assembled Extruder Front View	62
Fig. 37. Assembled Extruder Side View	63
Fig. 38. Simplified Heat Flow Diagram	66
Fig. 39. Simplified Thermal Resistance Diagram	67
Fig. 40. Space Heater Mounting Solution	70
Fig. 41. Connections to SKR 2 Schematic	71
Fig. 42. Connections to Raspberry Pi Schematic	72
Fig. 43. Connections to AC Schematic	73
Fig. 44. Connections to Buck Converters Schematic	74
Fig. 45. Power Plate Design	75
Fig. 46. Power Plate Heat Block Design	75
Fig. 47. Installed Power Plates	76
Fig. 48. OctoPrint Landing Page	92
Fig. 49. OctoPrint Temperature Control Page	93
Fig. 50. Cad Lid Handle Design	94
Fig. 51. Case Front Sheet Metal Design	95
Fig. 52. Case Back Sheet Metal Design	95
Fig. 53. Case Left Sheet Metal Design	95
Fig. 54. Case Right Sheet Metal Design	96
Fig. 55. PLA Mounting Plate	96

Fig. 56. Case CAD Model	97
Fig. 57. Finished Case Assembly Without Lid	98
Fig. 58. Finished Case Assembly With Lid	98
Fig. 59. 3DPP CAD Model Front	100
Fig. 60. 3DPP CAD Model Back	101
Fig. 61. 3DPP Front Without Door	102
Fig. 62. 3DPP Front With Door	103
Fig. 63. 3DPP Back	104
Fig. 64. 3DPP Inside Bottom	105
Fig. 65. 3DPP Inside Top	105
Fig. 66. Counterweight System Design Concept	107
Fig. 67. Y-Axis Belt Holder	110
Fig. 68. Male-Male Power Cable	111
Fig. 69. Air Velocity in Heated Chamber	114
Fig. 70. Average Fluid Temperature with 3-Inch Thick Insulation	115
Fig. 71. Floor, Right, and Front Wall Temperature Distribution	116
Fig. 72. Top, Left, and Back Wall Temperature Distribution	116
Fig. 73. Temperature Distribution Across X and Z Plane	117
Fig. 74. PLA Benchy Printed with the 3DPP	119
Fig. 75. Minor Print Defects in the PLA Benchy	120
Fig. 76. PPS Benchy Printed with the 3DPP	121
Fig. 77. Print Defects in the PPS Benchy	122
Fig. 78. PEEK Benchy Printed with the 3DPP	123
Fig. 79. Tall PLA Static Mixer	123
Fig. 80. Surface Finish of the PLA Static Mixer	124

LIST OF TABLES

<i>Table</i>	<i>Page</i>
Table 1. Properties of Common Filament types	21
Table 2. Available Commercial PEEK Printers	23
Table 3. X-Axis Torque Calculation Parameters	29
Table 4. Torque Efficiency vs. Microsteps	32
Table 5. Y-Axis Torque Calculation Parameters	39
Table 6. X-gantry Weight Distribution	51
Table 7. Lead Screw Torque Values	54
Table 8. Thermal Air Properties at 80°C	65
Table 9: 3DPP Dimensions for Thermal Analysis	66
Table 10: Power Draw for Components Powered by Buck Converters	113
Table 11. Power Draw for Components Powered by an AC-DC Power Supply	113
Table 12. Project Schedule	129
Table 13. Total Unit Cost	130
Table 14. Total Wasted Cost	133

LIST OF SYMBOLS AND ABBREVIATIONS

LIST OF SYMBOLS	
μ	Coefficient of friction
$^\circ$	Degrees
LIST OF ABBREVIATIONS	
3D	3-dimensional
FDM	Fused Deposition Modeling
3DPP	3D PEEK Printer
PLA	Polylactic acid
SLA	stereolithography
PEEK	Polyether Ether Ketone
ABS	Acrylonitrile Butadiene Styrene
PETG	Polyethylene terephthalate glycol
CAD	Computer-aided Design
TPU	Thermoplastic Polyurethane
PC	Polycarbonate
POM	Polyoxymethylene

1 CHAPTER 1: INTRODUCTION

1.1 *Problem Statement and Purpose*

Over the past decade, 3D printing has become a popular manufacturing technique, due to its rapid per-unit production speed and low cost for both prints and the printer itself. However, traditional FDM printing is seldom used in applications requiring usage in high-temperature environments or that require high structural strength. This can be attributed to the low printing temperatures (~200 °C), and thus weak plastics available for use in most printers. As the industry grows, more companies have been designing commercial-grade, high-temperature printers that cost five figures, making them unobtainable to most hobbyists and consumers. This report covers the design and fabrication of a 3D printer capable of printing large items (1'x1'x5') at high temperatures (450 °C with an 80 °C build chamber) while maintaining a price under \$2,500.

1.2 *Project and Design Objectives*

The goal of this project is to build a 3D printer capable of printing high-temperature thermoplastics for the sponsor's needs, which is mainly printing PEEK objects for structural purposes. There are currently no printers on the market that fit the sponsor's needs and budget requirements, so the goal is to build one using existing 3D printing technologies. Due to the large scale of this project and limited time, the goal is to build a fully functional prototype that serves as a proof of concept. Future work would include adapting the final design for manufacturability.

1.3 Intended Outcomes and Deliverables

For the 3DPP, there are 3 sets of requirements for evaluating the end product. The functional requirements (mechanical systems), the user experience requirements (how easily the user can interact with the printer), and the safety requirements (protection mechanisms the printer has.)

Functionally, the 3DPP will:

- Respond to movement commands in the X, Y, Z, and E directions
- Heat the nozzle to 450 °C, bed to 200 °C, and chamber to 80 °C
- Print all common filament types without heated chamber (PLA, ABS, PETG)
- Have a build volume of 300x280x1330mm
- Operate at maximum chamber temperature for 3 days continuously
- Print PEEK objects

For the user experience requirements, the user will be able to:

- Monitor and control movement and temperature locally through an LCD
- Through a web-interface:
 - Control movement and temperature
 - Send Marlin commands
 - Start, stop, and monitor prints
 - View print through a real-time stream

For the safety requirements, the 3DPP will:

- Be able to operate on a single 15A circuit without the heated chamber and operate on three separate 15A circuits with the heated chamber on
- Have thermal protection for the hotend, heated bed, and chamber

- Have fused connections in the event of a short circuit

Meeting all of these requirements means the 3DPP is fully functional, is easy for anyone to use, and is safe to operate. The deliverable is a single, completed prototype of the 3DPP that is ready to print from.

1.4 Summary of Report Structure

This report will start by giving a brief history of existing 3D printing technologies, where the 3DPP stands compared to other comparable printers on the market, and cover the design choices taken for the printer given the design requirements. Then it will discuss the construction process of the printer, along with changes to the design that were needed. The results of the finished prototype will be examined, and then the report will cover the logistics of the project (budget, project management, etc) followed by the future applications of this project and its technologies.

2 CHAPTER 2: BACKGROUND

2.1 *A Brief History of 3D Printing*

3D printing dates back to the early 1980s when Dr. Hideo Kodama first introduced the concept of stereolithography as a method of rapid prototyping. This type of 3D printing, also called SLA, may be very different from the type of 3D printing most are familiar with. SLA uses lasers to precisely cure resin to build up prints. It was not until the 1980s when Scott Crump created the first fused deposition modeling, or FDM, printer that laid the groundwork for most consumer printers available today [1]. The initial creators of these different 3D printing technologies patented their products, which greatly slowed the development of 3D printing technology until the patents expired in the mid-2000s [1]. After the patents for FDM printing expired, many companies began developing the technology further into the modern printer ecosystem that exists today. As the technology progressed, 3D printing established itself as a way to rapidly manufacture parts with complex geometric properties cheaply. Additionally, printers did not take up anywhere near the space comparable machines like CNCs. As the printer industry grew, the prices of the printers continually dropped, with quality printers costing less than \$1,000. FDM printing has become a consumer favorite, due to its low setup and material cost, which will be explored further in this paper.

2.2 *FDM 3D Printing Process Overview*

FDM operates by precisely moving a high-temperature nozzle over a print bed, which is just a flat surface, to lay a bead of plastic down in a 2-dimensional shape. Another bead of plastic is

laid on top of the first in a slightly different shape. This process is repeated over and over until the 2D shapes stacked on top of each other form a 3D. FDM printers need to be able to accurately, reliably, and quickly move the heated nozzle to the desired location while extruding filament at the correct rate relative to the movement. If the filament is extruded too quickly, it will cause a bulge in the object, and if it is extruded too slowly, the object will lose structural integrity.

To translate an object from a CAD model to an actual print, the CAD model is exported in a standard file format and fed into a slicer. The slicer converts the model into 2D slices, a series of linear moves on the same Z-axis location (this is a simplification, as non-planar slicers do not require the moves to be on the same Z-axis location.) These moves are encoded in G-Code, a simple programming language that tells the motors where to move, how fast to move, and what path to follow. An example G-Code command might look like “G1 X10 Y150 E3 F50”. G1 might correspond to the move command, so move to X position 10, Y position 150, and move the extruder to position 3 with a feed rate of 50. After the model is sliced and converted to the G-Code, it is loaded into the 3D printer’s motherboard, whose firmware will read the G-code and drive the stepper motors to mimic that motion. It is a complex series of events, and the slicing software and printer firmware are constantly improving to increase the quality of prints.

2.3 FDM Movement Systems

While G-Code handles the theoretical coordinates the nozzle should be traveling to, the firmware needs to translate those coordinates into actual space. This is accomplished through the use of a movement system that can accurately, precisely, and reliably move each axis to the correct

position. The reliability is especially important, as the control board does not know where each axis actually is. It only knows the relative position. Normally on power-up, the control board will move each axis to position 0, which is typically found by moving each axis until it hits a physical switch, signaling to the board the axis is at position 0. From there, all moves are relative to the control board's believed position. If the movement system binds when the control board tries to move the X-axis to position 10, the control board believes the X-axis is at position 10, even though it is stuck at position 0. Until it is manually corrected, all future moves will be 10 positions off in the X-direction. For the 3DPP, it was important to choose the most effective movement system to meet the 3DPP's cost requirement while maintaining the necessary accuracy, precision, and reliability. Out of the plethora of options, the most viable was a cartesian movement system, where an X, Y, and Z-axis are all controlled by separate stepper motors, a delta movement system, where a combination of 3 vertical motors, or a coreXY movement system, where the X and Y directions are controlled by a single continuous belt and the Z-axis is independently controlled.

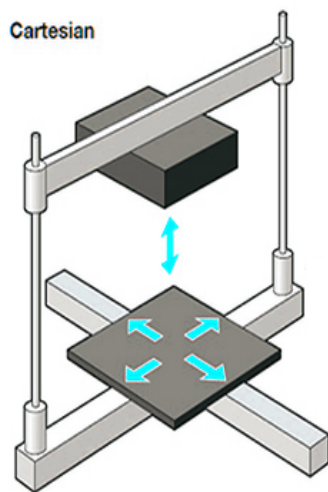


Figure 1. Cartesian Movement System Diagram [2]

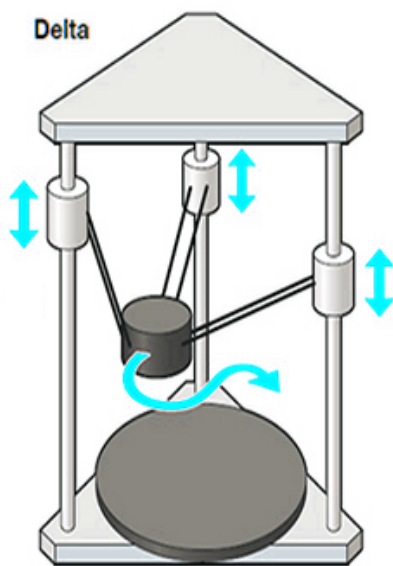
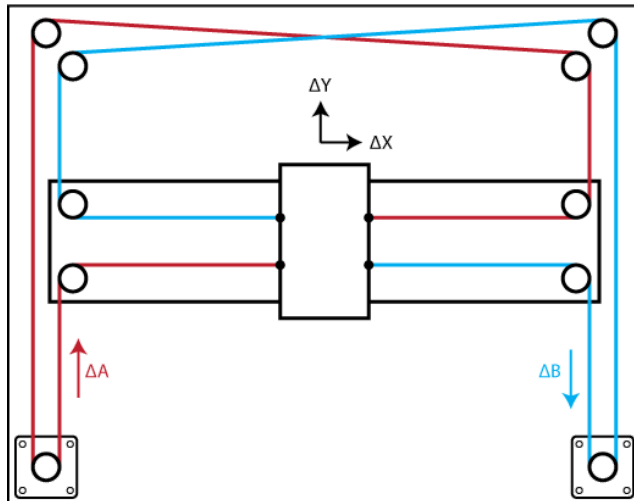


Figure 2. Delta Movement System Diagram [2]



Equations of Motion:

$$\Delta X = \frac{1}{2}(\Delta A + \Delta B), \quad \Delta Y = \frac{1}{2}(\Delta A - \Delta B)$$

$$\Delta A = \Delta X + \Delta Y, \quad \Delta B = \Delta X - \Delta Y$$

Figure 3. CoreXY Movement System Diagram [2]

For the 3DPP, a cartesian or CoreXY system seemed easier to implement, due to the tight time frame. The delta system would be harder to troubleshoot as each axis can not be tested individually. Since all axes work together to move the nozzle, it would have been harder to troubleshoot issues. It would not have been until all axes were constructed that a single one could be tested. Also, the sponsor will have to determine basic issues with the printer when using it himself, so a more simplistic movement system will help him narrow down problems, without requiring an in-depth understanding of the printer's movement system. With a cartesian and CoreXY printer, print defects can easily be isolated to a specific axis, which makes solving an issue easier. Between CoreXY and cartesian, the CoreXY requires the bed to move up and down in the Z-direction, as opposed to the nozzle moving in the Z-direction like in a cartesian system. The cartesian system appeared more favorable once again due to its simplistic movements. There is a single motor responsible for each axis. While a printer could be made using either CoreXY or delta movement systems, cartesian was chosen for this project because it was easy for the entire group to visualize how each movement axis would work, and the division of labor for designing each movement axis could be split among the group members.

2.4 Filament Types

Filament is the plastic extruded to make a 3D printed part. Different types of filament have different material properties, making each filament useful in different ways. For example, PLA, one of the most common filaments, is relatively strong and is great for most prints that are not in direct heat, as even direct sunlight could soften the plastic. TPU is a filament that is flexible and is useful for snap-fit parts since the plastic will not break when snapped into position. If both

filaments are used to make the same part, the resulting objects would look identical but would be useful in very different ways.

Table 1 highlights some of the different material properties of common filament types. While not exact, there is a positive correlation between the extrusion temperature and the deflection temperature, which is the temperature at which the part will begin to deform. While the strength of the part does not necessarily increase as the extrusion temperature increases, the deflection temperature normally does. A high-temperature printer opens 3D printing technology to a plethora of applications it was not able to be used in when dealing with high-temperature plastics, including some of the world's largest industries such as automotive, oil, and medical [3].

Filament Type	Tensile Strength (MPa)	Flexural Strength (MPa)	Deflection Temperature at 0.45 MPa (°C)	Extrusion Temp. (°C)	Bed Temp. (°C)	Chamber Temp. (°C)
PLA [4]	56	115	80	200	60	N/A
PETG [5]	45	72	70	240	80	N/A
PC [6]	62	78	135	290	110	40
PPS [7]	50	52	90	330	130	70
PEEK [8]	100	130	140	390	140	80

Table 1. Properties of Common Filament Types

2.4 Heated chamber

In Table 1, notice the materials requiring the highest printing temperatures require a “chamber temperature” parameter. When the filament is heated by the nozzle to print, the material undergoes thermal expansion. After it has been extruded, the material cools and shrinks. For lower temperature extrusion, the amount the material shrinks as it cools to room temperature is negligible for affecting print quality. But, as the temperature gradient between the nozzle temperature and ambient print temperature increases, the amount the part shrinks as it cools is enough to warp the print, cause print defects, or cause the part to lose bed adhesion. The solution to this issue is to introduce a heated chamber, which decreases the temperature gradient, keeping the extruded plastic warm, so the entire part can cool at once after it has been printed. The requirement of a heated chamber is one of the main causes of the high cost and the low number of printers that print these high-temperature materials. All the components inside the chamber need to be able to withstand the chamber temperature, which increases printer cost and complexity.

2.6 Existing Printer Solutions

PEEK Printer Name	Build Volume (mm ³)	Max Extruder Temp (°C)	Max Bed Temp. (°C)	Max Chamber Temp. (°C)	Price
Intamsys Funmat HT	1.76E+07	450	160	90	6,000
Tractus3D T850P	3.14E+07	450	175	80	15,000
CreatBot PEEK-300	3.60E+07	500	200	120	17,000
Apium P220	4.77E+06	540	160	220	46,000

Zortrax Endureal	3.60E+07	480	220	200	58,000
Roboze One+400 Xtreme	1.65E+07	500	150	N/A	50,000
3ntr Spectral 30	2.70E+07	500	300	250	110,000
Essentium HSE 180 HT	2.07E+08	550	100	200	149,000
3DGence Industry F340	2.65E+07	500	160	85	30,000
MiniFactory Ultra	1.07E+07	480	250	250	50,000
Stratasys Fortus 450mc	5.85E+07	450	250	350	160,000
Aon-M2+	1.30E+08	450	200	135	50,000
Averages	5.01E+07	490	193	165	61,000
M3DD Printer	1.12E+08	450	200	80	2,500

Table 2. Available Commercial PEEK Printers [9]

Table 2 is a list of existing commercially available printers that can print PEEK. All available commercial PEEK printers have some tradeoff that makes them unappealing. The most affordable printer out of the bunch, the Intamsys Funmat HT, has a build volume 10x smaller than the 3DPP at double the price. The printer that was closest in build volume to the 3DPP costs \$50,000, making it far from affordable. The 3DPP strikes a middle-ground no other company has touched as of yet.

2.7 Market Analysis

In 2018, the 3D printing industry was worth 1.53 billion. By 2026, it is predicted to more than double to 3.78 billion [10]. While printer software and related services make up part of that, the printers themselves account for half the market. 3D printing is expanding into even the largest of industries, such as medical, automotive, and oil [3]. As shown by the large number of companies in Table 2 that are trying to expand into printing high-temperature plastics, printing PEEK and similar engineering-grade thermoplastics has a promising future since it overcomes a lot of the temperature and strength shortcomings of lower-temperature plastics.

3 CHAPTER 3: METHODS AND MATERIALS

3.1 *System Design and Components*

The 3DPP is made up of 2 main systems: the printer system and the thermal system. The printer system operates as a regular, low-temperature 3D printer would, and the thermal system is a combination of the heated enclosure and the necessary provisions within the printer system that allows it to operate in a high-temperature environment. The printer system was built from the ground up with the thermal system in mind, using high-temperature resistant components. This made integrating the two systems easy.

3.1.1 *Chamber Frame*

The chamber frame serves as the foundation for the 3DPP. Not only does the chamber frame provide structural support for the movement system, but it also serves as the demarcation of the heated chamber. The insulation is mounted to the outside of the chamber frame, forming the heated chamber inside. While aluminum extrusions are the de-facto standard for most 3D printing frames due to their structural rigidity, low cost, and high functionality, building the prototype into a server rack proved to be more cost-effective and provided more mounting options for the cost. For the internal frame that guides the movement system, aluminum extrusions were chosen for the reasons just listed. If the 3DPP were to be mass-produced, the server rack chamber frame is one component that could be swapped out for something less unique. To stay under the sponsor's budget, this was the best solution.



Figure 4. Nearly Empty Chamber Frame

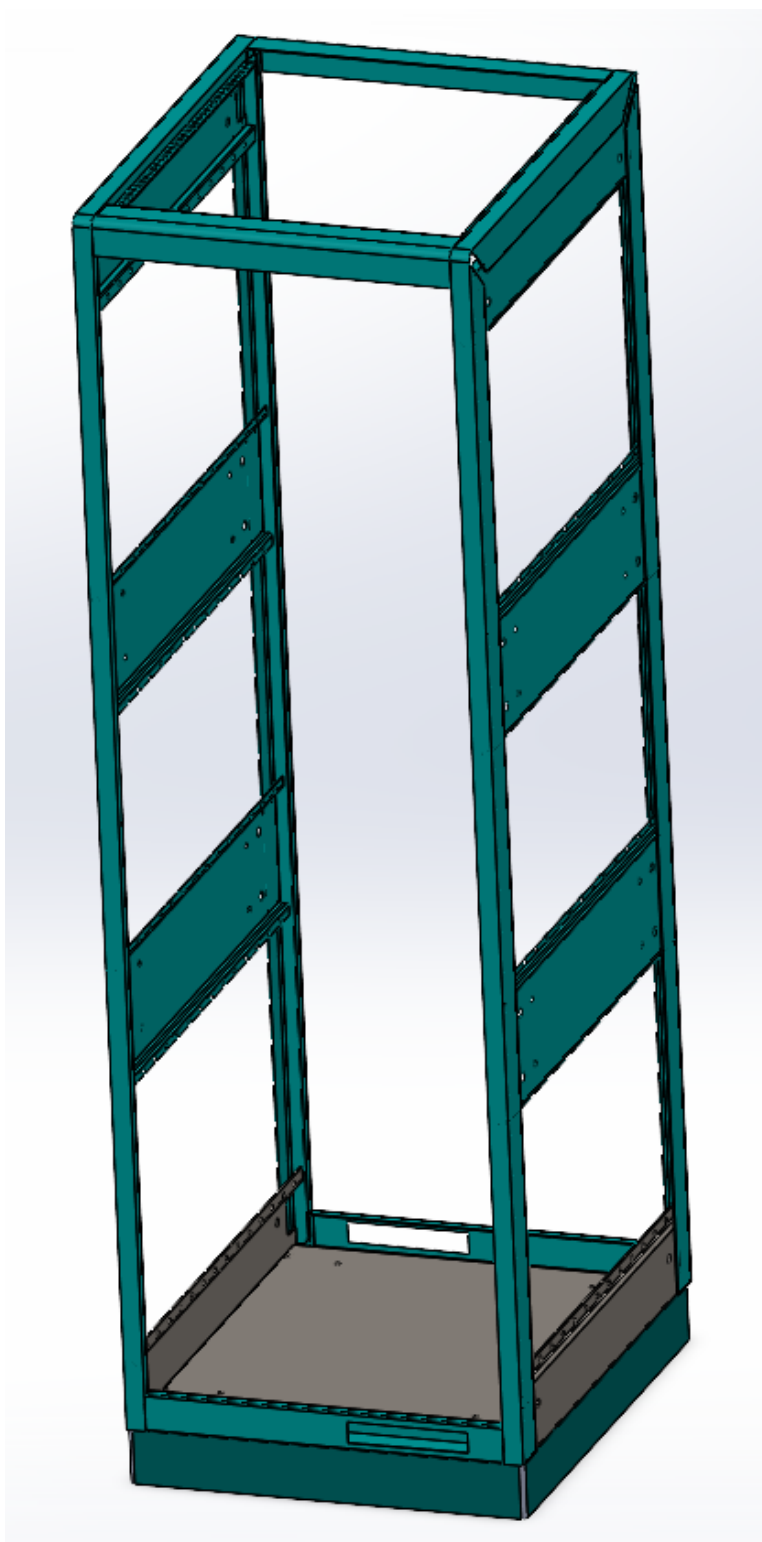


Figure 5. CAD Model of Empty Chamber Frame

3.1.2 X-Axis

3.1.2.1 X-Axis Movement

The X-axis movement system needs to allow for accurate and reliable movement in the X-direction to any coordinate 0-280 mm, per the design requirements. A belt and motor combination was a cheap solution with plenty of accuracy for the application. The X-axis movement system operates using a stepper motor-driven GT2 belt. The belt attaches to the X-carriage, which holds the hotend. The carriage slides along aluminum extrusions using V-wheels. Basic movement analysis to show that NEMA 17 stepper motors have plenty of power to move along the X-axis.

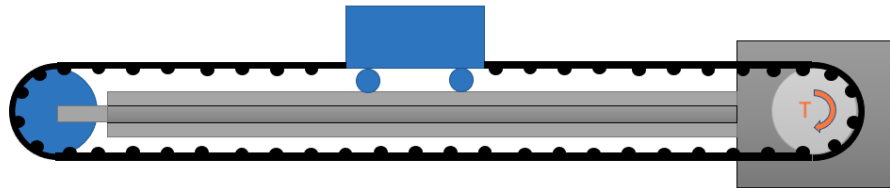


Figure 6. Simplified X-Axis Movement Diagram

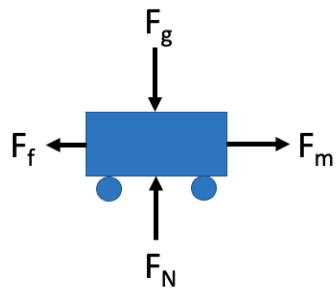


Figure 7. X-axis Free Body Diagram

Variable	Value	Units	Name
m_c	0.297	kg	Mass of the X-carriage
r_m	0.0047	m	Radius of the Motor
a_{max}	0.500	m/s^2	Maximum acceleration
v_{max}	200	mm/s	Maximum Velocity
μ	0.0015 [11]	N/A	Coefficient of friction
g	9.81	m/s^2	Gravitational acceleration

Table 3. X-Axis Torque Calculation Parameters

Where $F_g = \text{Weight of the Carriage} = m_c * g = 0.297 * 9.81 = 2.62N$

$$\Sigma F_y = 0 = F_N - F_g \longrightarrow F_N = \text{Normal Force} = Fg = 2.62N$$

$$F_f = \text{Force of Friction} = \mu * F_N = 0.0015 * 2.62N = 3.93 * 10^{-3}N$$

$$\Sigma F_x = m_c * a_{max} = 0.297 * 0.5 = 0.149 = F_m - F_f$$

$$F_m = 0.1485 + 3.93 * 10^{-3} = 0.152N$$

$$T_m = r_m * F_m = 0.0047 * 0.152 = 0.0714 Ncm \longrightarrow \text{Minimum required motor torque}$$

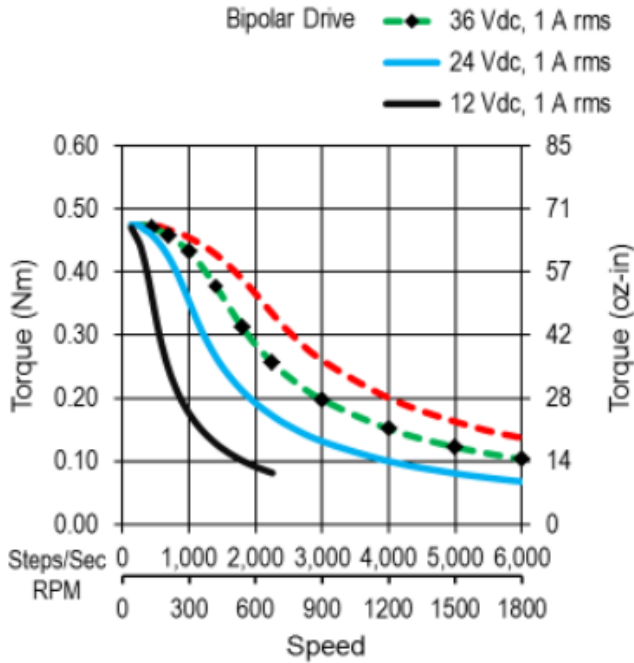


Figure 8. Speed vs Torque Curve for 1A NEMA 17 Stepper Motor [12]

Stepper motors do not have 100% torque efficiency when operating at high speeds, so a max speed needs to be found at which the minimum torque can be supplied. The 24V, 1A NEMA 17 stepper motor chosen for the X-axis operates at 200 steps/revolution [12]. By considering the GT2 belt with a pitch of 2mm and the shaft coupling pulley with 16 teeth, the linear displacement and max step speed can be calculated.

$$\text{Linear Displacement} = 16 * 2 = 32 \text{ mm/revolution}$$

$$\text{Distance per step} = \frac{32 \text{ mm/rev}}{200 \text{ steps/rev}} = 0.16 \text{ mm/step}$$

$$\text{Max step speed} = \frac{v_{\max}}{0.16 \text{ mm/step}} = \frac{200 \text{ mm/s}}{0.16 \text{ mm/step}} = 1250 \text{ step/sec}$$

At 1250 step/sec, Figure 8 shows that the stepper motor supplies a torque of 30 Ncm at 1250

step/sec, but this is assuming that this motor is taking full steps. Stepper motors are capable of microstepping, where instead of rotating fully between coil pairs, multiple adjacent coil pairs partially energize, rotating the motor between a full step. The number of partial power ratios between the pairs of coils determines how many microsteps a stepper motor has. The X-axis motor is running at a common 16 microsteps which improves motor precision but reduces the efficiency of the motor. The benefit is greater accuracy because of the fine movement capability.

Microstep/full step	% Torque/Microstep
1	100.00%
2	70.71%
4	38.27%
8	19.51%
16	9.80%
32	4.91%
64	2.45%
128	1.23%
256	0.61%

Table 4. Torque Efficiency vs. Microsteps [13]

Considering Table 4, at 16 microsteps / full step and 30 Ncm of torque,

$$\text{Effective Torque} = 30 \text{ Ncm} * 9.80\% = 2.94 \text{ Ncm}$$

Since only 0.0714 Ncm is required to move in the X-carriage, the NEMA 17 motor which provides 2.94 Ncm of torque will be capable of moving the X-carriage. This gives a safety factor of about 40 for the motor binding due to lack of torque.

To avoid terminology confusion, a distinct differentiation should be made between the X-gantry and the X-carriage. The X-gantry refers to the entire assembly that is raised and lowered by the Z-axis, while the X-carriage is the piece of metal the X-axis moves back and forth that the hotend and extruder are mounted to. The X-gantry was constructed from a horizontal aluminum extrusion with brackets on either side to hold the stepper motors, camera, wiring, and end stops. This is connected to two vertical aluminum extrusions, which guide it up and down the printer for the Z-axis movement. The stepper motor was put on one end of the aluminum extrusion, and a tensioning mechanism was attached to the other. As seen in figure 5, the belt then wrapped around both, connecting to the X-carriage. The tensioning mechanism used was a metal plate with a bearing attached to the X-gantry aluminum extrusion with T-nuts. To tension, the T-nuts were loosened, the belt pulled taught, then the T-nuts were tightened, holding the belt's tension. When the stepper motor turned, it would move the X-carriage left and right.

When the printer first boots up, it needs to determine its relative location in space. To calibrate the X-axis, an X-stop switch was installed on the left side of the X-gantry. When the X-axis performed "homing", it would move left until it hit the switch, allowing the control board to know where the X-axis origin was. From there, the control board knew where in space the X-axis

was. This same homing system was implemented on the Y-axis as well. Due to the long wire runs, electrical interference and voltage drop were problems. Both false positives and false negatives were occurring when homing, causing the printer to spontaneously enter an error state. To counter this, a combination of a 10nF capacitor in series with the switch and software debouncing fixed all of the end-stop issues.

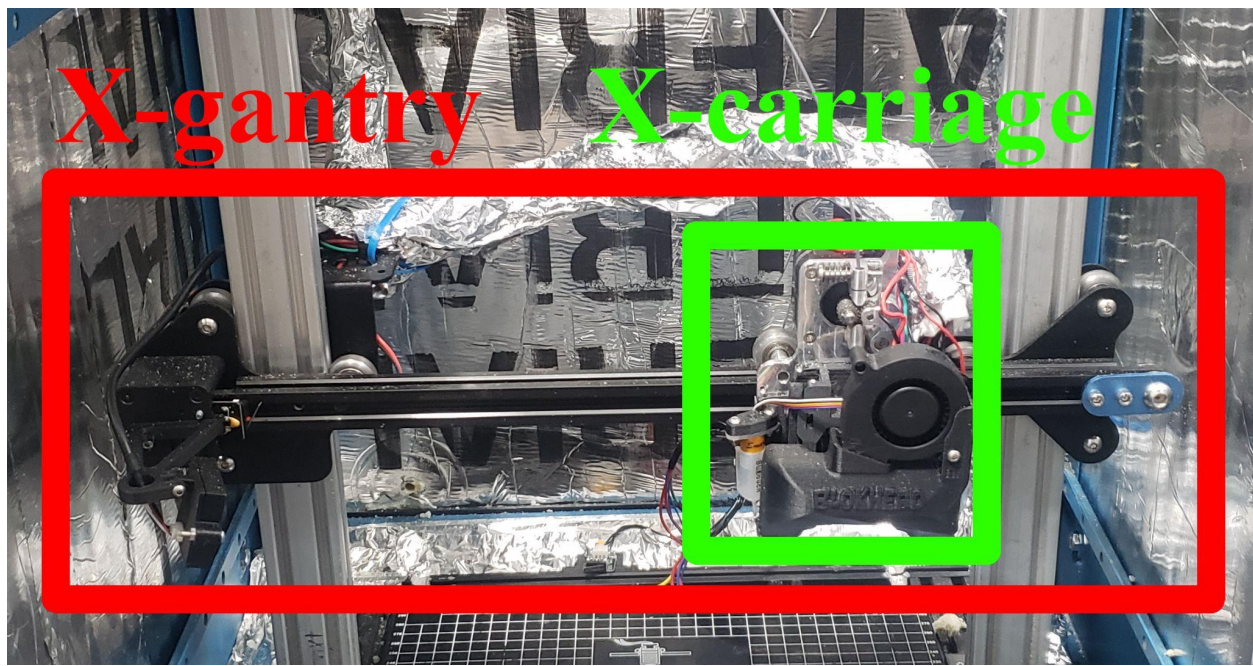


Figure 9. X-gantry vs. X-carriage

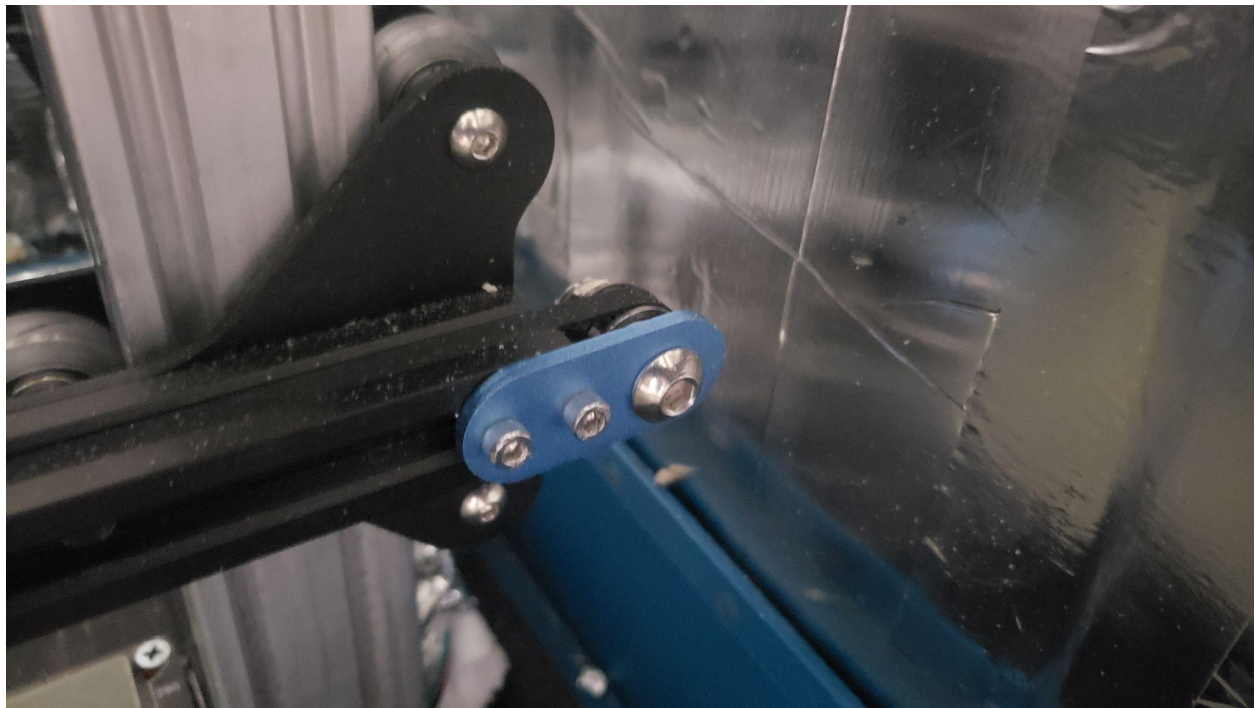


Figure 10. X-axis Tensioner



Figure 11. X-Stop With 10nF Filter Capacitor

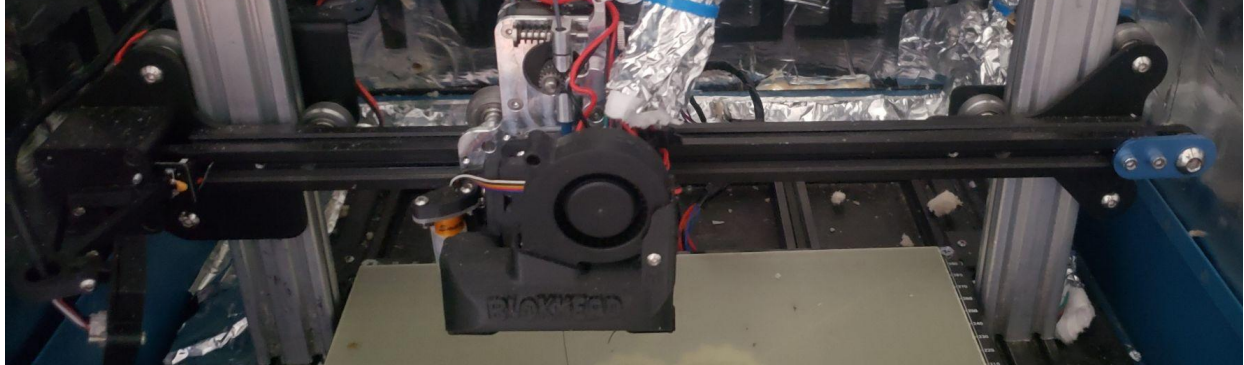


Figure 12. Finished X-Gantry

3.1.2.2 X-Axis Thermal Solution

Due to the components it drives, the X-axis stepper motor is required to be in the heated chamber.

Since the stepper motor is only rated to operate up to 50°C [12], a system is needed to cool the motor. First, the current was limited on the X-axis motor to 800mA, as opposed to the maximum rated current of 1A, which helped keep the motor cool, regardless of the ambient temperature. Then, a TEC-12706 Peltier plate was installed with the cold side on the backside of the motor and the hot side attached to a heatsink and fan. A Peltier plate is not the most energy-efficient method of cooling. In fact, they are only about 5% efficient [14]. However, since such a small area needed to be cooled and their power draw was relatively low, they served as an ideal cooling solution. Additionally, Peltier plates have a small footprint and only require a positive and negative wire to work, as opposed to the other cooling alternative, liquid cooling.

Other components that were on the X-axis that could potentially get damaged in an ambient temperature of 80°C were the GT2 drive belt and the V-wheels. The GT2 belt was replaced with a high-temperature EPDM GT2 belt that can withstand temperatures up to 135°C [15]. The

V-wheels were replaced with ones made out of POM, which has a deflection temperature of 158°C [16]. All other components on the X-axis were able to withstand 80°C.

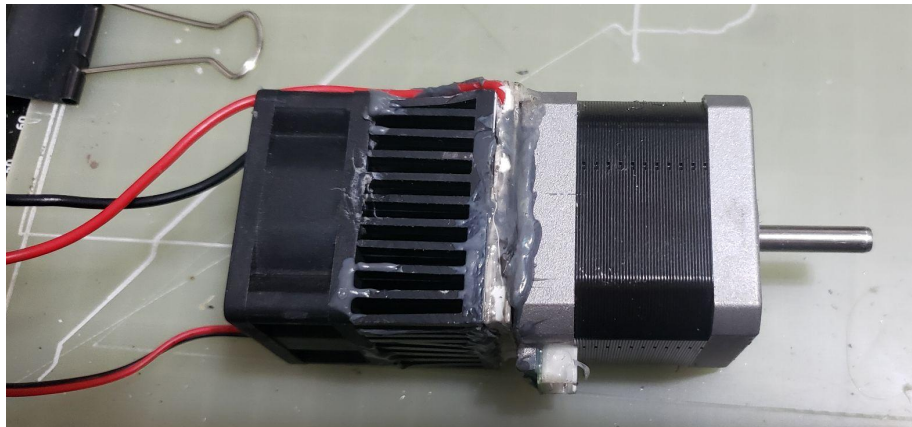


Figure 13. X-axis Stepper Motor with Peltier Plate, Aluminum Heat Sink, and Fan

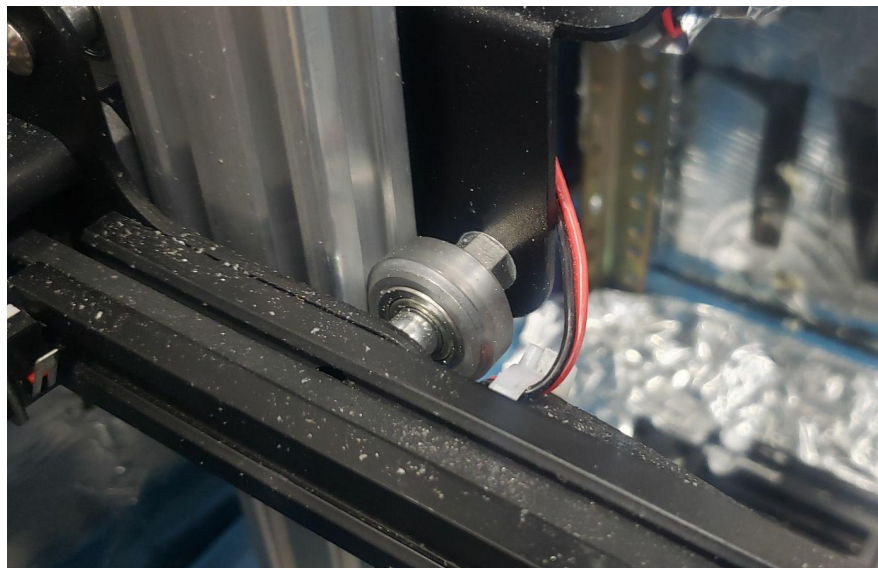


Figure 14. Installed POM V-Wheel

3.1.3 Y-Axis

3.1.3.1 Y-Axis Movement

Similar to the X-axis movement system, the Y-axis used a belt and pulley system. The belt attaches to the bed plate, which slides along aluminum extrusions using V-wheels. Due to the increase in mass of the bed, a 2A stepper motor was selected to maintain roughly the same safety factor as the X-axis movement system. Basic movement analysis to show that the 24V, 2A NEMA 17 stepper motor had enough power to move the Y-axis.



Figure 15. Simplified Y-Axis Movement Diagram

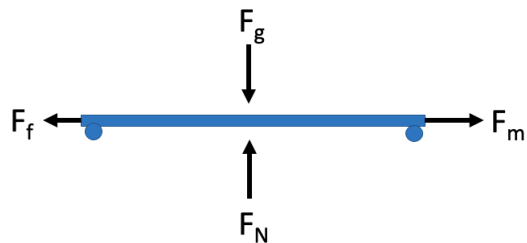


Figure 16. Y-Axis Free Body Diagram

Variable	Value	Units	Name
m_c	2.70	kg	Mass of the Bed Assembly
r_m	0.0047	m	Radius of the Motor
a_{max}	0.500	m/s^2	Maximum acceleration
μ	0.0015 [11]	N/A	Coefficient of friction
g	9.81	m/s^2	Gravitational acceleration

Table 5. Y-Axis Torque Calculation Parameters

Where $F_g = \text{Weight of the Carriage} = m_c * g = 2.7 * 9.81 = 26.5N$

$$\Sigma F_y = 0 = F_N - F_g \longrightarrow F_N = \text{Normal Force} = Fg = 26.5N$$

$$F_f = \text{Force of Friction} = \mu * F_N = 0.0015 * 26.5N = .0398N$$

$$\Sigma F_x = m_c * a_{max} = 2.70 * 0.500 = 1.35 = F_m - F_f$$

$$F_m = 1.35 + .0398 = 1.39N$$

$$T_m = r_m * F_m = 0.0047 * 1.39 = 0.653Ncm \longrightarrow \text{Required motor torque}$$

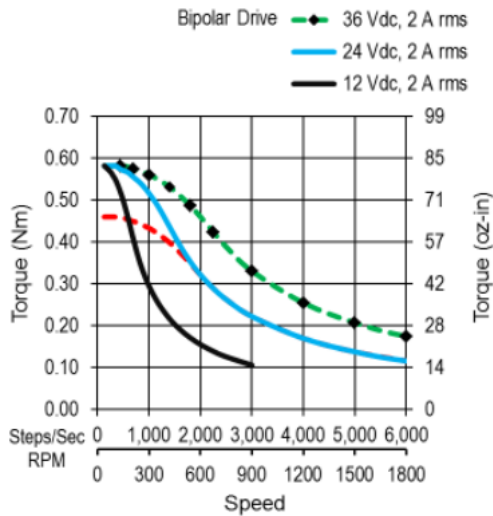


Figure 17. Speed vs Torque Curve for 2A NEMA 17 Stepper Motor [12]

No parameters for linear displacement or max step speed change from the X-axis calculations, so the max step speed of the motor is still 1250 step/sec. Figure 17 shows that the stepper motor supplies a torque of 49 Ncm at 1250 steps/sec with full steps. Using table 4, with 16 microsteps per full step, the effective torque has an efficiency of 9.80%.

$$\text{Effective Torque} = 49 \text{ Ncm} * 9.80\% = 4.80 \text{ Ncm}$$

This brings the effective torque of the Y-axis stepper motor to 4.80 Ncm. Only 0.653 Ncm is required to move in the Y-carriage, so the 24V, 2A NEMA 17 stepper motor will provide enough torque and have a factor of safety of 7.

While the fundamental movement principles were the same, a couple of special parts were needed to be fabricated for the Y-axis. To minimize the stepper motors inside the heated chamber, the Y-axis stepper motor was mounted beneath the chamber frame, with only the shaft sticking up through the floor. Mounting the motor outside the chamber frame was a very easy

way to prevent the motor from being subjected to the hostile printing environment and keeping it below its rated operating temperature of 50°C [12]. To tension the Y-axis, a modified version of Roger Cable’s “CR10S Pro V2 Y axis tension” design was 3D printed [17]. All 3D printed parts for this project were printed out of PLA. If the parts were going to be inside the heated chamber, they were then replaced with Carbon-Fiber impregnated Polycarbonate (PC) after functionality had been verified since the PC can withstand heated chamber temperatures up to 135°C [6]. The belt tensioner design uses a 3D printed screw and nut combination to create tension on a bearing the belt is driven around. During testing, the nut would occasionally loosen, so a second locking nut was added, resolving the problem.

To allow for unlevelness in the build, the heated print bed was designed to be connected to a potentially unlevel base plate using four screw and spring combinations, similar to the strut of a car. Tightening one of the screws would pull that corner of the print bed down, while loosening it would allow it to be pushed up, allowing for manual adjustment of the levelness of the print bed. To construct this, first, a metal plate was cut out of a piece of sheet metal that would ride forward and backward on two aluminum extrusions. Two extrusions were used instead of a single extrusion for stability purposes. The metal plate’s only critical dimensions were the holes for the eight V-wheels that guide the bed along the extrusions and the mounting points for the heated bed that was going to be on top of the plate. To allow for manufacturing inaccuracies, four of the V-wheels used concentric nut spacers that can be twisted to change how far the wheel is from the aluminum extrusion. This tightens the wheels against the extrusions to account for imperfect manufacturing and wheel wear. The belt was attached to the lower metal plate using an aluminum GT2 belt clamp. From there, the heated build plate was installed on top of the metal

plate using the screw and spring combination, creating the finished assembly.

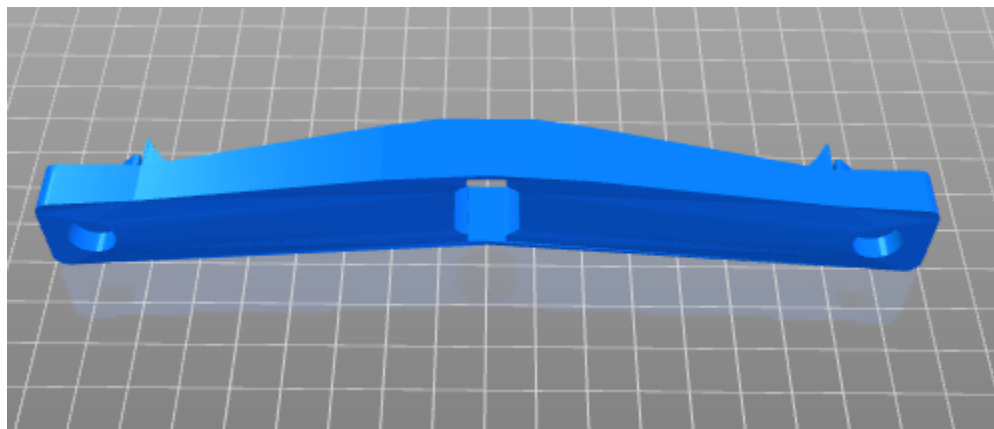


Figure 18. CR10S Pro V2 Y-Axis Tensioner Base

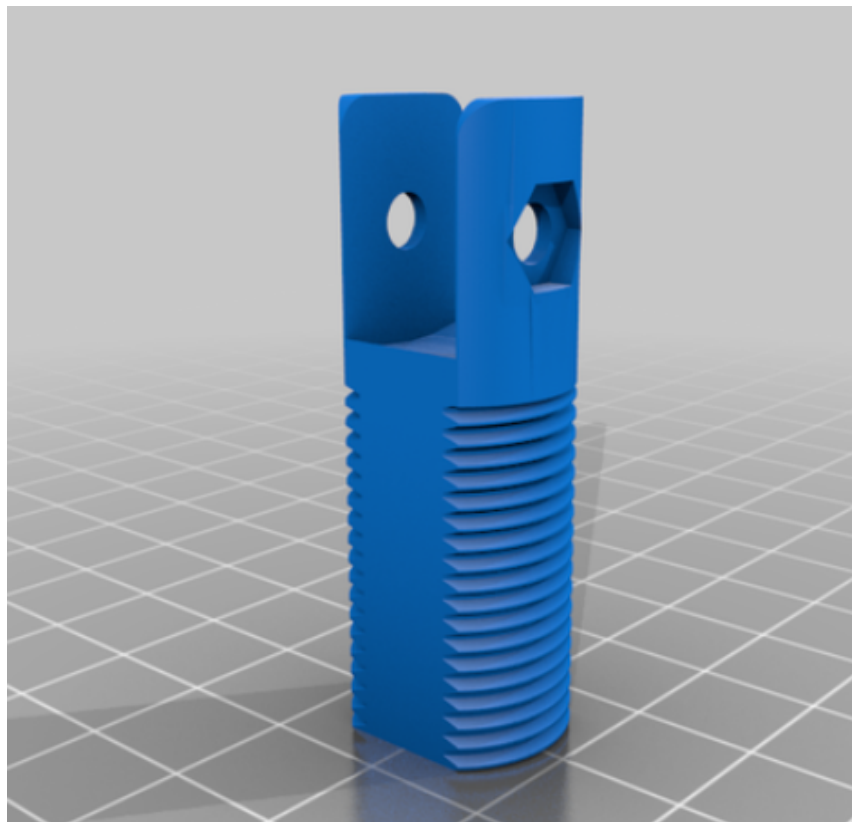


Figure 19. CR10S Pro V2 Y-Axis Tensioner Screw

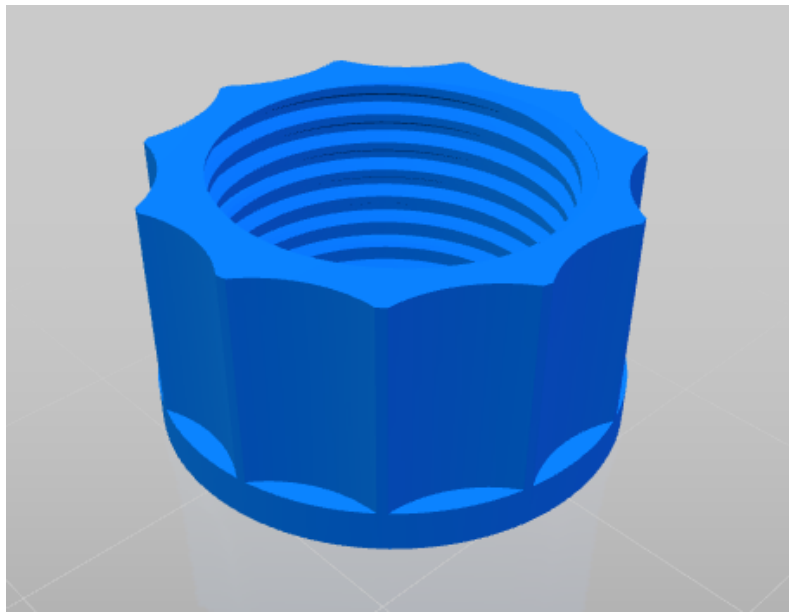


Figure 20. CR10S Pro V2 Y-Axis Tensioner Nut

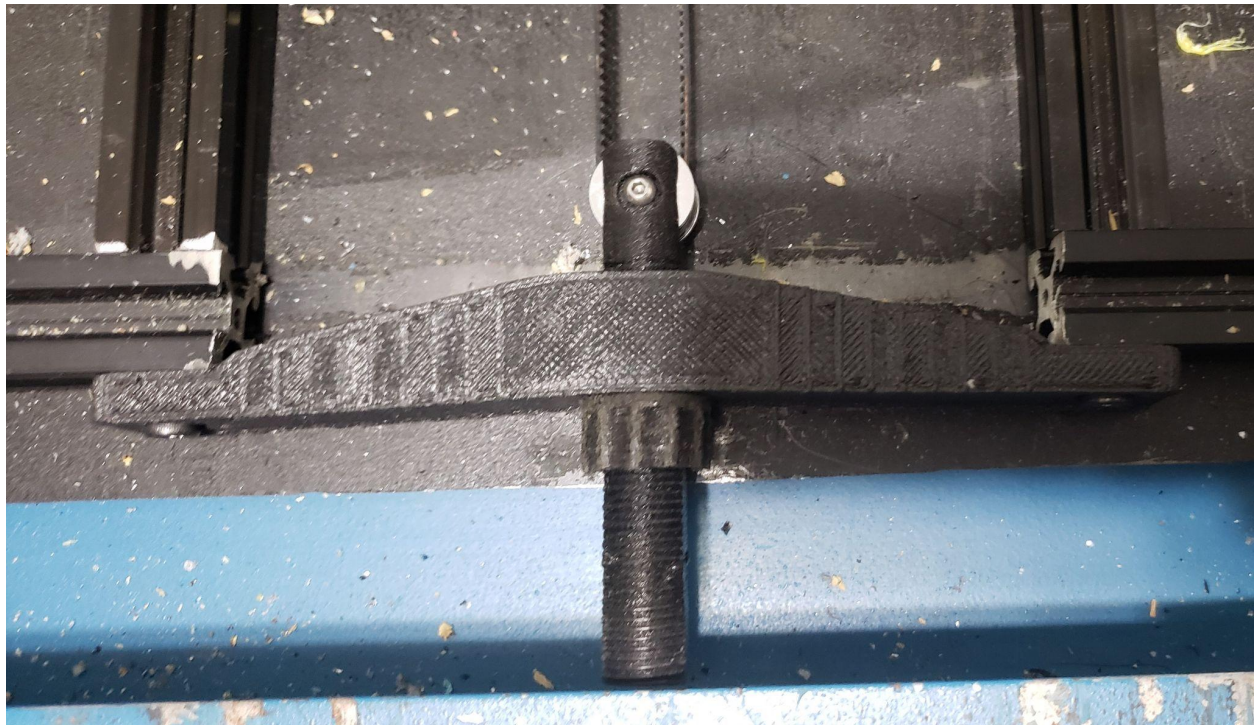


Figure 12. Assembled Y-Axis Tensioning Mechanism

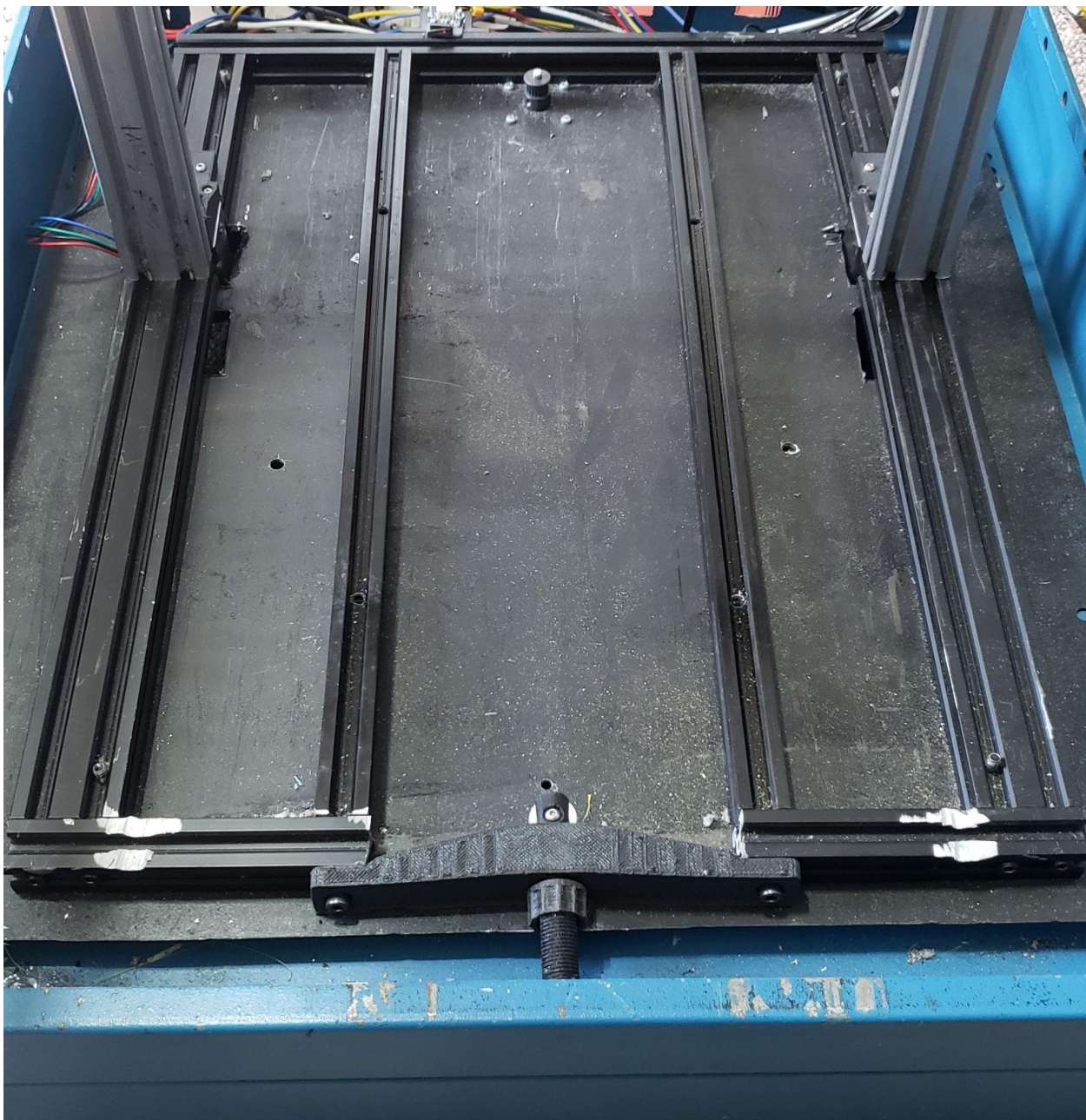


Figure 13. Y-Axis Aluminum Extrusions



Figure 23. Bed Base Plate

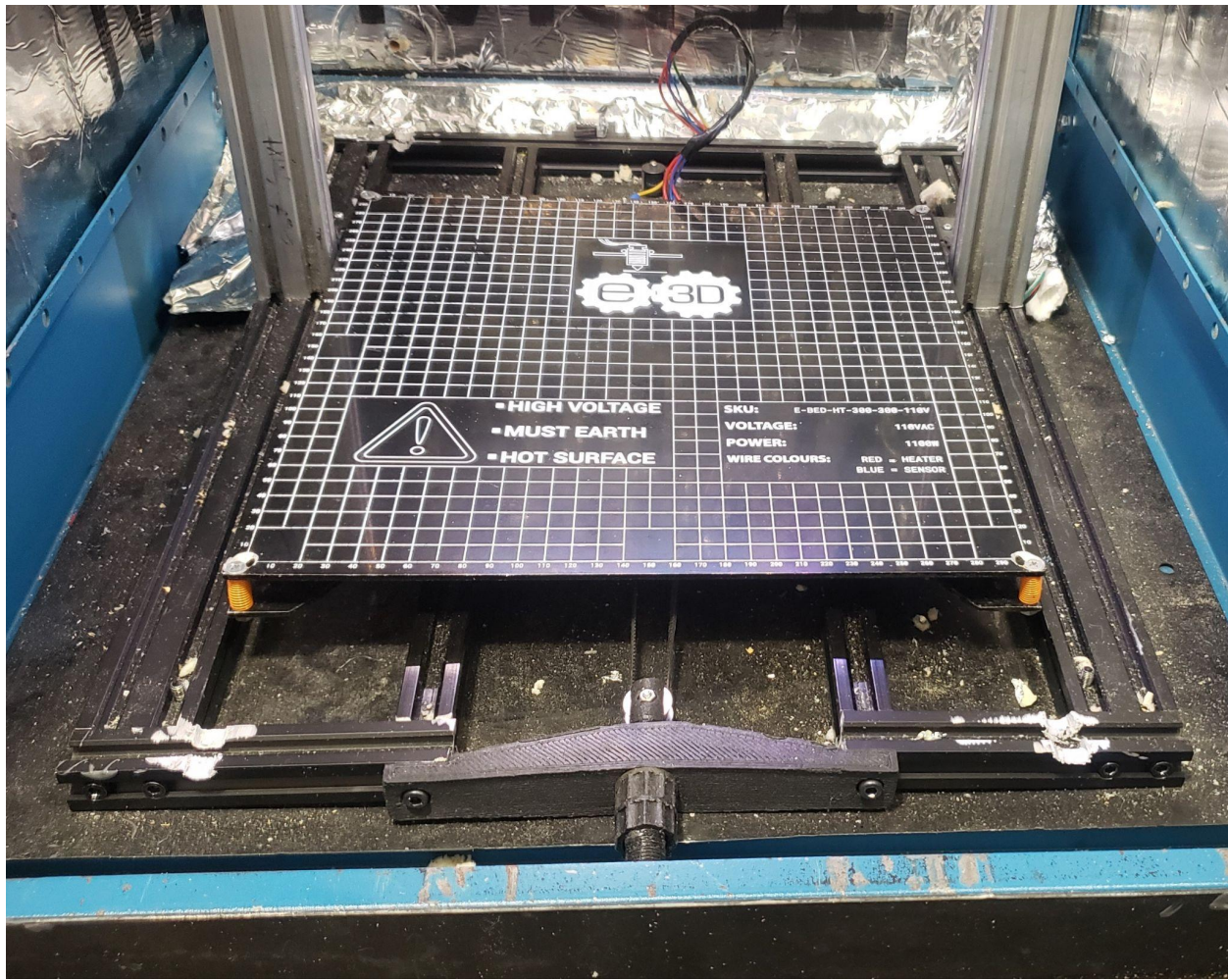


Figure 24. Finished Y-axis

3.1.3.2 Y-axis thermal solution

Mounting the Y-axis stepper motor outside the heated chamber alleviated most of the work needed for thermal protection provisions. However, just like the X-axis, the drive belt was also upgraded to a high-temperature EPDM GT2 belt and the V-wheels were upgraded to POM V-wheels. Apart from protecting from high temperatures, the print bed heats up to allow prints to better adhere to it. By keeping the bottom of the print warm, the print does not warp up off the

print from temperature contractions, similar to the purpose of the heated chamber. The base of the print is much more critical, as all prints are built from the bottom up, so having a foundation that will not move is important to reliable print success. The bed used in this printer is a 300mm x 300mm “High Temperature Heated Bed” from E3D, capable of maintaining a constant temperature of 200°C [18]. The heated bed uses AC power and is turned on and off via a relay. The electrical working of the heated bed is covered in more detail in section 3.1.7.

3.1.4 Z-axis movement

The design requirements dictated 1330mm of build height, which is much larger than either the X or Y-axes. Also, the Z-axis has to counteract the force of gravity, presenting an engineering challenge. To get the Z-axis movement system working properly, it went through two major design iterations, with many smaller iterations. The failed iterations are covered more in section 3.3. The final working version of the Z-axis movement system used dual 5 foot (1500mm) tall, 8mm T8 lead screws to raise and lower the X-gantry. A dual-lead screw/dual-Z motor setup was used to make sure the system had enough torque overhead to work reliably in the event of Z-axis binding. The Z-axis stepper motors were mounted outside the heated enclosure at the bottom of the chamber frame, similar to the Y-axis. A modified version of Brian Deger’s “Ender 3 - Z Motor Mount” was used to mount the Z-axis motors to the frame [19]. The original design only gave perfect alignment in the X direction, but allowed play in the Y direction. If the stepper motor shaft and the lead screws were not perfectly concentric, the lead screw would bind when trying to be moved since even a small amount of mis-alignment would result in significant movement at the top of the lead screw due to its height. The play introduced in the Y direction was due to the original design expecting to be placed on top of another aluminum extrusion. For

the 3DPP, this was not possible, since the Z-motors needed to be mounted outside the heated chamber. The modified version added a plate that extended across from the top of the motor to mount onto a nearby horizontal aluminum extrusion, giving Y-axis support.

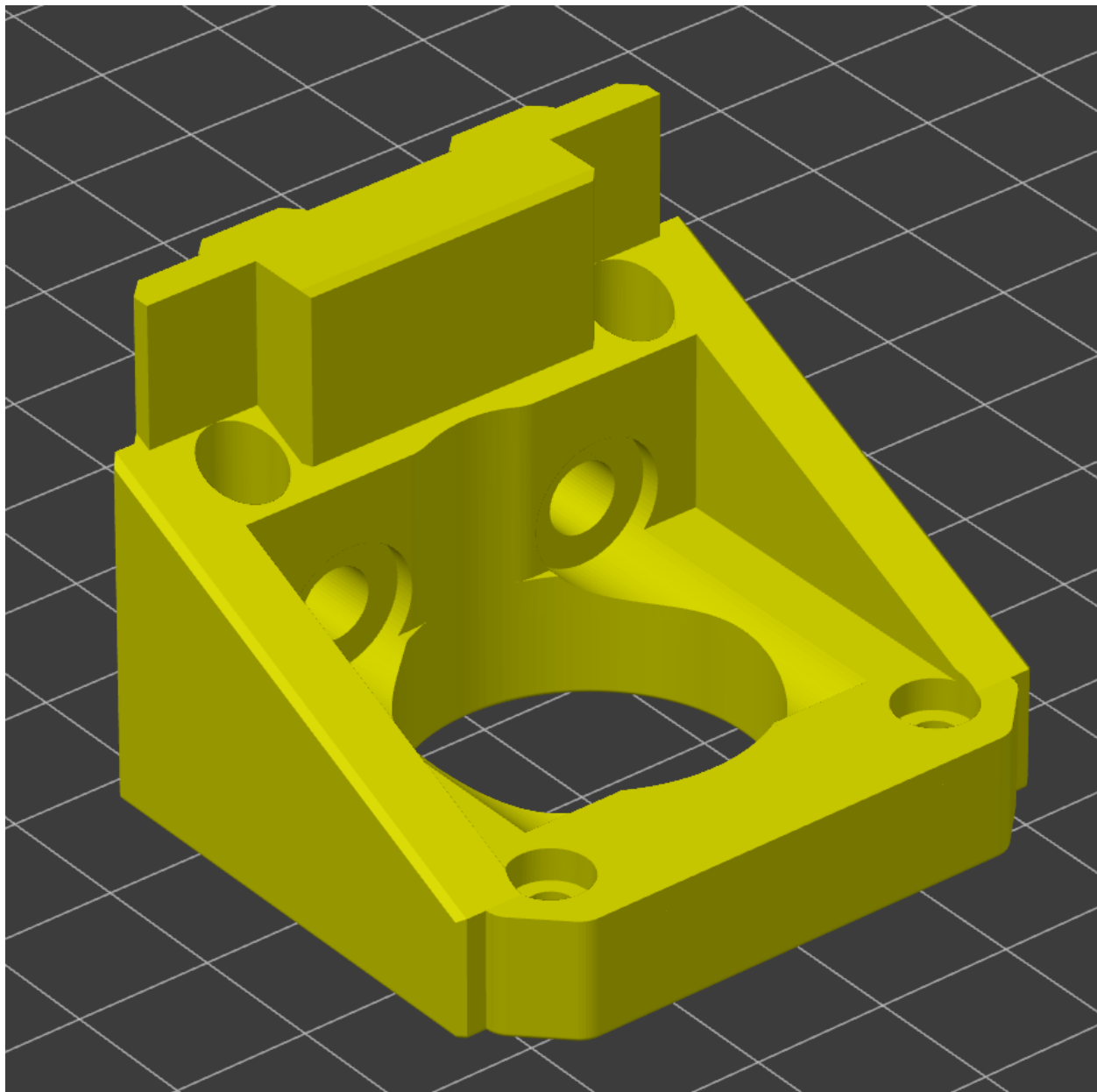


Figure 25. Ender 3 - Z Motor Mount [19]

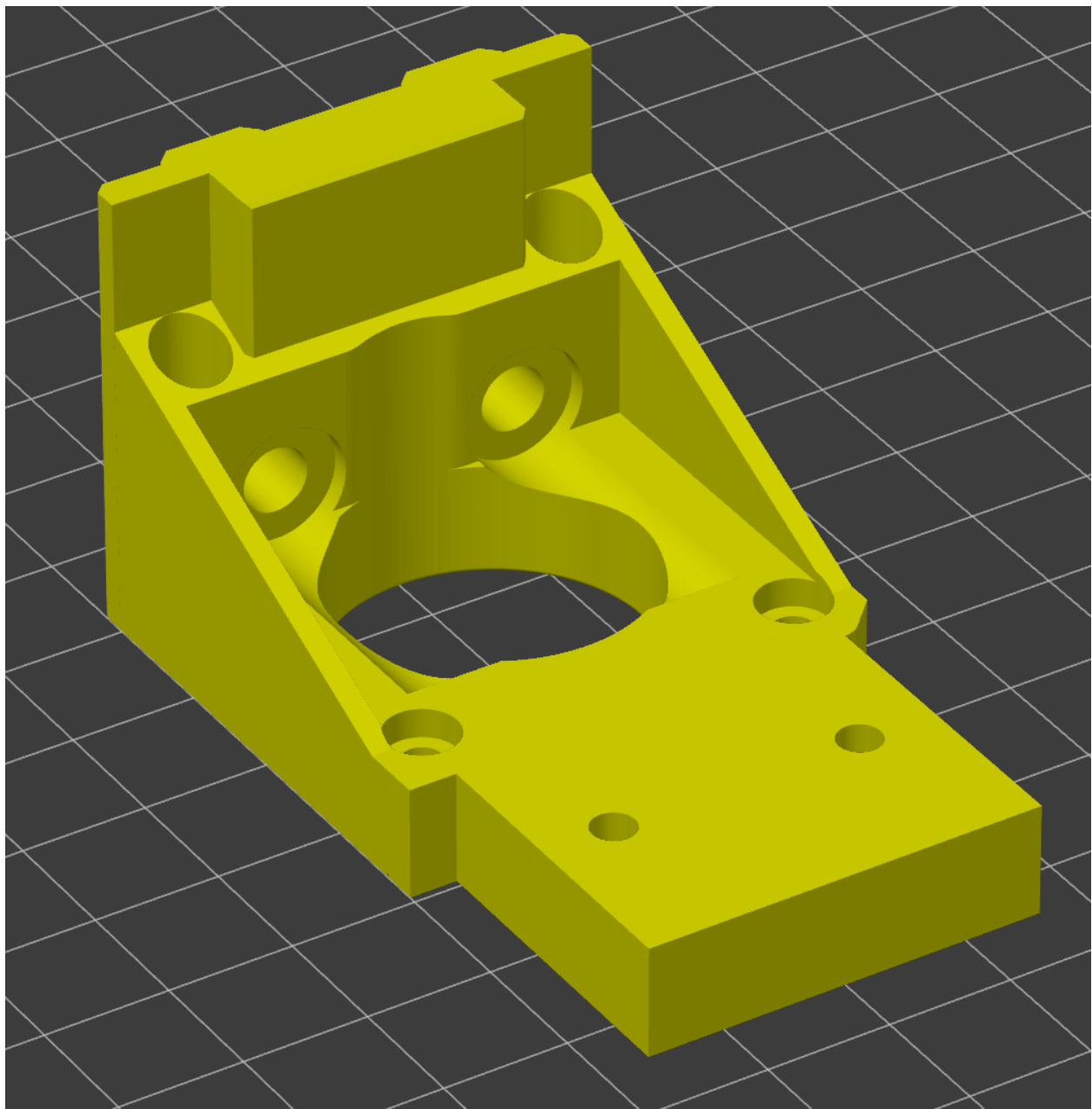


Figure 26. Modified Z-Axis Motor Mount

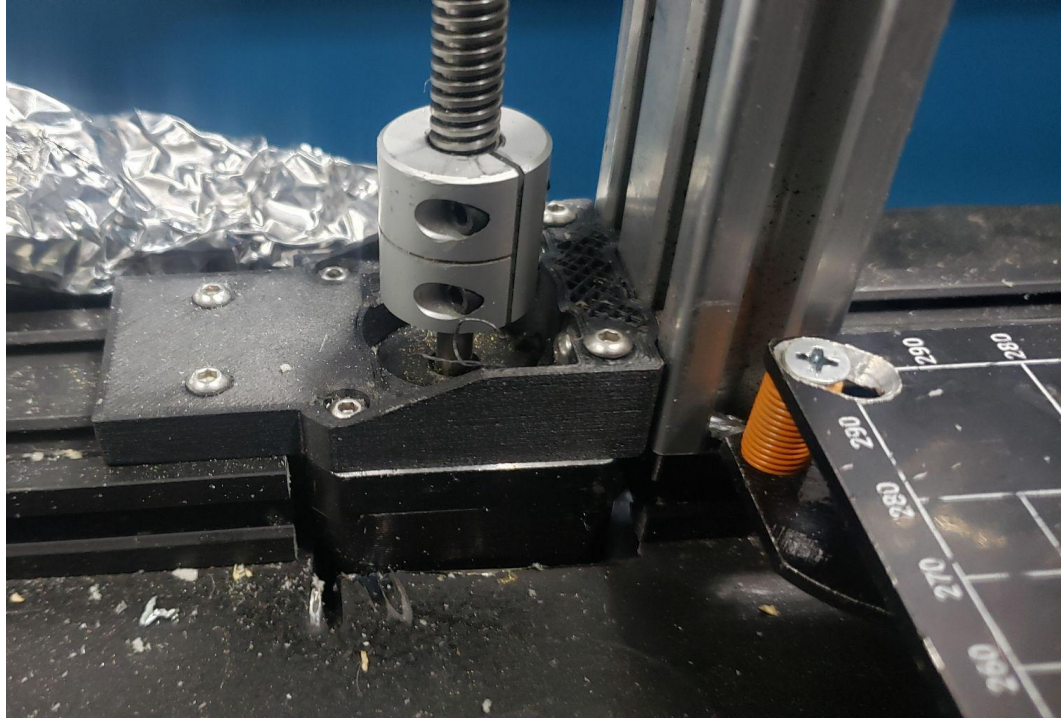


Figure 27. Assembled Z-Axis Mount

The modified design made the Z-axis stepper motors completely square compared to the X-gantry so the lead screws and the motor shaft shared a nearly perfect concentric axis. A 5mm to 8mm coupling nut was used to interface the motor shafts with the lead screws. Brass nuts were attached to the X-gantry, which threaded through the lead screws to raise and lower the gantry. Kinematic calculations were performed to determine the force, and thus torque needed to move the Z-axis.

Location	Total Mass (kg)	Parts Found in this Location
Left	0.627	Brackets, X-Motor, V-wheels, X-motor fan, peltier plate
Center	0.836	Aluminum extrusion, extruder assembly
Right	0.214	Brackets, V-wheels

Table 6. X-Gantry Weight Distribution

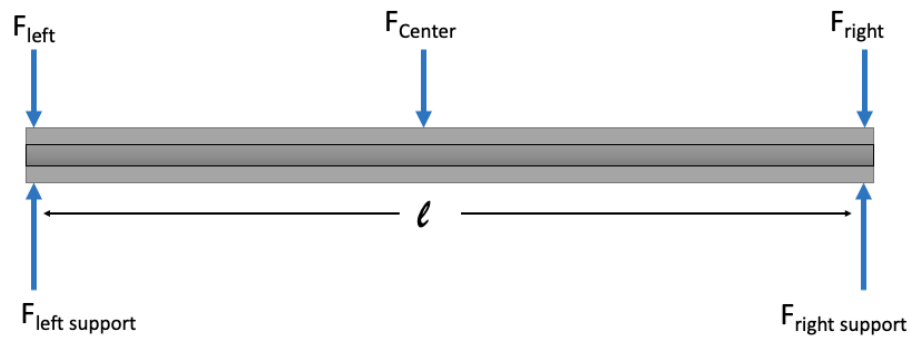


Figure 28. X-Gantry Free Body Diagram

The X-gantry had a total length of 0.416m.

$$F_{left} = mass_{left} \times 9.81 = 0.627 \times 9.81 = 6.151N$$

$$F_{center} = mass_{center} \times 9.81 = .836 \times 9.81 = 8.201N$$

$$F_{right} = mass_{right} \times 9.81 = .214 \times 9.81 = 2.099N$$

To find Left and Right support forces:

$$\Sigma M_L = 0 = F_{center}(l/2) + F_{right}(l) - F_{right\ support}(l)$$

$$F_{right\ support} = [8.201(0.416/2) + 2.099(0.416)] = 2.579/0.416 = 6.200N$$

$$\Sigma F_z = 0 = F_{left\ support} - F_{left} - F_{center} - F_{right} + F_{right\ support}$$

$$F_{left\ Support} = 6.151 + 8.201 + 2.099 - 6.200 = 10.251N$$

Lead Screw Property	Variable	Value
Pitch	p	0.050"
Major Diameter	d	0.250"
Minor Diameter	d _r	0.175"
Collar Diameter	d _c	0.3"
Friction Coefficient	f	0.15 [19]
Collar Friction Coefficient	f _c	0.15 [19]
Force on Right Screw	F _R	6.200N (1.394lbf)
Force on Left Screw	F _L	10.251N (2.305lbf)

Table 5: Lead screw kinematic variables

$$Pitch\ Diameter = d_m = d - 2(\frac{p}{4}) = 0.125 - 2(\frac{0.05}{4}) = 0.225"$$

$$\text{lead} = l = np = 1(0.05) = 0.05"$$

Torque Required to raise/lower load for the Right Screw

$$\text{To Raise} \rightarrow T_{R,\text{Total}} = T_R + T_{R,C} = \frac{Fd_m}{2} \left(\frac{l+\pi Fd_m}{\pi d_m - fl} \right) + \frac{Ff_c d_c}{2}$$

$$T_{R,\text{Total}} = \frac{(1.394)(0.225)}{2} \left(\frac{0.05 + \pi(0.15)(0.225)}{\pi(0.225) - (0.15)(0.05)} \right) + \frac{(1.394)(0.15)(0.3)}{2} = 0.087 \text{ lbf.in} = 0.983 \text{ N.cm}$$

$$\text{To Lower} \rightarrow T_{L,\text{Total}} = T_L + T_{R,C} = \frac{Fd_m}{2} \left(\frac{\pi Fd_m - l}{\pi d_m + fl} \right) + \frac{Ff_c d_c}{2}$$

$$T_{L,\text{Total}} = \frac{(1.394)(0.225)}{2} \left(\frac{\pi(0.15)(0.225) - (0.05)}{\pi(0.225) + (0.15)(0.05)} \right) + \frac{(1.394)(0.15)(0.3)}{2} = 0.043 \text{ lbf.in} = 0.486 \text{ N.cm}$$

Torque Required to raise/lower load for the Left Screw

$$\text{To Raise} \rightarrow T_{R,\text{Total}} = T_R + T_{R,C} = \frac{Fd_m}{2} \left(\frac{l+\pi Fd_m}{\pi d_m - fl} \right) + \frac{Ff_c d_c}{2}$$

$$T_{R,\text{Total}} = \frac{(2.305)(0.225)}{2} \left(\frac{0.05 + \pi(0.15)(0.225)}{\pi(0.225) - (0.15)(0.05)} \right) + \frac{(2.305)(0.15)(0.3)}{2} = 0.144 \text{ lbf.in} = 1.63 \text{ N.cm}$$

$$\text{To Lower} \rightarrow T_{L,\text{Total}} = T_L + T_{R,C} = \frac{Fd_m}{2} \left(\frac{\pi Fd_m - l}{\pi d_m + fl} \right) + \frac{Ff_c d_c}{2}$$

$$T_{L,\text{Total}} = \frac{(2.305)(0.225)}{2} \left(\frac{\pi(0.15)(0.225) - (0.05)}{\pi(0.225) + (0.15)(0.05)} \right) + \frac{(2.305)(0.15)(0.3)}{2} = 0.071 \text{ lbf.in} = 0.804 \text{ N.cm}$$

Torque Description	Torque (N.cm)
Torque to raise right screw	0.983
Torque to lower right screw	0.486
Torque to raise left screw	1.63
Torque to lower left screw	0.804

Table 7: Lead Screw Torque Values

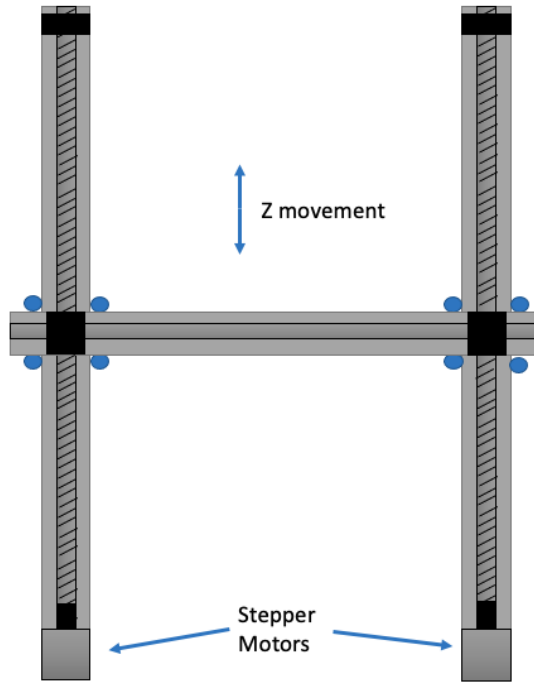


Figure 29. Simplified Z-Axis Movement Diagram

The same 24V, 2A stepper motor used for the Y-axis was used for both Z-axis stepper motors.

With 16 microsteps/full step, each motor is capable of providing 4.8Ncm of torque each (as shown in the Y-axis torque calculations), for a total of 9.6 Ncm. The total torque required to raise the X-gantry is 2.613 Ncm, giving the Z-axis a factor of safety of about 3.5. However, this is assuming the torque required to raise each side is symmetrical. Each side of the X-gantry has a different weight because different components are mounted to each side. To distribute the available torque evenly across the system, a Z-sync belt was added to the top of the lead screws so one could not rotate without the other. This also stops the X-gantry from becoming unlevel when the printer turns off since when the Z-motors are disabled, they can rotate slightly. Over time, this would result in a crooked X-gantry. Now, the torque provided to the system would distribute across the lead screws, making sure one side did not bind from lack of torque while the other was operational. The Z-sync mechanism consisted of 2 GT2-16T-B5 idler pulleys attached to the top of each lead screw with a grub screw. A high-temperature GT2 belt was attached to each pulley, and a tensioner was added to keep the belt taut. The tensioner was simply a bracket with a free-spinning pulley whose distance could be changed and locked in place using a screw and lock nut combination. The tension needed to be very small to not cause the lead screws to bend inward and deflect, binding the system. The last part added to the Z-axis was lead screw guides. If the X-gantry was at the bottom of the printer, the top of the lead screw would not be supported by anything, causing it to bend due to imperfect manufacturing. A simple mount by Franic Conrad of a bearing in a loosely constrained channel was added to contain movement of the lead screw without holding it tightly [20]. Unlike the X and Y-axes, to determine its location in space, a traditional limit switch was not used. Instead, a hall effect sensor called a BLTouch was used to calibrate the Z-axis to position 0. The BLTouch was mounted to the X-carriage and

would work by deploying a magnetic probe and moving the Z-axis down until the probe touched the bed. This causes the magnet to move slightly closer to the hall effect sensor, indicating how far from the bed the sensor is. The advantage of a probe like this, as opposed to a limit switch, was the ability to probe the entire build platform and construct a virtual mapping of the levelness of the bed, allowing for software compensation if the bed or X-gantry was not perfectly square.

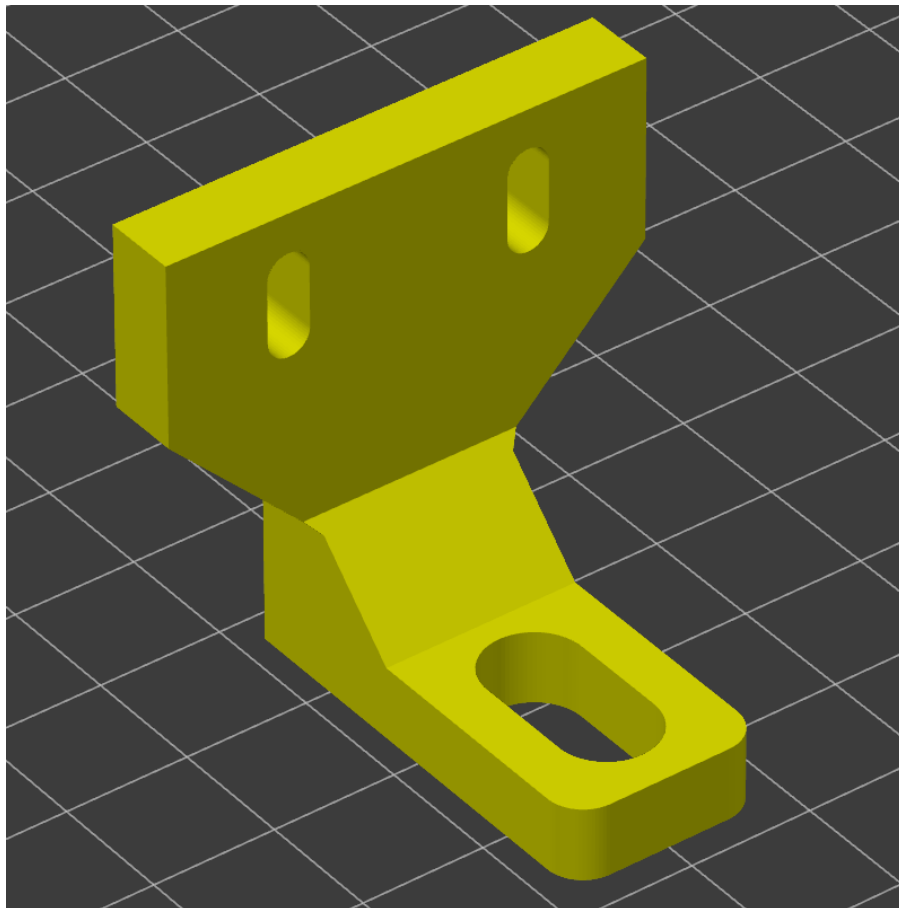


Figure 30. Z-Sync Tensioning Mechanism

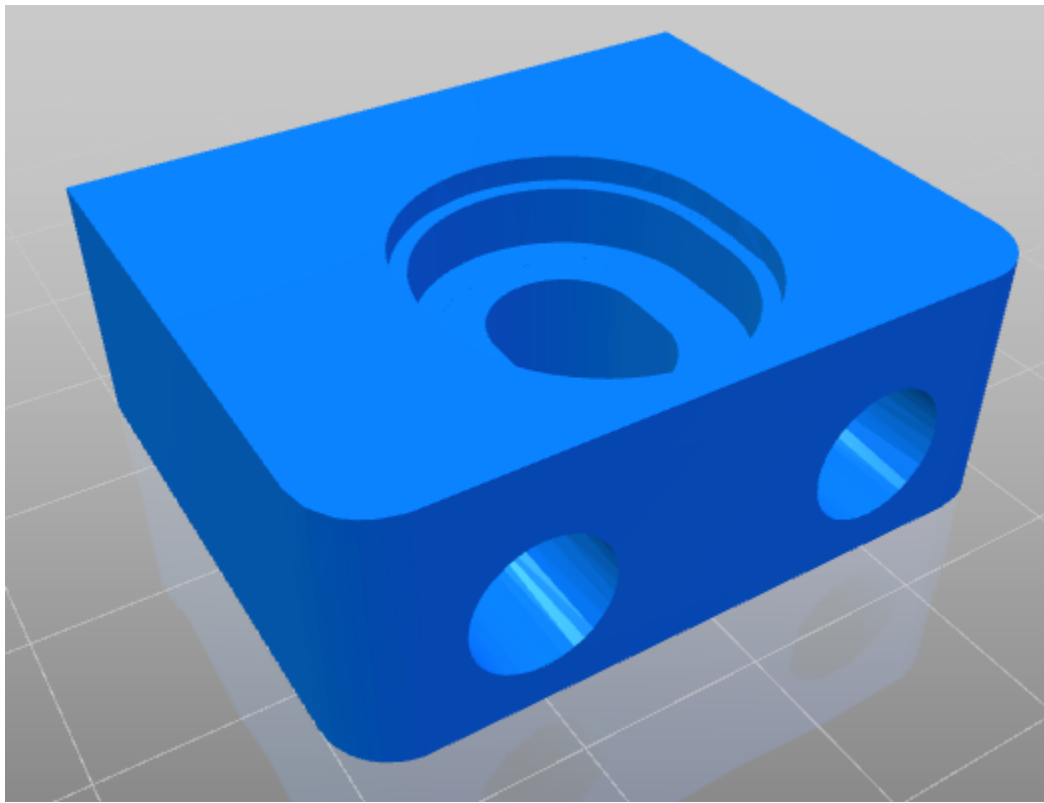


Figure 31. Lead Screw Guide [20]

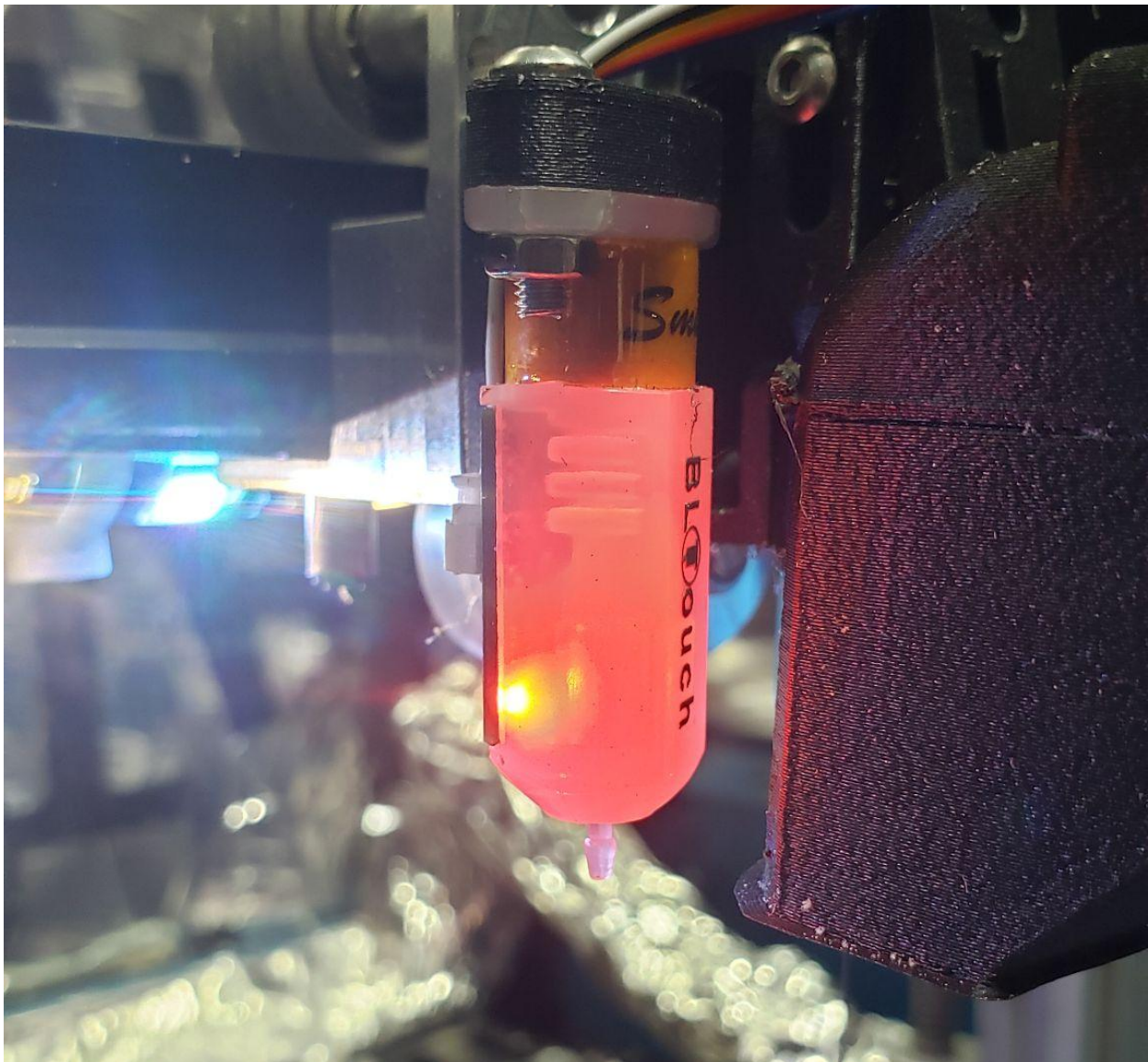


Figure 32. BLTouch Stowed

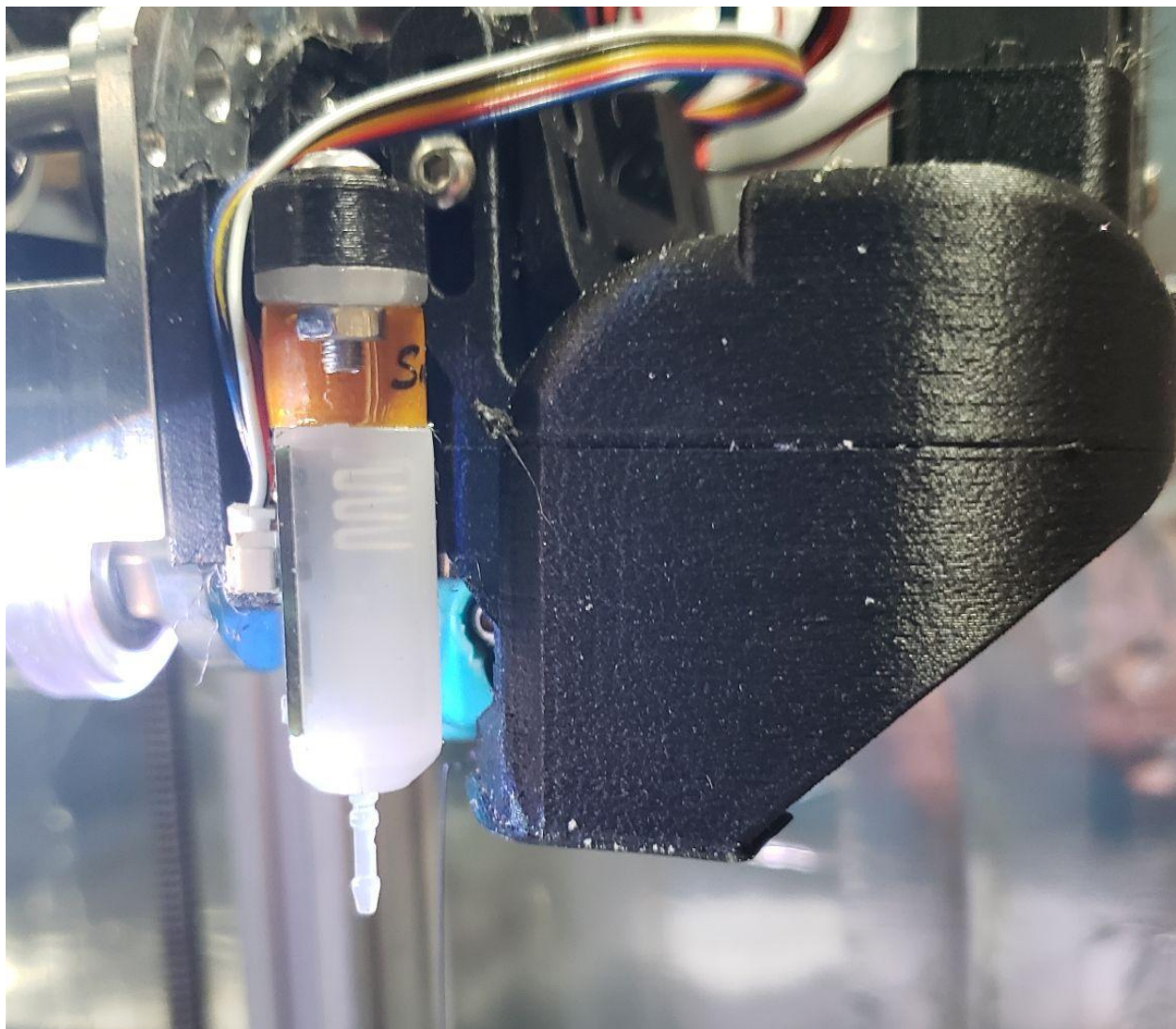


Figure 33. BLTouch Deployed

3.1.5 *Extruder*

The extruder is the heart of the 3DPP. All 3 axes work together to move it to the exact spot so the filament can be perfectly extruded. This piece must be as light as possible so it has less inertia and can be moved quickly by the X and Z-axes, improving print quality and reducing print time. The extrusion mechanism still needs to be strong enough to force plastic through the

hotend, the hotend needs to be able to reach 450 °C to melt PEEK and PSU while not melting surrounding components, and the nozzle needs airflow directly below it to cool the plastic quickly so the print does not become sloppy due to overhangs. The Slice Engineering Mosquito® Hotend, which “Eliminates heat creep, reduces jamming, and improves printing resolution through Bimetallic Heat Break™ technology”, “conducts 85% less heat than a standard threaded heat break,” and has a “low mass on the carriage for maximum X-Y acceleration” [21] was selected as the hotend. The Mosquito® Hotend also comes with a custom hotend fan that keeps the heat isolated to the heater block to prevent heat creep from clogging the heat break. Heat creep occurs when heat from the heater block (shown in figure 33) is able to permeate up the heat break and into the heat sink unrestricted. If the temperature in the heat sink or break gets hot enough, the filament will liquefy until the printer is turned off. Next time the printer is turned on, the filament will be jammed in the heat break or heat sink where it last liquified until the heat creeps back up again. Blowing air across the heat break and heat sink keeps the air isolated to the heater block. The hotend assembly was mounted to a Micro Swiss Direct Drive Extruder, which provides a strong direct drive interface while maintaining the required lightweight of the X-carriage. It has a dual-gear extruder, so the plastic is gripped from both sides during extrusion. The increase in grip allowed for a reduced force required to extrude the plastic since no force was lost to the grip slipping, so the size of the stepper motor could also be reduced, which was the heaviest component of the extruder by far. Direct drive was used as opposed to a Bowden tube solution because since the filament spool is outside the build chamber, feeding the filament into a direct drive solution is much easier. Since the extruder is lightweight, it has nearly all the advantages of direct drive, such as more reliable extrusion, better retraction, and needing a less-powerful motor, without the disadvantages [22]. A part cooling

solution was also needed, called a K-fan. The K-fan blows air directly below the nozzle, cooling the filament as soon as it comes out. This stops the filament from drooping anywhere there are overhangs or filament bridges. The quality of the K-fan's airflow directly impacts the finish of prints, so having a quality design is instrumental. The open-source design by David Petsel called "Petsfang" was selected [23]. David Petsel designed a fan duct that interfaces with the Micro Swiss direct drive mount and has already run flow analysis to make sure the fan is cooling optimally. As a side note, since the extruder stepper motor has to be inside the build volume, the same Peltier plate and fan cooling solution used on the X-axis was also used here.

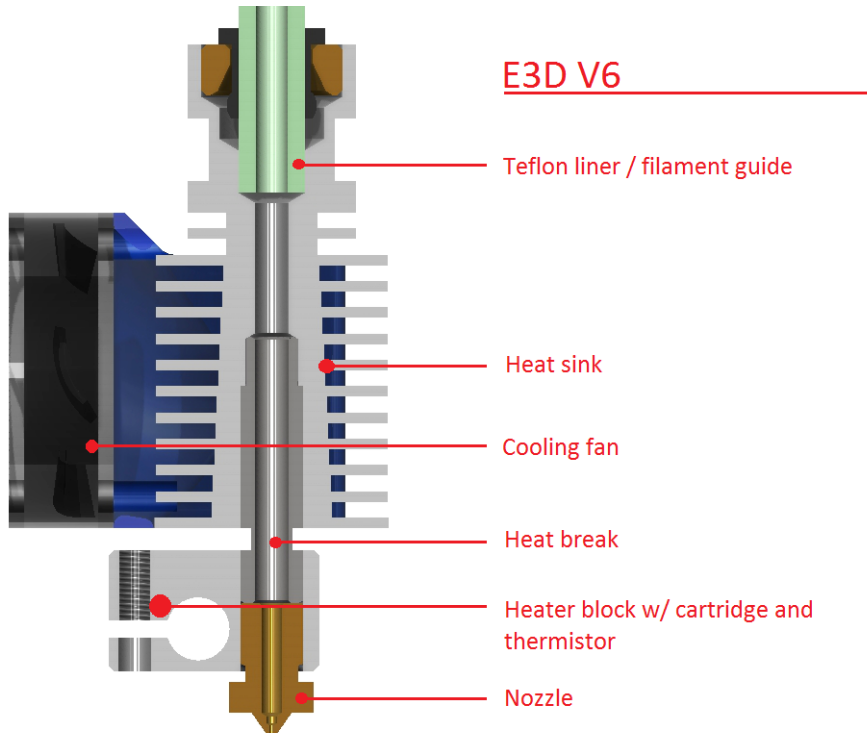


Figure 34. E3D V6 Hotend Diagram

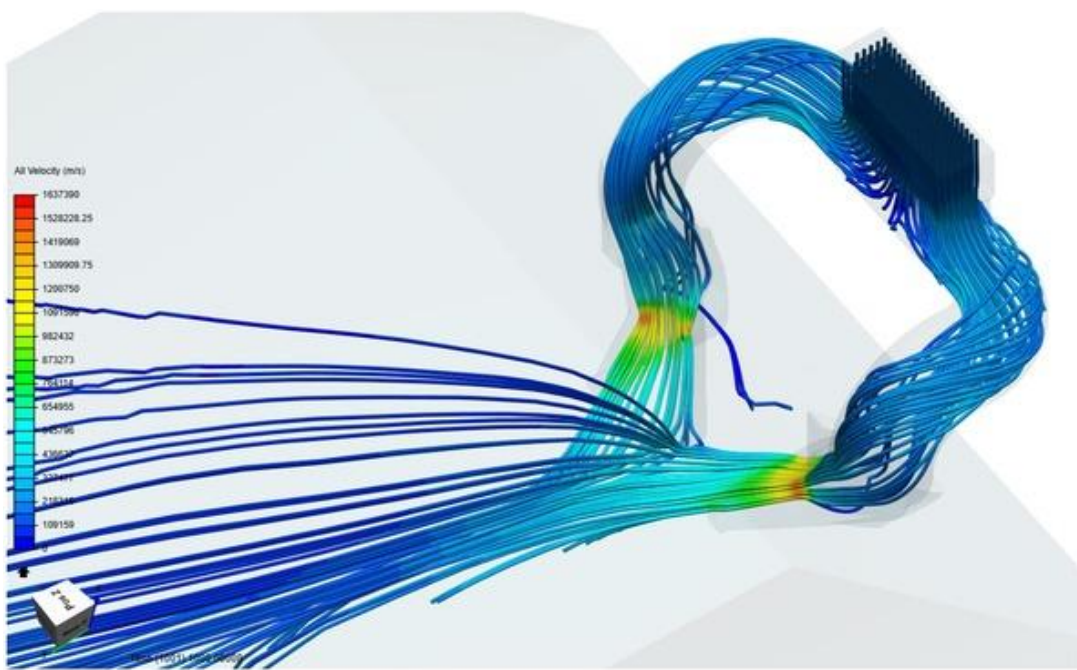


Figure 35. Airflow Analysis from Petsfang Duct [23]

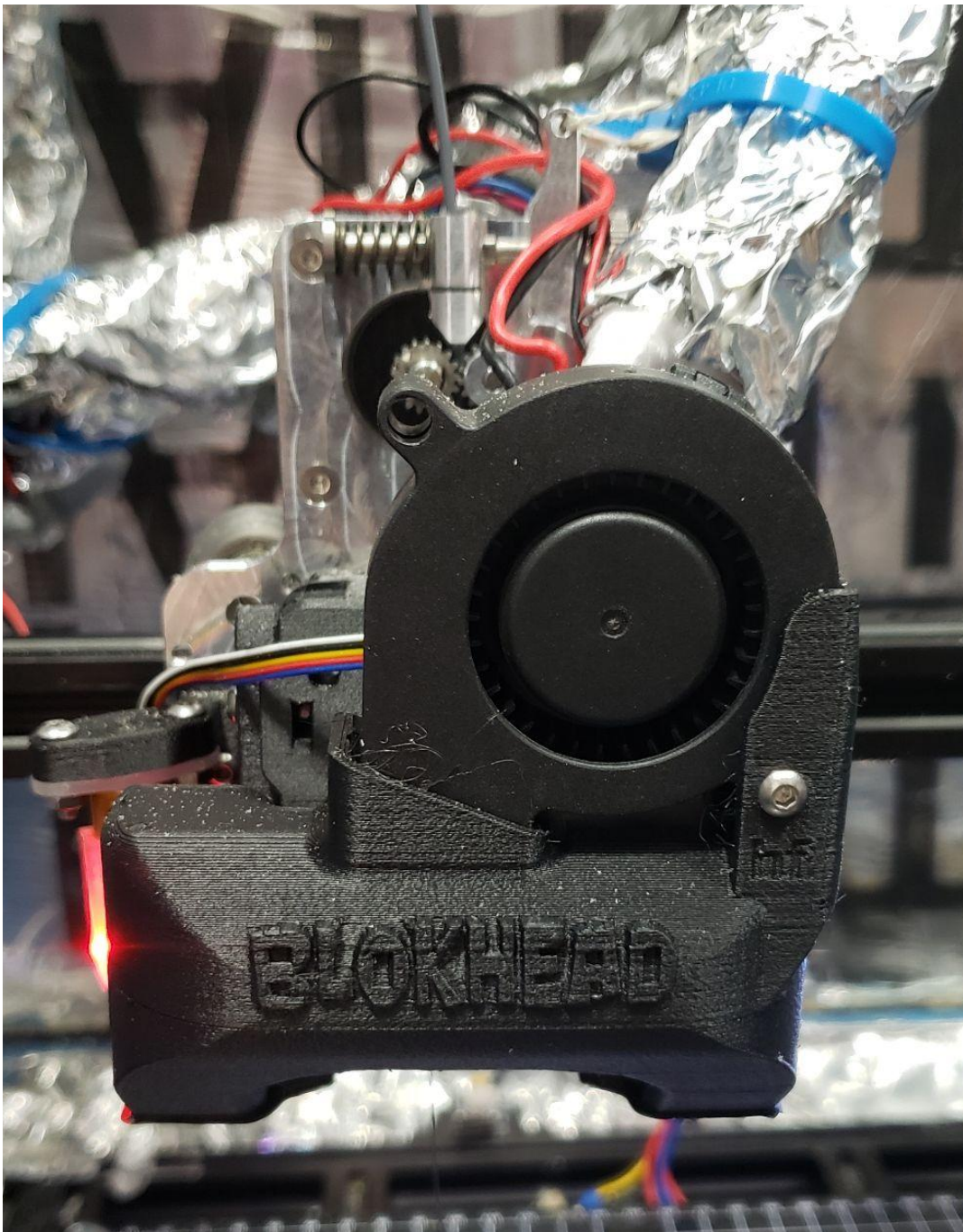


Figure 36. Assembled Extruder Front View

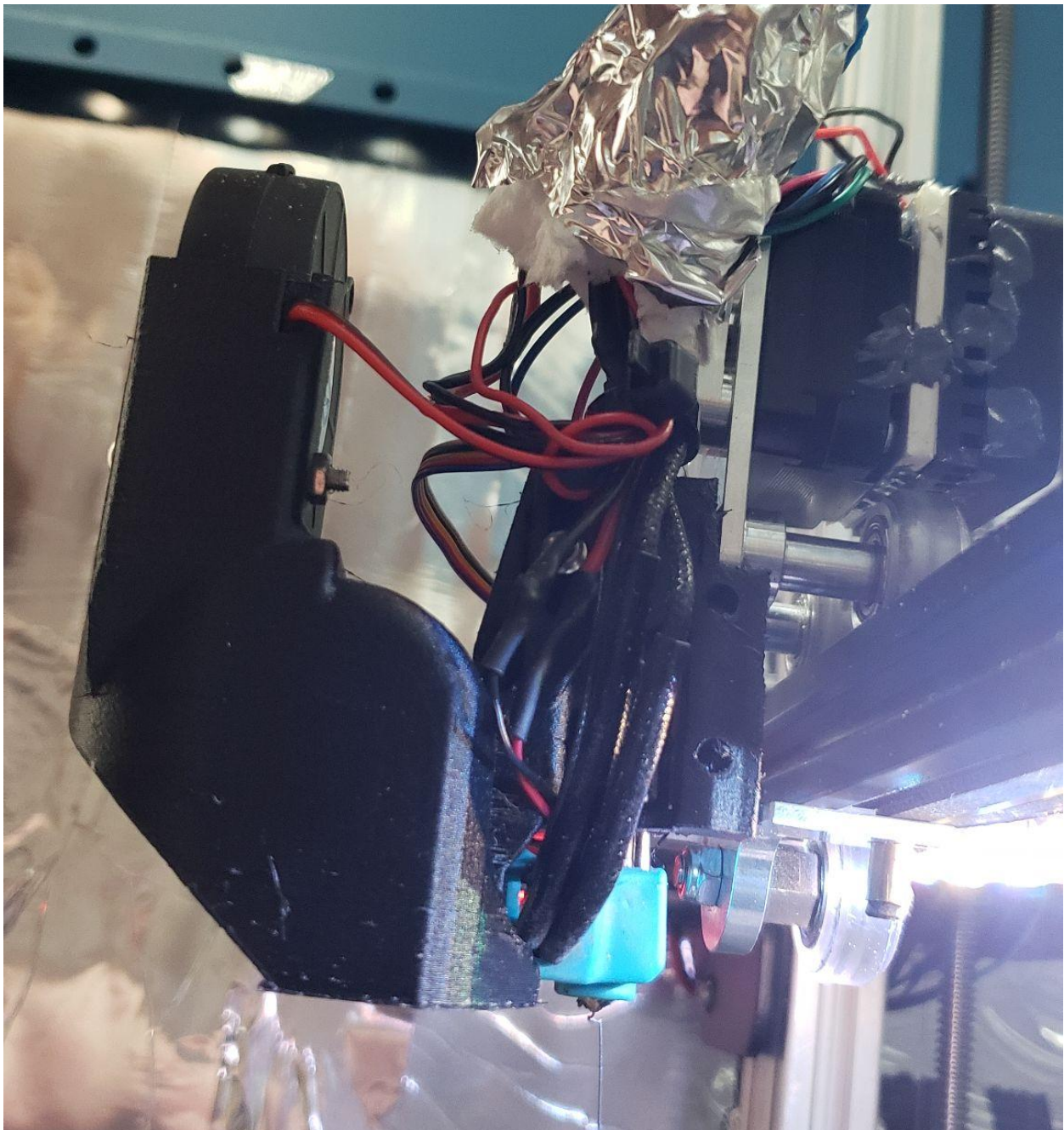


Figure 37. Assembled Extruder Side View

3.1.6 Heated Chamber

To heat the chamber, 2 space heaters, each with a heat power of 1500W, are used to bring the temperature of the chamber up to 80°C. This was the most cost-effective heating solution that provided enough power and could fit within the 3DPPs available chamber. The larger the heating elements, the less space is available for prints, so it makes sense to have a heating element with the smallest footprint possible. Since the bottom of the printer enclosure was filled with the heated bed, the space heaters were mounted at the top of the enclosure. Two 120mm X 120mm fans were then mounted above the space heaters to force the heated air downwards, creating a type of convection oven. Since the wattage of the heating elements is known, the necessary thickness of insulation can be determined through calculations. The first step is to estimate the convection heat transfer coefficient, which gives a mathematical ratio between the heat flux and the change in temperature.

Air Property at 80°C	Variable	Value
Thermal conductivity	k	0.02953 W/mK
Kinematic viscosity	ν	$2.097 \times 10^{-5} \text{ m}^2/\text{s}$
Prandtl Number	Pr	0.7154

Table 8: Thermal Air Properties at 80°C [24]

Printer Dimension	Variable	Value
Height	h_p	1.676 m
Width	w	0.533 m
Length	L	0.635 m
Area of front,back walls	A_{FB}	0.894 m ²
Area of left,right walls	A_{LR}	1.065 m ²
Area of top,bottom walls	A_{TB}	0.339 m ²
Total Area	A_{total}	4.596 m ²

Table 9: 3DPP Dimensions for Thermal Analysis

Fan Cross-sectional area: $0.1016 \times 0.1016\text{m} = 0.01032 \text{ m}^2$

$$\text{Fan Airflow} = 120.3 \frac{\text{m}^3}{\text{hr}} * \left(\frac{1\text{hr}}{3600\text{s}}\right) * \left(\frac{1}{0.01032\text{m}^2}\right) \rightarrow \text{Fan Velocity} = V = 3.235 \frac{\text{m}}{\text{s}}$$

$$Re_{h_p} = \frac{Vh}{v} = \frac{(3.235)(1.676)}{2.097 \times 10^{-5}} = 258553 < 5 \times 10^5 \rightarrow \text{laminar flow}$$

$$Nu = \frac{hl}{k} = 0.664 Re_{h_p}^{0.5} Pr^{1/3} \rightarrow h = \frac{0.664 Re_{h_p}^{0.5} Pr^{1/3} k}{h_p} = \frac{0.664(258553)^{0.5}(0.7153)^{1/3}(0.02953)}{1.676} = 5.32 \text{ W/m}^2\text{K}$$

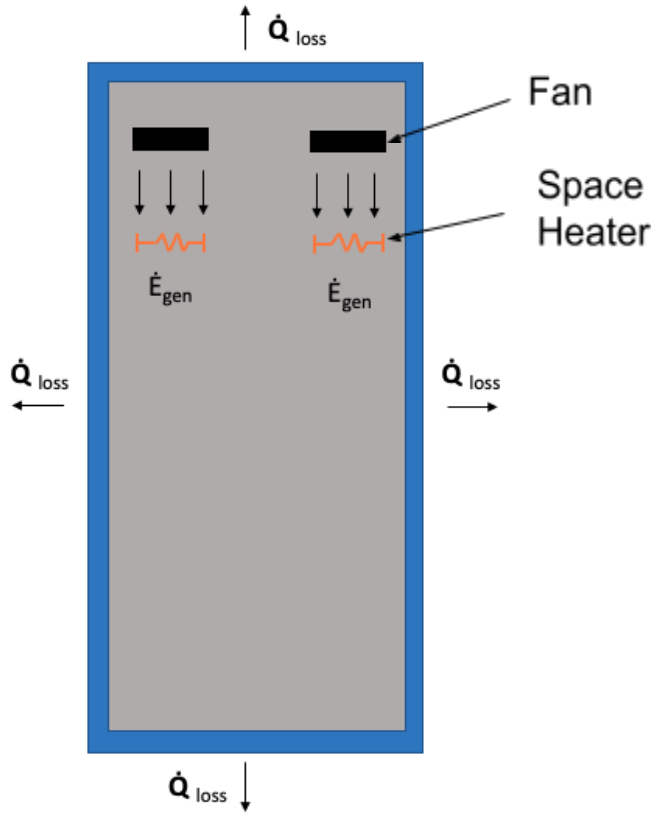


Figure 38. Simplified Heat Flow Diagram

Figure 37 shows the heat generation, or \dot{E}_{gen} , from the space heaters in the chamber and the heat loss flowing out of the chamber through the insulation, or \dot{Q}_{loss} . By setting heat generation equal to heat loss in the system, the minimum thickness of insulation required to keep the chamber at 80°C can be determined.

In other words: $-\dot{Q}_{loss} = \dot{E}_{gen}$

Where $\dot{E}_{gen} = \dot{Q}_{heater} = 3000W$, the combined power of the space heaters

The 3000W is distributed along all the faces of the interior, so the proportion of heat transferred on each face can be found.

$$\text{For the front and back face: } Q_{heater,FB} = \frac{A_{FB}}{A_{total}} Q_{heater} = \frac{0.894}{4.596} (3000) = 583.6W$$

For the left and right face: $Q_{heater,LR} = \frac{A_{LR}}{A_{total}} Q_{heater} = \frac{1.065}{4.596} (3000) = 695.2W$

For the top and bottom face: $Q_{heater,TB} = \frac{A_{TB}}{A_{total}} Q_{heater} = \frac{0.339}{4.596} (3000) = 221.3W$

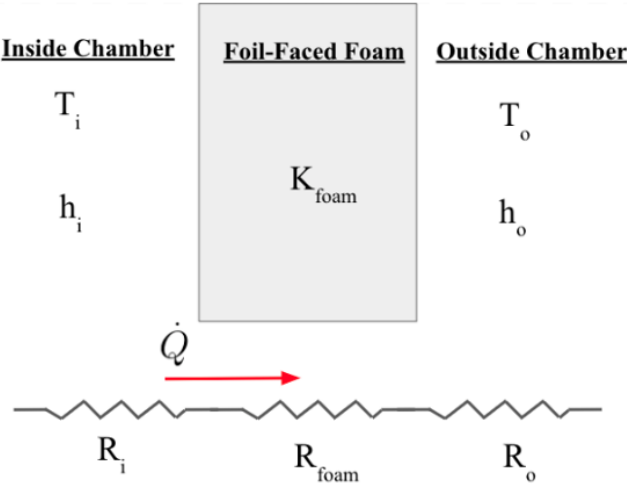


Figure 39. Simplified Thermal Resistance Diagram

By using thermal resistance simplification, $-\dot{Q}_{loss}$ can be calculated. When it is set equal to \dot{Q}_{heater} at each face, the minimum thickness of insulation to sustain 80°C can be found.

$$Q_{loss} = \frac{T_i - T_o}{R_{total}} \text{ and } R_{total} = \frac{1}{h_i A} + \frac{t}{k A} + \frac{1}{h_o A}$$

Through equation manipulation, the insulation thickness (t) can be isolated

$$t = \frac{kA(t_i - t_o)}{-Q_{heater}} - \frac{k}{h_i - h_o}$$

Minimum thickness for front and back:

$$t = \frac{0.02953(0.894)(80-22.2)}{-583.6} - \frac{0.02953}{5.32-10} = .00370m = 0.146in$$

Minimum thickness for left and right:

$$t = \frac{0.02953(1.065)(80-22.2)}{-695.2} - \frac{0.02953}{5.32-10} = .00370m = 0.146in$$

Minimum thickness for top and bottom:

$$t = \frac{0.02953(0.339)(80-22.2)}{-221.3} - \frac{0.02953}{5.32-10} = .00370m = 0.146in$$

The minimum thickness of each wall came out to be the same at 0.146 inches. By rounding up to market standard would be $\frac{1}{4}$ " insulation is required to sustain the heated chamber at 80°C. This theoretical value assumes a perfectly sealed chamber. The insulation chosen was 3" foil-faced polyisocyanurate rigid foam insulation. One main advantage of this insulation is it provides its own structural integrity, so a separate apparatus is not needed to mount the foam. The foam can be bolted directly to the chamber frame. The 3" of foam is excessive relative to the required value, but there were not any space constraints in the design requirements, so thicker insulation only helped. The insulation thickness was capped at 3" since that was the largest thickness available. While this is much larger than our calculated minimum thickness, it will drastically decrease the amount of time to heat the chamber and use significantly less energy as well. Since the heat-sensitive electronics were mounted to the top of the chamber, where heat was most likely to escape, a thin ceramic fiber insulation blanket was added between the electronics and the top insulation to provide extra protection.

Mounting the space heaters proved a difficult task as well. Each space heater had an independent, fused AC connection for safety as well as 2 fast shut-off switches. Since each space heater can get up to 300°C, only metal could be used to mount them, as other materials would deform. The problem arises because a space heater element is simply many ceramic heating elements

surrounded by metal fins to dissipate the heat. One side of the metal touching the ceramic heating element is positively charged, and the other side is grounded. The current flowing through the ceramic plate heats it up. This system is compounded in a sandwich fashion where there is a common ground on the inside metal fins, 2 columns of ceramic plates, and 2 then positive outside metal fins. To mount the space heater elements, a metal assembly was manufactured to mount to the positively charged outsides. These mount points can not touch the case, since the case is earthed. Using any metal to suspend the space heaters from the ceiling was difficult because the head of the screw was touching sheet metal at the top, so if the space heater mount touched the screw, it would cause a short. A rubber grommet and 2 nylon washers insulated the screw from the top sheet metal so the screw was now electrically isolated from the top sheet metal. However, after installing the foil-faced polyisocyanurate rigid foam insulation, if the foil on the insulation touched the screw, it would also cause a short since the electrically conductive foil was also touching the case. The final solution was a triple-insulated method, where the screw was insulated from the top sheet metal with a rubber grommet and two nylon washers, a nylon spacer insulated the screw until it was past the insulation, then as an extra precaution, a rubber grommet with 2 Delrin washers insulated the space heater from the screw.



Figure 40. Space Heater Mounting Solution

3.1.7 Electrical System

The electrical system was designed by first planning out all circuits and components that needed to be in the 3DPP and drawing up the schematics shown in figures 40-43. The schematics are broken up into 4 parts.

1. Parts connected to the main control board, the SKR 2. This is a 3D printer control board by BIGTREETECH, powered by an STM32F407.
2. Parts connected to the supporting board, a raspberry pi. This board hosts a web server for the end-user to monitor the status of the printer, feed G-CODE commands to the SKR, and run custom code to control the heated chamber.
3. AC circuits. As noted in the design requirements, the electrical system is split into 3 15A AC circuits. The first is for all of the control and computation systems of the printer and

the last two are for heating the chamber. All three lines connect to a 15A fuse, then to individual power switches, and finally to their loads.

4. Buck Converter schematic. This schematic contains anything that requires power that does not run off the main 24V of the power supply. The voltage is stepped-down to the appropriate voltage and then sent to that component.

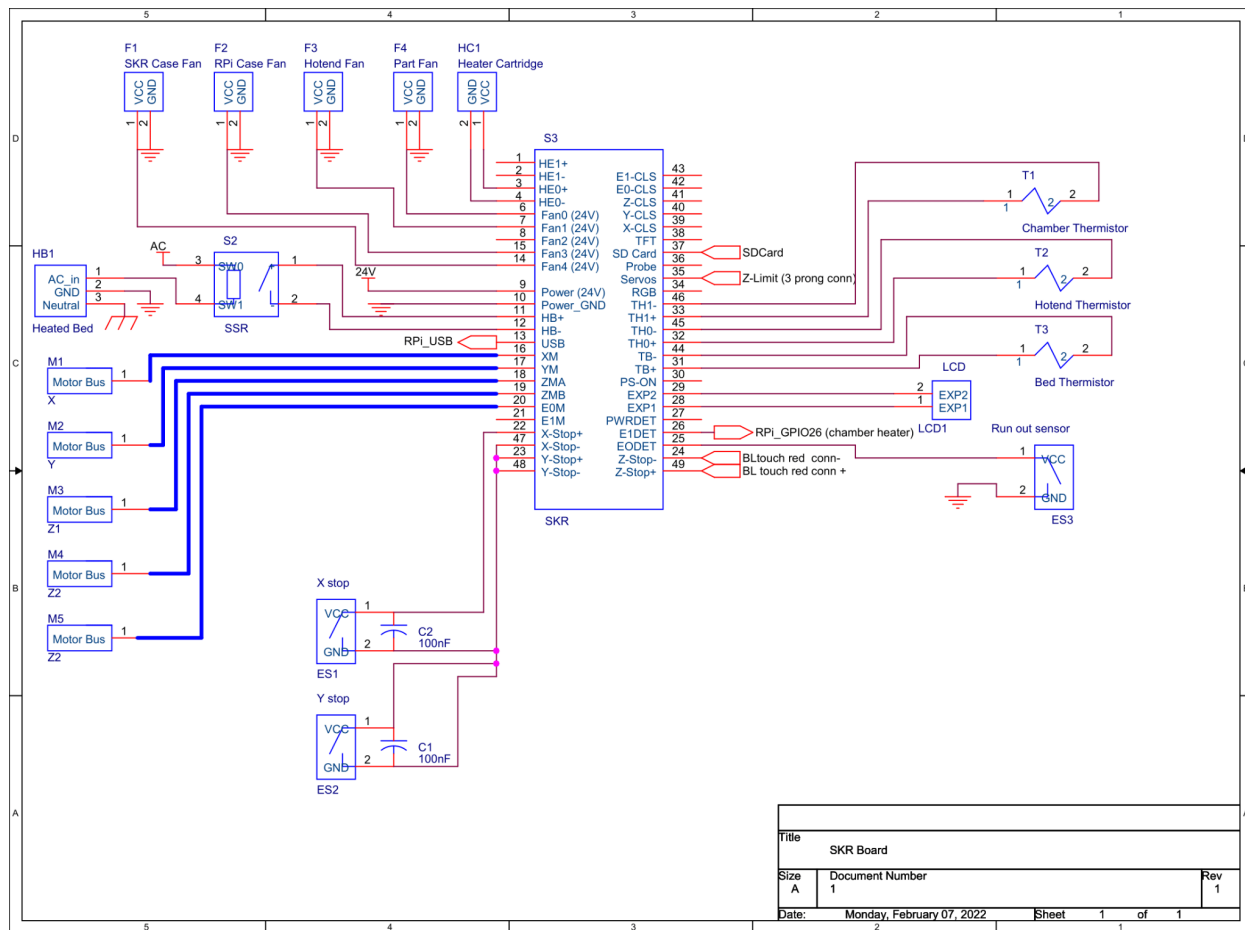


Figure 41. Connections to SKR 2 Schematic

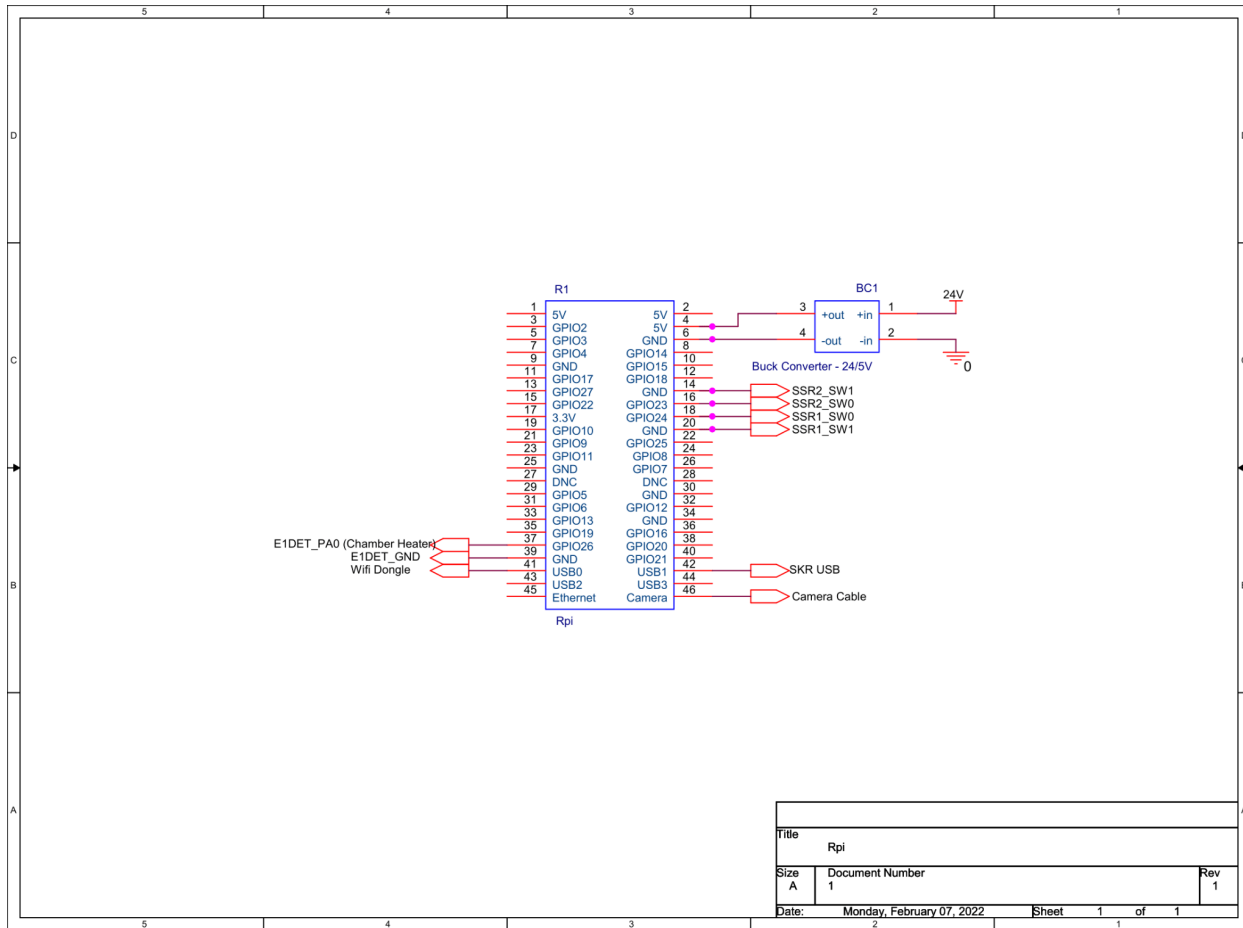


Figure 42. Connections to Raspberry Pi Schematic

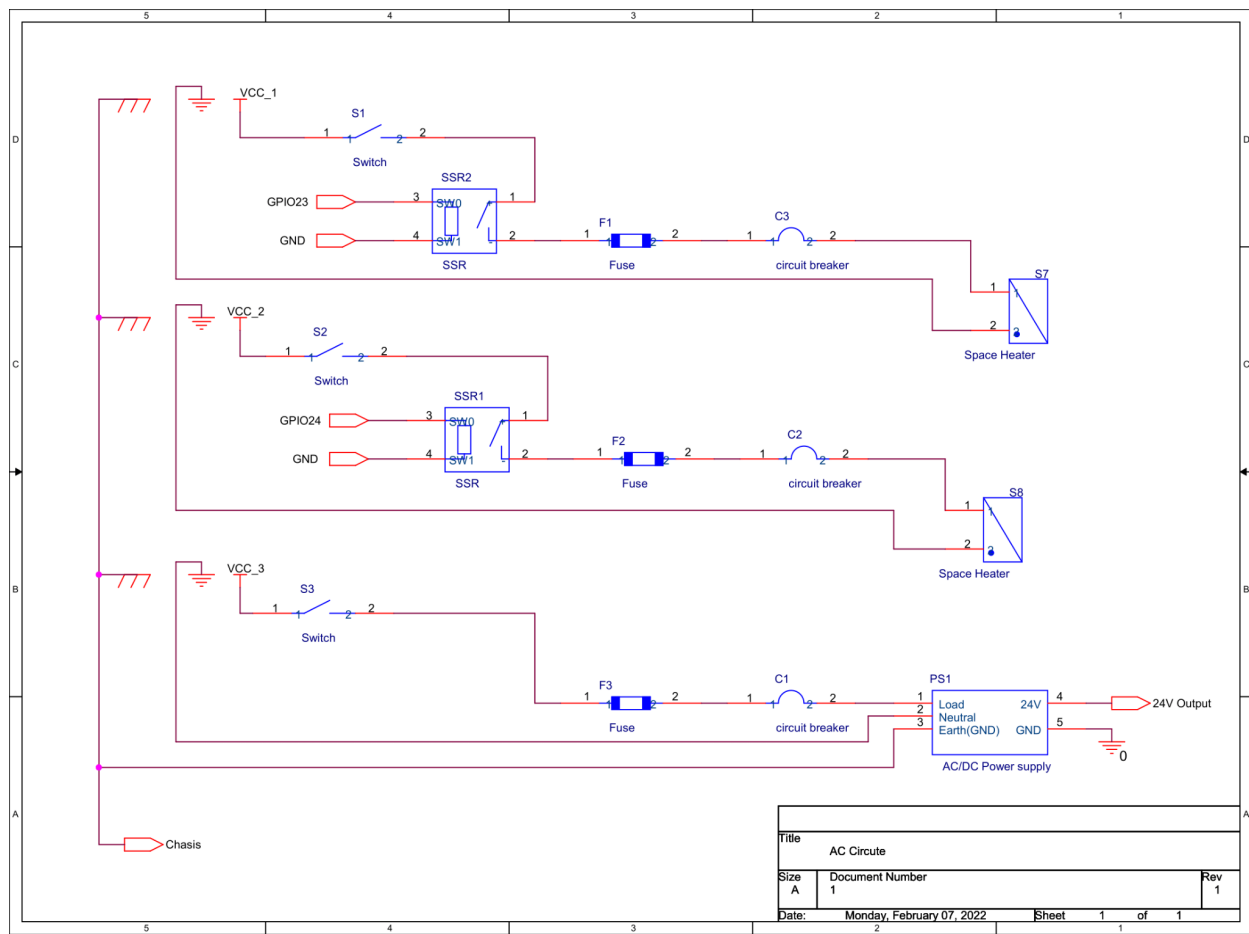


Figure 43. Connections to AC Schematic

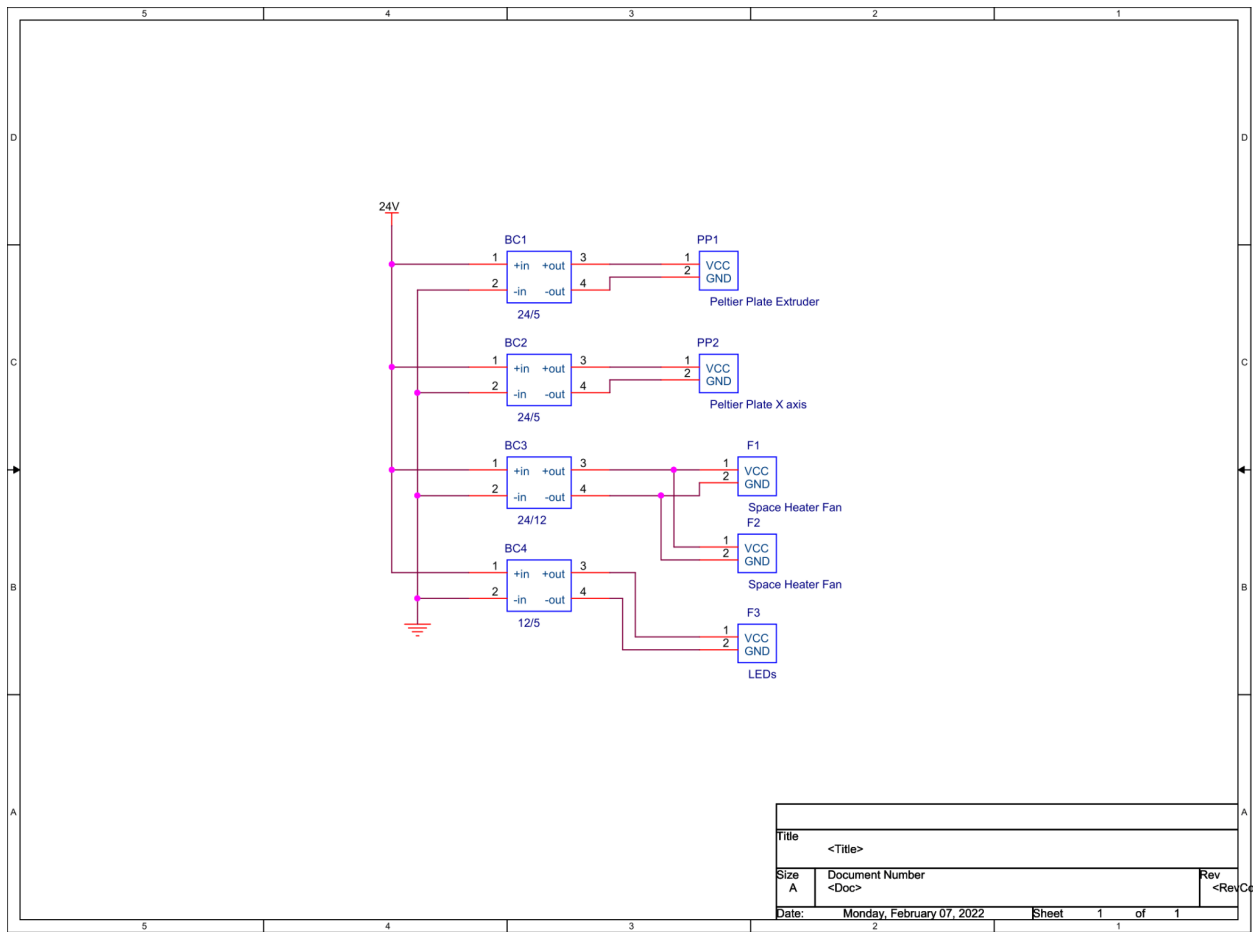


Figure 44. Connections to Buck Converters Schematic

To mount the 3 AC female receptacles, custom plates had to be printed so no heat would escape out the holes cut for the AC female receptacles.

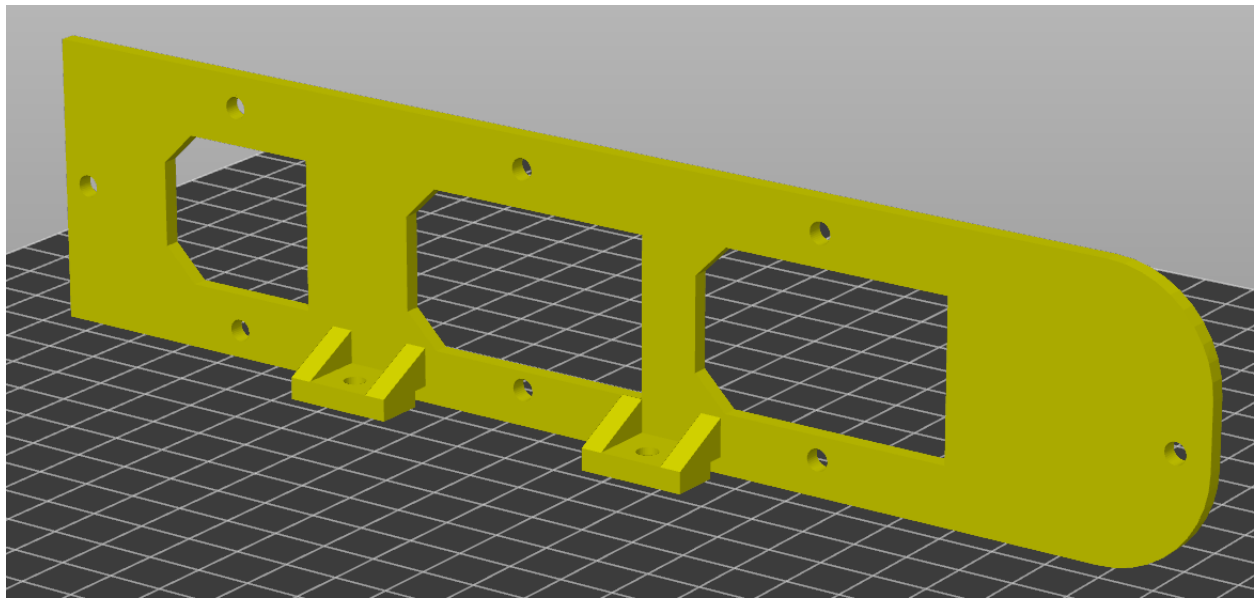


Figure 45. Power Plate Design

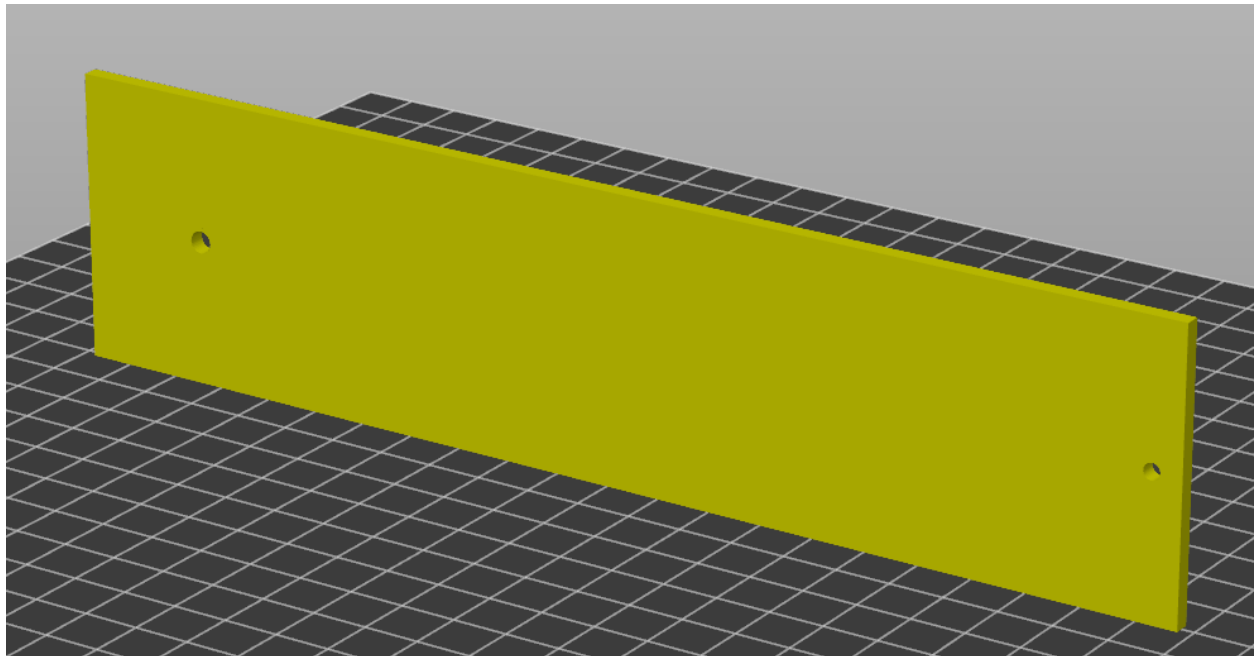


Figure 46. Power Plate Heat Block Design



Figure 47. Installed Power Plates

Two of the AC circuits are very simple. They just power the space heaters, while offering a fused connection and a safety shutoff switch. The last AC circuit connects to a 24V 21A power supply. From there, the power supply powers buck converters, which drop the voltage to provide power to various supporting components or the main processing board, an SKR 2. The SKR 2 is a 3D Printer control board by BIGTREETECH, powered by an STM32F407 microcontroller.

Each aspect of the printer system connected back to the SKR 2 and was controlled by firmware. The SKR 2 supports 5 stepper motors drivers, X, Y, Z1, Z2, and E motor drivers, for each stepper motor used. TMC2209 motor drivers were selected due to their low cost, 2A continuous drive current, and ease of use. Additionally, they are silent so they will not be making annoying noises while printing.

Following the SKR Schematic, other components connected to the SKR are both the X and Y end stops, which were discussed in the X-axis and Y-axis movement sections, as well as the

BLTouch connections, which serve as the Z-stop and software bed leveling system. The SKR powers 4 cooling fans. Two of them are 80mm X 80mm fans mounted to the rear of the electronic case to the electronics. The other two fans were the extruder fan and the K-fan. The SKR 2 supports an LCD connection, which allows the printer to be controlled by a local LCD, as per the design requirements. The SKR also controlled the temperature and temperature monitoring for all 3 heating systems: the hotend, the bed, and the heating chamber. For the heated bed and chamber, this consists of turning on and off a relay that is connected to AC power. For the hotend heater cartridge, the board directly powers the cartridge. For each heating system, a thermistor was also connected to monitor the individual temperatures of the hotend, the heated bed, and the heated chamber. All 3 heating systems required a different temperature range, so different thermistors were used for each. The hotend used an RTD PT1000 thermistor, which can reach up to 500°C [25]. The bed uses an Semitec 104NT, which can reach temperatures of 300°C [26]. The chamber thermistor uses an NTC 100K thermistor, which can reach temperatures of 250°C [27]. Each thermistor has a lookup table that relates the thermistor's current resistance to the corresponding temperature that would cause it to be at that resistance. To efficiently heat each system, PID tuning was performed on the hotend and heated bed to minimize heat-up time and overshoot. Additionally, PID tuning allows each of the two temperature systems to be more accurate. The heated chamber would not benefit from PID tuning due to its long heat up and cool down time. The heated chamber used an alternative control system called bang-bang control. One of the design requirements was thermal protection for each heating system, so if the temperature range varies too much, this could be interpreted as a heating failure, triggering the printer to go into an error state for safety. The exception to this rule was the heated chamber, as monitoring the temperature range is not sufficient for thermal

protection. Normal thermal protection knows that if the heating element is on, the temperature should be rising. If the temperature falls or does not move, it assumes the thermistor is not working, meaning the heating element is at an unknown temperature, which is a fire hazard. This is sufficient for the hotend and bed thermal protection, but for the heated chamber, this logic does not work. If the heated chamber is at temperature and the printer door is opened, it would cause the temperature to plummet, triggering an error. Opening the door is not always safe, but it is not necessarily an error, especially at the beginning of a print. Instead, chamber thermal protection was disabled in the SKR's firmware, and the SKR passes the power signal to a raspberry pi. The raspberry pi handles turning on and off the heated chamber and the thermal protection logic. The chamber thermal protection logic just uses temperature maximum and minimum values instead of relative temperature comparisons.

For the raspberry pi connections, the raspberry pi communicates over UART with the SKR2 sending commands and exchanging status information. Additionally, the raspberry pi drives a camera inside the heated chamber so the print can be monitored when the chamber is closed.

The buck converter schematic drives both the X and E Peltier plates at 5V, the space heater fans that run at 12V, and 5V LEDs that are inside the chamber so the camera has light to see the print. Without this, the inside of the chamber is dark.

For the thermal protection of the wires, nearly all wires inside the chamber were replaced with high-temperature silicone wire. All wires were wrapped in strips of thin ceramic fiber insulation blanket, wrapped in aluminum foil and then aluminum tape, protecting the few wires that could not be replaced with silicone wire.

3.1.8 Firmware

The difference between a good 3D printer and a great 3D printer comes down to the printer's firmware. Fine-tuning the firmware configuration leads to prints having fewer defects, faster speeds, and an overall better printing experience. The firmware chosen for the 3DPP was Marlin, an open-source firmware designed for FDM printers [28]. The Marlin simplifies the process of getting a printer up and running by tiering the configuration parameters. It has a regular configuration file, which uses preprocessor macros to select the main configuration options, and a second, advanced configuration file that does the same thing, but for more niche options. If neither of the preprocessor macro configuration options solves an issue, the raw C code can be modified since the project is open source. Below will go through most of the important options chosen for the 3DPP.

```
#define BAUDRATE 250000
```

The baud rate determines how quickly the SKR receives print commands. Selecting the highest baud rate allows for faster data transfer making sure the G-CODE transfer mechanism is not the bottleneck.

```
#define DEFAULT_NOMINAL_FILAMENT_DIA 1.75
```

Set the filament diameter expected for the printer.

```
#define TEMP_SENSOR_0 1047
```

Use the lookup table for a PT1000 with a 4.7k pullup resistor. This is the thermistor for the hotend.

```
#define TEMP_SENSOR_BED 5
```

Bed thermistor setting. Use the lookup table for a 100k thermistor with a 4.7k pullup resistor, specifically a Semitec 104GT

```
#define TEMP_SENSOR_CHAMBER 1
```

Chamber thermistor setting. Use the lookup table for a generic 100k thermistor with a 4.7k pullup resistor.

```
#define TEMP_RESIDENCY_TIME 10
```

Time in seconds to wait for hotend temperature to "settle" instead of start printing as soon as the actual temperature reaches the set temperature. This helps avoid printing if there is a temperature overshoot, resulting in a too high first layer temperature.

```
#define TEMP_WINDOW 1
```

Temperature (°C) proximity for the "temperature reached" timer for the hotend

```
#define TEMP_HYSTESIS 4
```

Temperature (°C) proximity considered "close enough" to the target temperature for the hotend

```
#define TEMP_BED_RESIDENCY_TIME 10
```

Time in seconds to wait for bed temperature to "settle", similar to the hotend.

```
#define TEMP_BED_WINDOW 1
```

Temperature (°C) proximity for the "temperature reached" timer for the bed

```
#define TEMP_BED_HYSTESIS 3
```

Temperature (°C) proximity considered "close enough" to the target temperature for the bed

```
#define TEMP_CHAMBER_RESIDENCY_TIME 60
```

Time in seconds to wait for the chamber temperature to "settle"

```
#define TEMP_CHAMBER_WINDOW 5
```

Temperature (°C) proximity for the "temperature reached" timer for the chamber

```
#define TEMP_CHAMBER_HYSTESIS 5
```

Temperature (°C) proximity considered "close enough" to the target temperature of the chamber.

```
#define HEATER_0_MINTEMP 5
```

```
#define BED_MINTEMP 5
```

```
#define CHAMBER_MINTEMP 5
```

The mintemp settings set the minimum sensical temperature. Any temperature below this probably indicates a broken thermistor wire, which will send the printer into an error state. (All temperature values from here on are in Celsius).

```
#define HEATER_0_MAXTEMP 450
```

```
#define BED_MAXTEMP 200
```

```
#define CHAMBER_MAXTEMP 90
```

Any reported temperature above the maxtemp values will cause the printer to enter an error state and shut down since the set values are the maximum values each element is rated for.

```
#define HOTEND_OVERSHOOT 15
```

(°C) Forbid setting temperatures over MAXTEMP - OVERSHOOT for the hotend

```
#define BED_OVERSHOOT 10
```

(°C) Forbid setting temperatures over MAXTEMP - OVERSHOOT for the bed

```
#define CHAMBER_OVERSHOOT 10
```

(°C) Forbid setting temperatures MAXTEMP - OVERSHOOT for the chamber

When heating up, even with very good PID tuning, a small temperature overshoot is likely to occur. Setting the target temperature too close to the maximum temperature almost guarantees a maximum temperature error and printer shutdown. The overshoot adds a margin of safety so the actual temperature can slightly overshoot the set temperature and not shut down.

```
#define DEFAULT_Kp 27.55
```

```
#define DEFAULT_Ki 2.90
```

```
#define DEFAULT_Kd 65.40  
  
#define DEFAULT_bedKp 16.52  
  
#define DEFAULT_bedKi 1.30  
  
#define DEFAULT_bedKd 140.31
```

These set the beginning values for the hotend and bed PID tuning. PID tuning is run over multiple iterations and these numbers change a lot as bed or nozzle conditions change. For example, a change in the printing surface on the bed or a heat-retaining silicone sock being added would change the PID values after re-tuning. These are just values that were hardcoded in the firmware after initial PID tuning to have relatively accurate PID values until more precision tuning can be done. The chamber uses a system called bang-bang, an alternative to PID tuning. It is useful when trying to limit how many times something is turned on and off. Bang-bang was easier to code the raspberry pi to accept as a signal, since the raspberry pi is controlling the space heater's power.

```
#define PREVENT_COLD_EXTRUSION  
  
#define EXTRUDE_MINTEMP 170
```

Stops the extruder from driving if the filament is below 170°C, where it is still solid. This will stop the filament from grinding if an extrude command is accidentally issued before the hotend is up to temperature.

```
#define PREVENT_LENGTHY_EXTRUDE
```

```
#define EXTRUDE_MAXLENGTH 200
```

Sets the max length a single extrude command can be. It is useful if the operator sends a command to extrude 100mm of filament but accidentally fat-fingers to extruder 1000mm of filament instead.

```
#define USE_XMIN_PLUG
```

```
#define USE_YMIN_PLUG
```

```
#define USE_ZMIN_PLUG
```

Tells the SKR 2 which pins have the X, Y, and Z limit switches connected, and that they are minimum switches, meaning the stop is the minimum coordinate (0) instead of the maximum coordinate for each axis.

```
#define X_DRIVER_TYPE TMC2209
```

```
#define Y_DRIVER_TYPE TMC2209
```

```
#define Z_DRIVER_TYPE TMC2209
```

```
#define Z2_DRIVER_TYPE TMC2209
```

```
#define E0_DRIVER_TYPE TMC2209
```

Tells the SKR which stepper motor drivers are being used, so it can properly communicate with them.

```
#define ENDSTOP_NOISE_THRESHOLD 4
```

Added maximum debouncing to the limit switches so they are not falsely triggered by an interference or voltage drop.

```
#define DETECT_BROKEN_ENDSTOP
```

Puts the print in an error state if an end stop is constantly reporting it is triggered.

These next settings are the most important for getting quality prints, as they control the movement settings. The steps per unit control how many stepper motor steps translate to a millimeter of movement on the printer. This is a function of the belts and movement systems used. For the GT2 belts the X and Y axes use with 6mm shaft pulleys, 80 steps/mm is close to the actual value. The lead screw is 1600 steps/mm and for the micro swiss extruder, it is 140 steps/mm. The firmware values get the printer relatively close to accurate movement. These values are fine-tuned by printing test objects, seeing how dimensionally accurate they are, then modifying the values appropriately, until 1 mm in software equals exactly 1 mm of actual movement.

```
#define DEFAULT_AXIS_STEPS_PER_UNIT { 80, 80, 1600, 140 }
```

Sets the steps per unit for the X, Y, Z, and E directions, respectively

```
#define DEFAULT_MAX_ACCELERATION { 500, 500, 100, 5000 }
```

The faster the acceleration, the more quickly the printer can print, but the more likely artifacts show up the printer from factors like inertia. The Z-axis movement is relatively slow to minimize screw deflection.

The next macros define the intricacies of the Z-homing mechanism, the BLTouch. While it may seem like a lot of information for such a trivial mechanism, the accuracy of the BLTouch determines the distance the nozzle is from the bed. Perfectly laying the first layer in a print often means the difference between a quality print, if the nozzle is too close, a print whose bottom flares out due to the overly squished first layer of plastic, or if the nozzle is too far, a print that fails halfway due to poor bed adhesion. The BLTouch accuracy comes down to ± 0.01 mm of precision. Additionally, the BLTouch is used to create a virtual mapping of the levelness of the bed, so getting it accurate is important.

```
#define Z_MIN_PROBE_USES_Z_MIN_ENDSTOP_PIN  
  
#define USE_PROBE_FOR_Z_HOMING  
  
#define BLTOUCH
```

These commands tell the firmware to use the BLTouch and which physical pins on the SKR 2 the BLTouch is connected to.

```
#define NOZZLE_TO_PROBE_OFFSET { -48, -10, 0 }
```

This offset is how far in the X, Y, and Z directions the BLTouch is from the nozzle. The important metric is how far the nozzle is from the bed, but since the BLTouch can not be in the exact same place as the nozzle, a mapping is created of the offset the BLTouch is from the nozzle so it can be compensated for in software. For the extruder mount used in the 3DPP, the BLTouch is slightly in front of the nozzle, and fairly to the left, resulting in the number used in the NOZZLE_TO_PROBE_OFFSET. The Z-axis offset is set to 0 and changed before a print since it

is constantly changed slightly depending on the filament used and the surface being printed on to maximize or minimize the first layer squish.

```
#define PROBING_MARGIN 15
```

Defines how far to keep the BLTouch away from the edge of the bed. This is useful if there are fasteners or something else the X-carriage can catch on when probing.

```
#define XY_PROBE_FEEDRATE (133*60)
```

```
#define Z_PROBE_FEEDRATE_FAST (2*60)
```

```
#define Z_PROBE_FEEDRATE_SLOW (Z_PROBE_FEEDRATE_FAST / 1.5)
```

```
#define MULTIPLE_PROBING 2
```

Set the BLTouch probe speed and make each BLTouch probe be verified with a second, slower probe.

```
#define Z_CLEARANCE_DEPLOY_PROBE 10
```

```
#define Z_CLEARANCE_BETWEEN_PROBES 5
```

```
#define Z_CLEARANCE_MULTI_PROBE 5
```

```
#define Z_AFTER_PROBING 5
```

```
#define Z_PROBE_LOW_POINT -3
```

```
#define Z_PROBE_OFFSET_RANGE_MIN -20
```

```
#define Z_PROBE_OFFSET_RANGE_MAX 20
```

These are various parameters of important clearances the printer follows when probing as to not run the probe into anything. Since before the Z-axis is homed, the printer does not know where it is in space, so these are relative limits from where the printer starts to not surpass or it might damage a component.

```
#define AUTO_BED_LEVELING_BILINEAR
```

```
#define GRID_MAX_POINTS_X 5
```

To make a mapping of the unlevelness of the bed, the BLTouch probes points in a GRID_MAX_POINTS by GRID_MAX_POINTS array. Bilinear bed leveling makes a mesh of these points and compensates for the unlevelness in software.

```
#define VALIDATE_HOMING_ENDSTOPS
```

Each time a limit switch is hit, move away and hit it again to verify functionality.

```
#define X_BED_SIZE 300
```

```
#define Y_BED_SIZE 280
```

```
#define X_MIN_POS 0
```

```
#define Y_MIN_POS 0
```

```
#define Z_MIN_POS 0
```

```
#define X_MAX_POS X_BED_SIZE
```

```
#define Y_MAX_POS Y_BED_SIZE
```

```
#define Z_MAX_POS 1330
```

These define the total build volume size.

```
#define PREHEAT_1_LABEL "PLA"
```

```
#define PREHEAT_1_TEMP_HOTEND 180
```

```
#define PREHEAT_1_TEMP_BED 70
```

```
#define PREHEAT_1_TEMP_CHAMBER 35
```

```
#define PREHEAT_1_FAN_SPEED 0
```

```
#define PREHEAT_2_LABEL "PC"
```

```
#define PREHEAT_2_TEMP_HOTEND 260
```

```
#define PREHEAT_2_TEMP_BED 100
```

```
#define PREHEAT_2_TEMP_CHAMBER 35
```

```
#define PREHEAT_2_FAN_SPEED 0
```

Two pre-heating profiles were added to the printer's firmware. They are simply for convenience.

```
#define NUM_Z_STEPPER_DRIVERS 2
```

Enables using a stepper motor driver for each Z-axis instead of a single driver for both.

```
#define MICROSTEP_MODES { 16, 16, 16, 16, 16, 16 }
```

Defines the number of microsteps the stepper motors used, which was used in the kinematic calculations.

The Marlin code was compiled and uploaded to the SKR 2's EEPROM. From there, a few calibration changes were still made. First, the steps/mm were fine-tuned. The X, Y, and Z steps were perfect, but the Extruder steps needed to be lowered from 140 steps/mm to 138 steps/mm. The maximum Z acceleration could be raised from 100 mm/s² to 300 mm/s² without noticeable print artifacts.

The stepper motor driver current was set to 800 mA for the X and Y axes, and 1450 mA for both Z axes. TMC2209 stepper motor drivers support 2 driving modes: stealthChop and spreadCycle. StealthChop is a quieter mode of operation. It uses PWM to vary the voltage. spreadCycle uses cycle-by-cycle current control, which is more powerful, but louder [29]. Since a slight increase in noise was not a concern, but a slight increase in power was very beneficial, spreadCycle was enabled on all stepper motor drivers.

3.1.9 Software

The design requirements dictate a web interface to control and monitor prints. To do this, a powerful piece of software named OctoPrint was used. OctoPrint is an open-source web interface for a 3D printer, offering full remote control and monitoring of the connected 3D printer as well as supporting a plethora of community-made plugins [30]. It was set up with a secure login for the project's sponsor. Octoprint allows print jobs to be sent wirelessly to the printer instead of having to use an SD card to upload the GCode. Through a web-based GUI, it can monitor the

print in real-time through a camera, issue movement commands, turn on and off fans, and set and monitor temperatures. It also allows the user to view the current GCode being executed during a print, compile print time-lapses, and communicate with the SKR 2 through UART. On top of all this functionality, community add-ons added to the 3DPP's OctoPrint installation are PrintTimeGenius, which uses multiple more accurate metrics to give precise time a print will take to complete, instead of the general estimate native to OctoPrint [31], and BetterHeaterTimeout, which shuts off the heaters on the printer after they have been on and idle for so long in case the user forgets to turn them off if they were turned on manually [32].

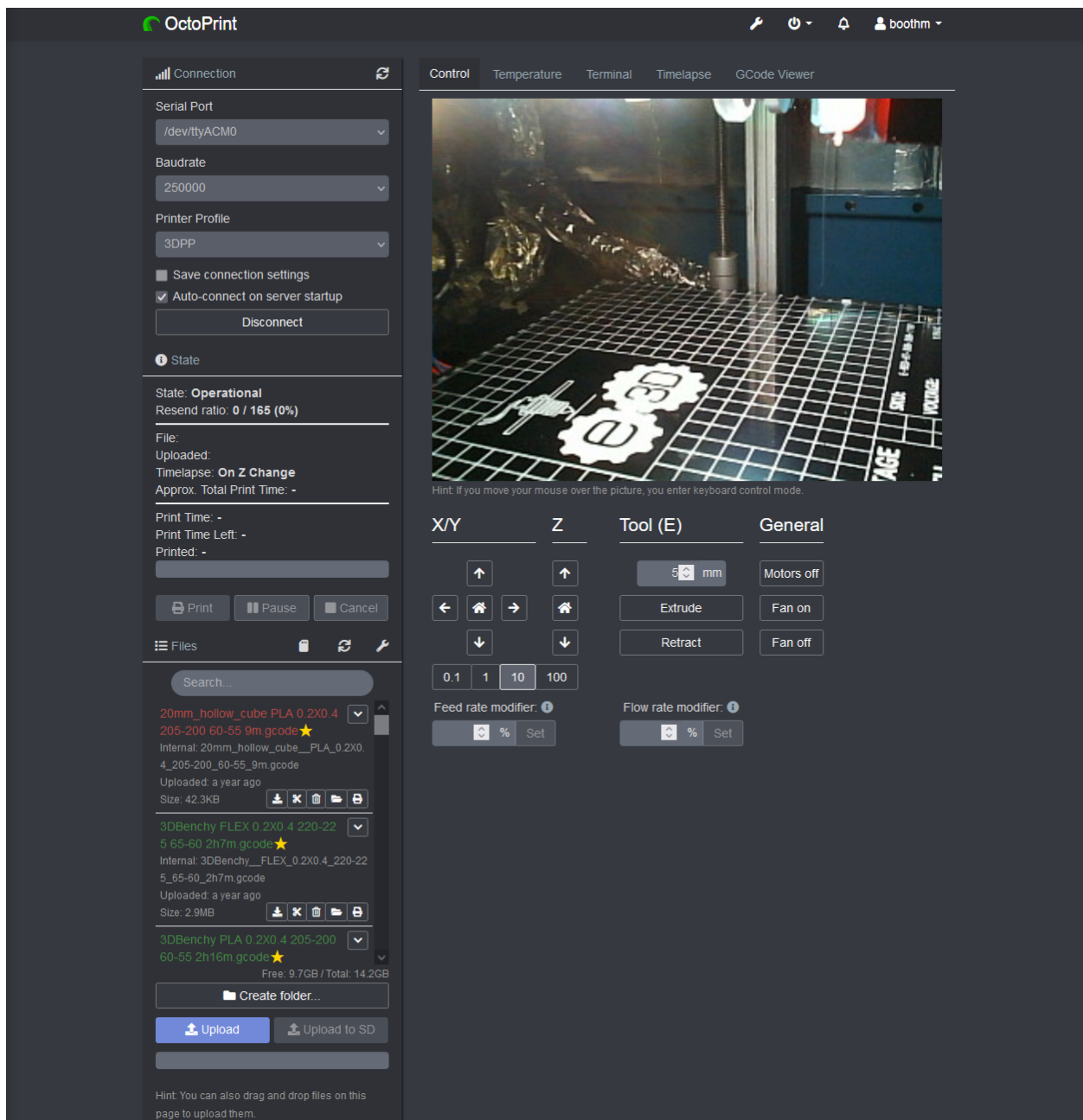


Figure 48. OctoPrint Landing Page

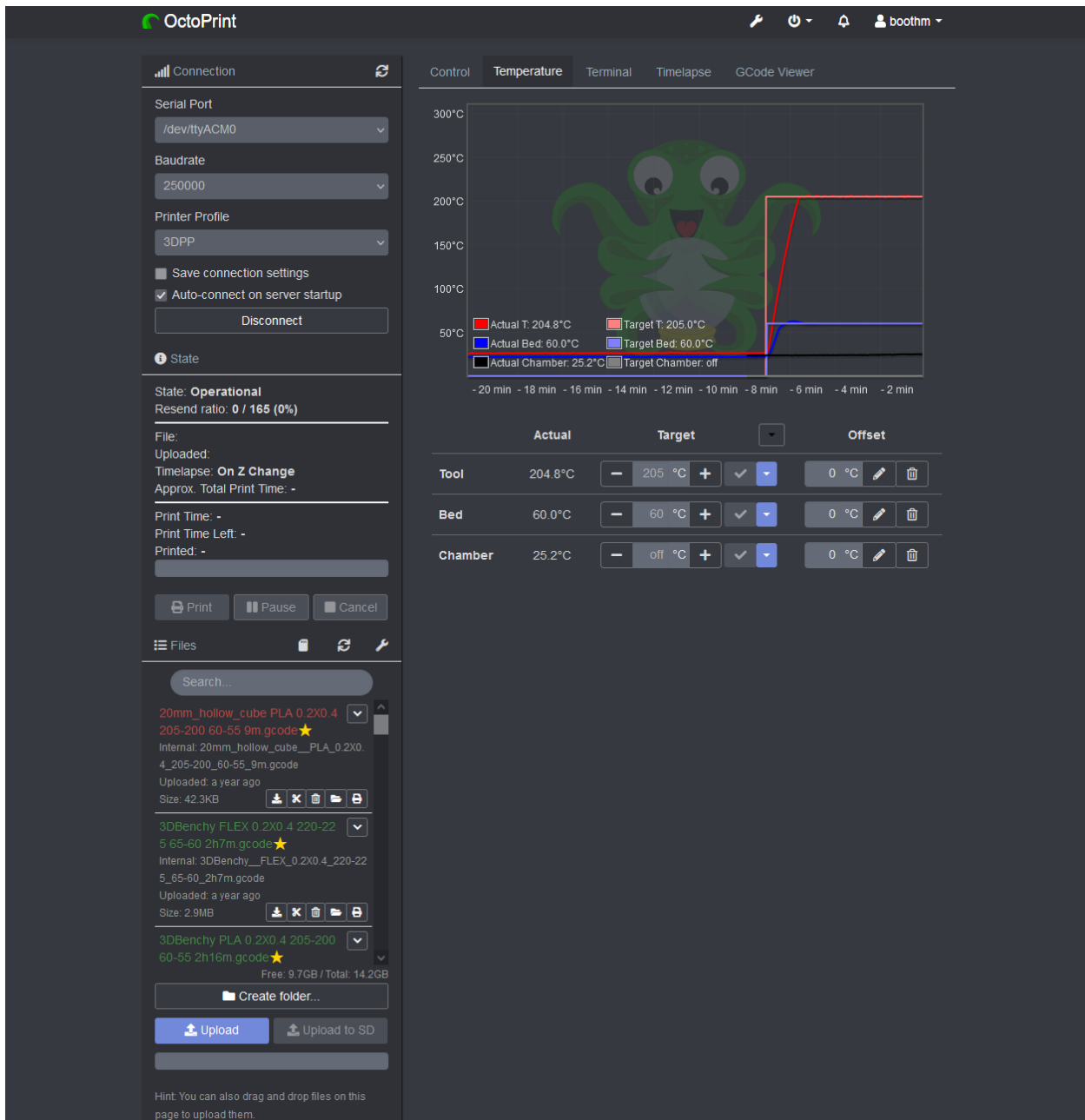


Figure 49. OctoPrint Temperature Control Page

3.1.10 Electronics Case

To house the electronics, a case was built around them, which were mounted on the top of the printer. The case was constructed out of sheet metal and was used to mount fans, the LCD, and

the safety shut-off switches. Inside the case, a base plate was 3D printed out of PLA that all the electronics were mounted to for organizational purposes. Threaded inserts were pressed into the PLA plate, then M3 screws mounted the various boards to the plate. The plate itself is mounted to a piece of wood on the top of the printer to not penetrate into the heated chamber, and mounted to the case's metal walls, giving plenty of structural rigidity. The power supply also mounted to the PLA plate. A lid was attached with magnets to the top of the case which can easily be removed to work on the electronics, if needed. A handle was added to the top, to aid in the removal of the lid while not adding much to the height of the printer.

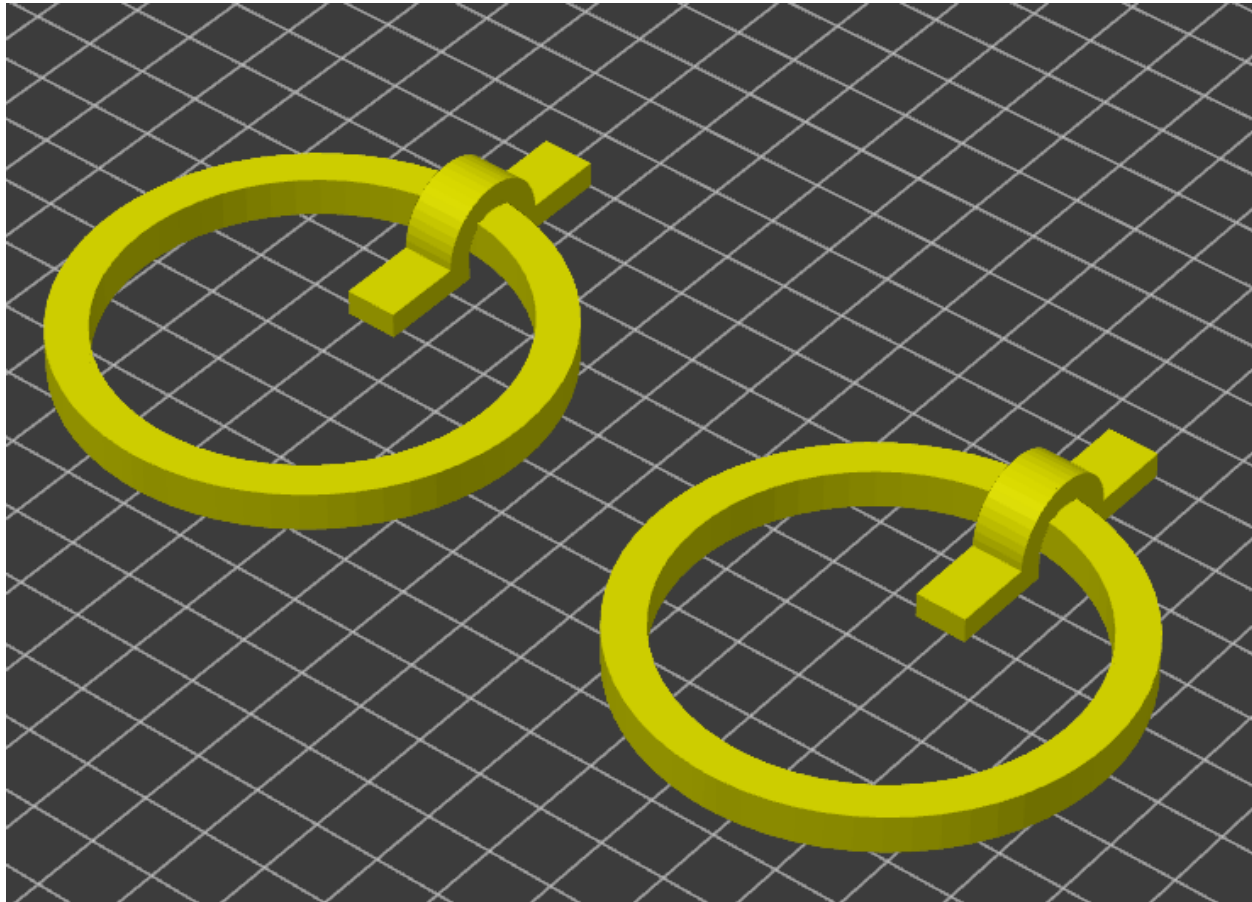


Figure 50. Case Lid Handle Design

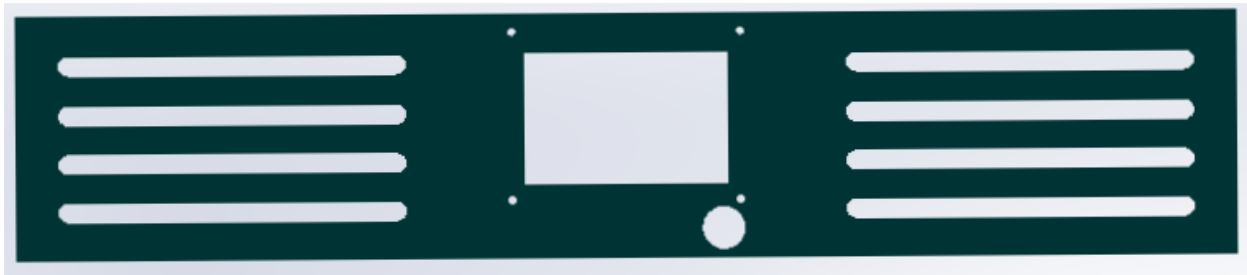


Figure 51. Case Front Sheet Metal Design

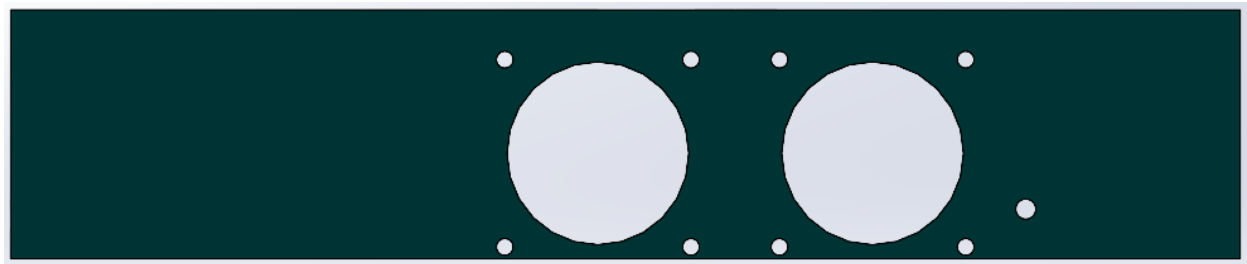


Figure 52. Case Back Sheet Metal Design

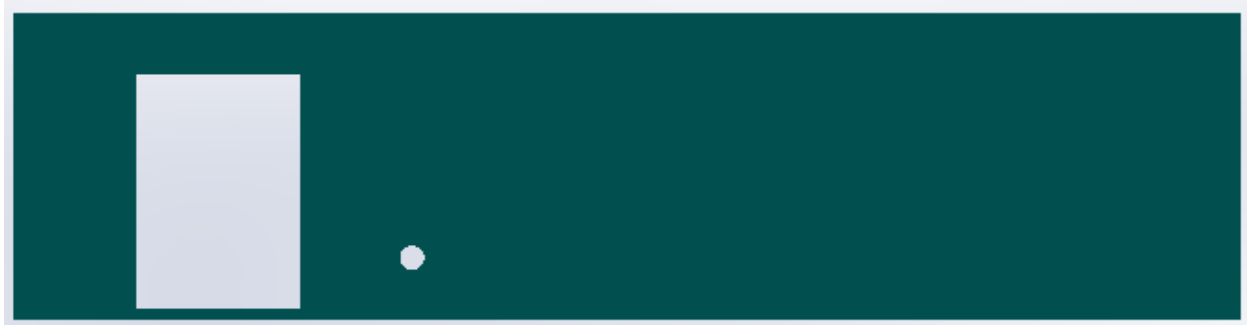


Figure 53. Case Left Sheet Metal Design

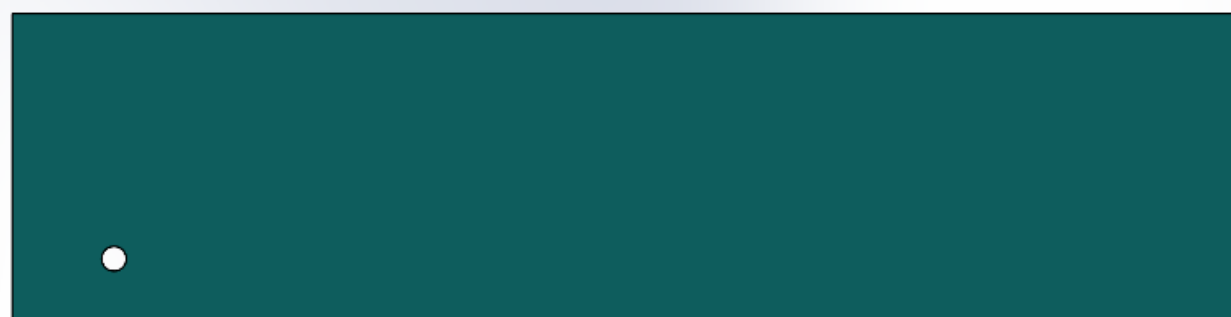


Figure 54. Case Right Sheet Metal Design

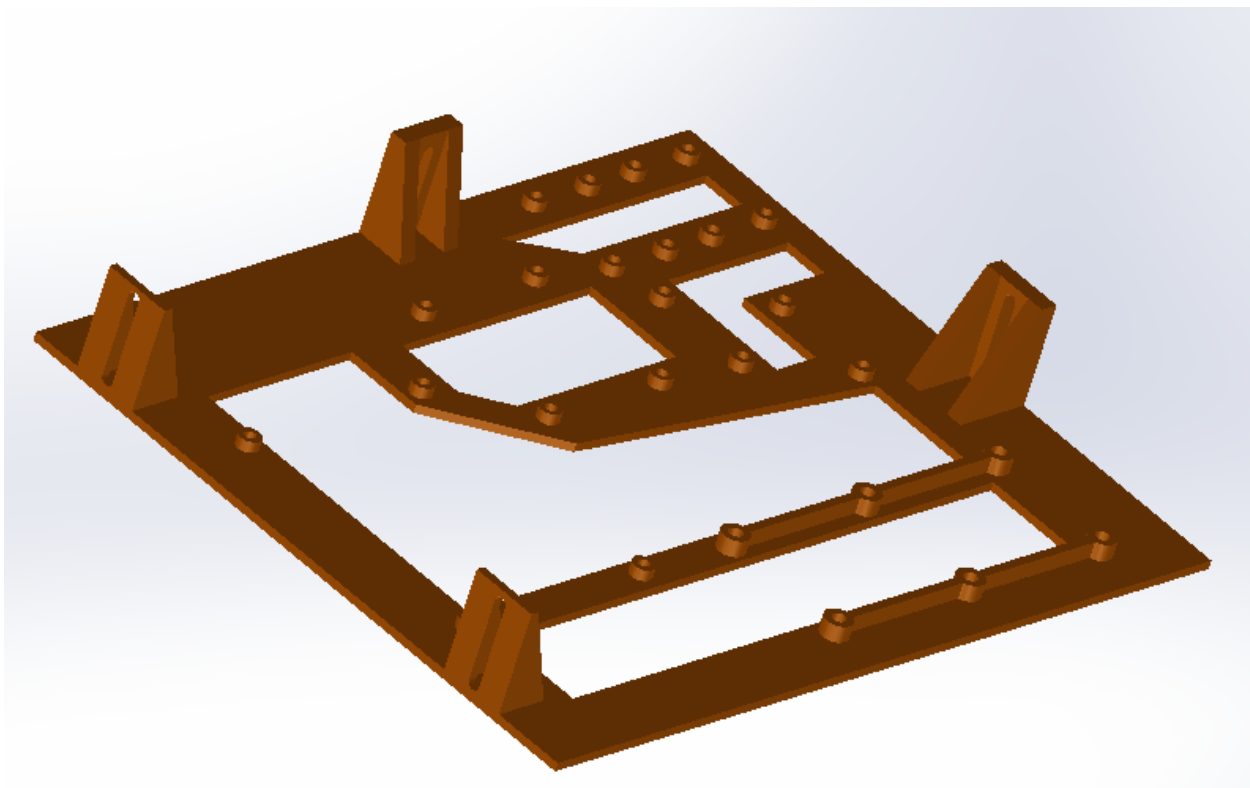


Figure 55. PLA Mounting Plate

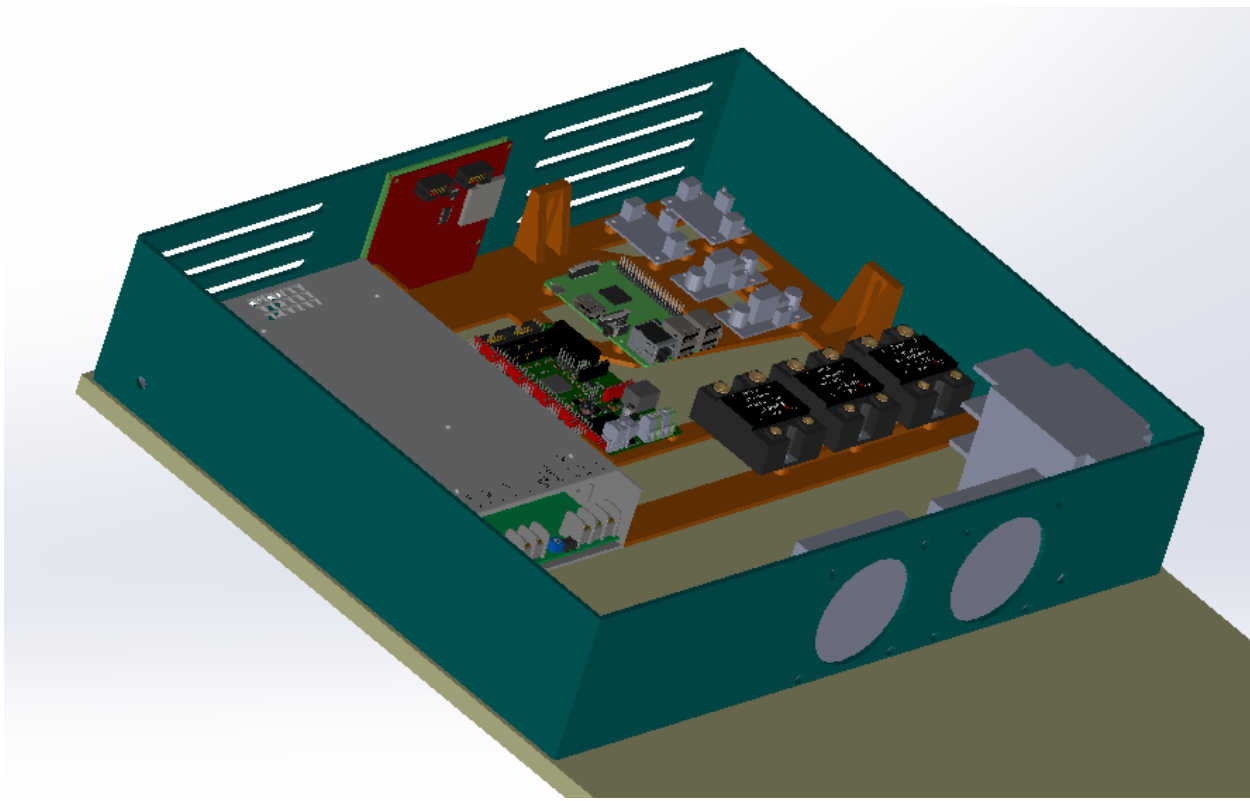


Figure 56. Case CAD Model

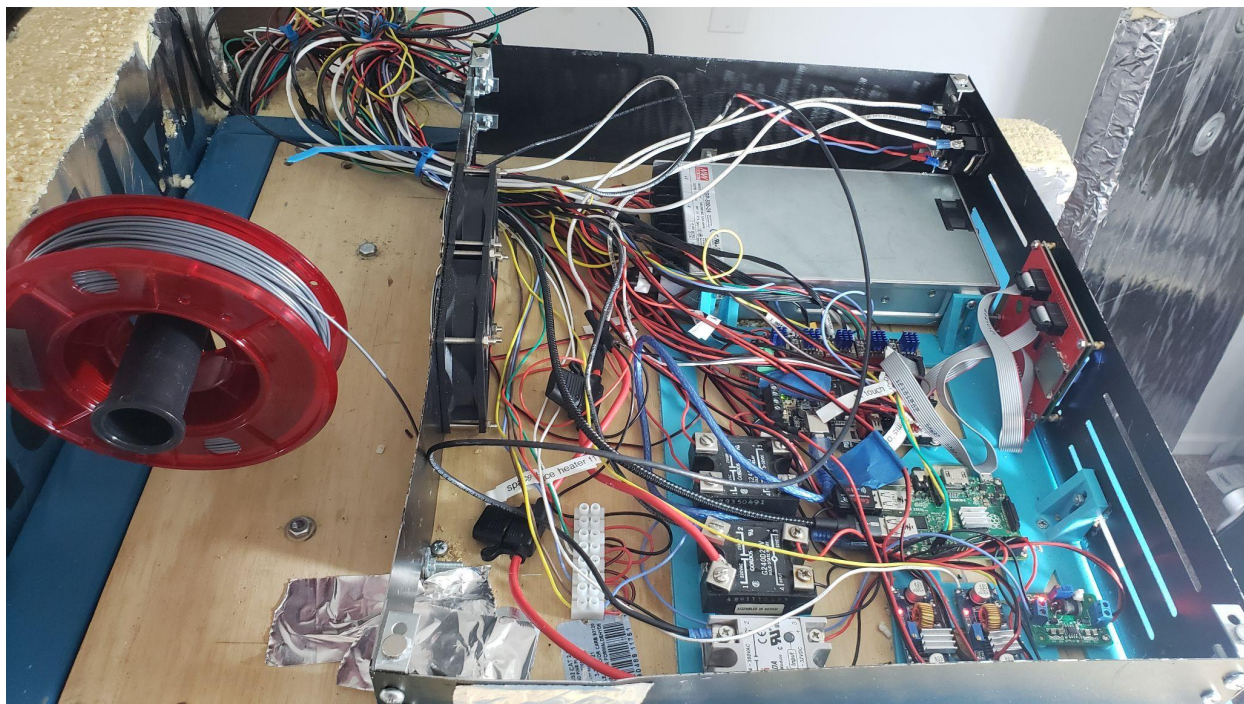


Figure 57. Finished Case Assembly Without Lid

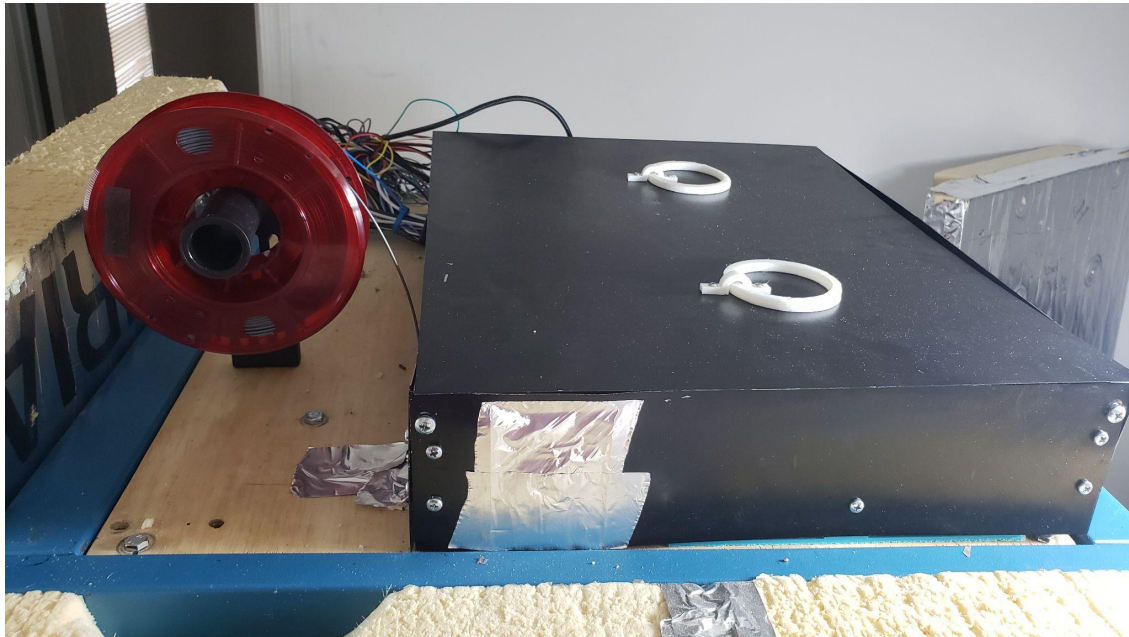


Figure 58. Finished Case Assembly With Lid

3.1.11 CAD Model

When building the 3DPP, many parts needed CADed to be 3D printed. The CAD model was also very helpful to visualize various systems in the 3DPP, test fitting parts before they arrived (or were 3D printed) given their dimensions, and run simulations. Many of the parts in the CAD assembly were drawn up manually, but some were pulled from already created models online to save time. Below is a list of parts in the final assembly pulled from an online source with the appropriate attributions:

- X-gantry base [33]
- X-carriage base [34]
- Meanwell Power Supply [35]
- Solid State Relay [36]
- LCD [37]
- Raspberry Pi [38]
- SKR 2 [39]
- Petsfang Models (hotend mount and K-fan duct) [23]
- Z-axis stepper motor to lead screw coupling nut [40]
- Safety Switches [41]
- 2A NEMA 17 Stepper Motors [42]
- Filament Spool [43]
- BLTouch [44]
- Extruder NEMA 17 Stepper Motor [43]
- IEC Power Socket [44]
- AC Power Socket [45]

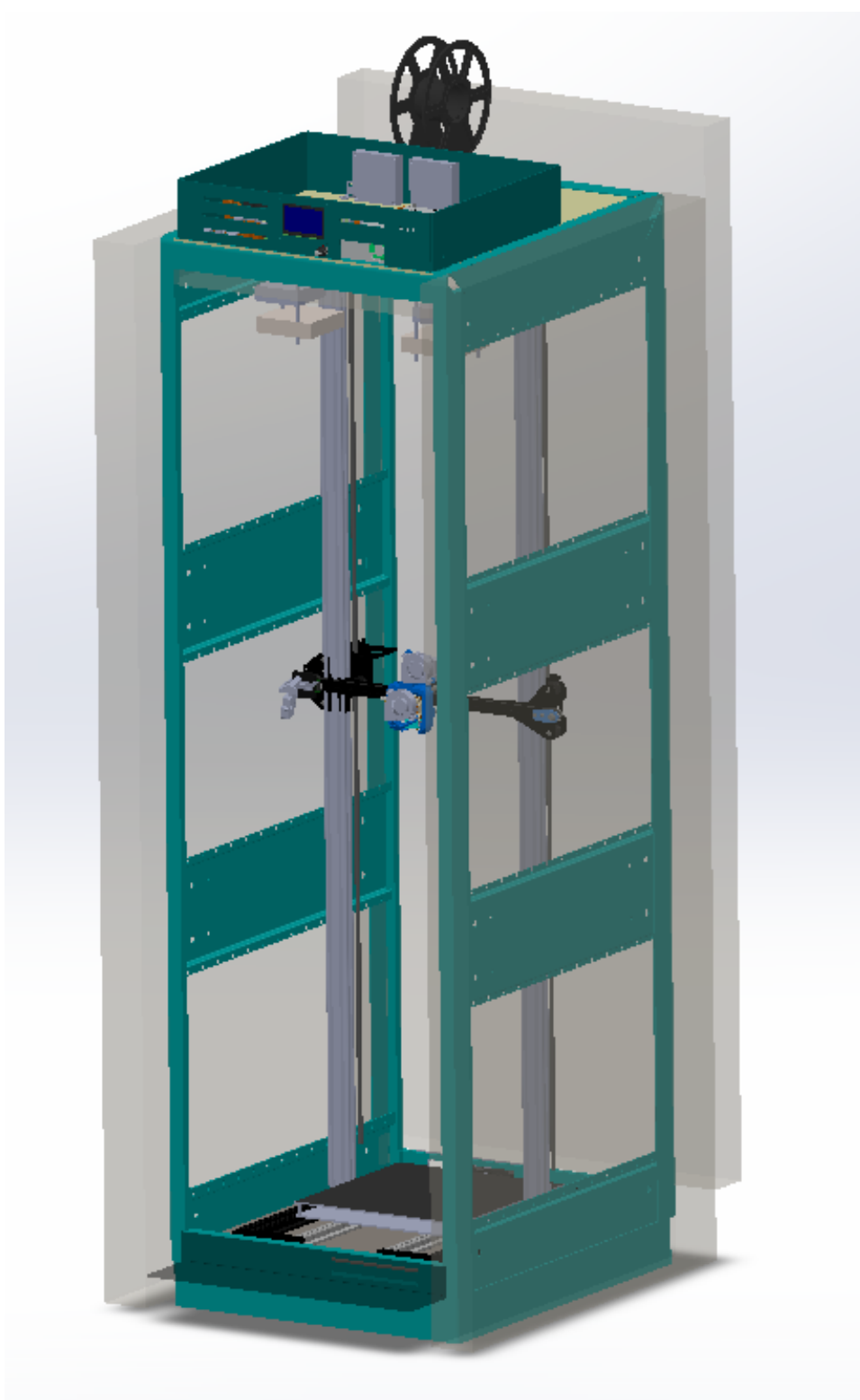


Figure 59. 3DPP CAD Model Front

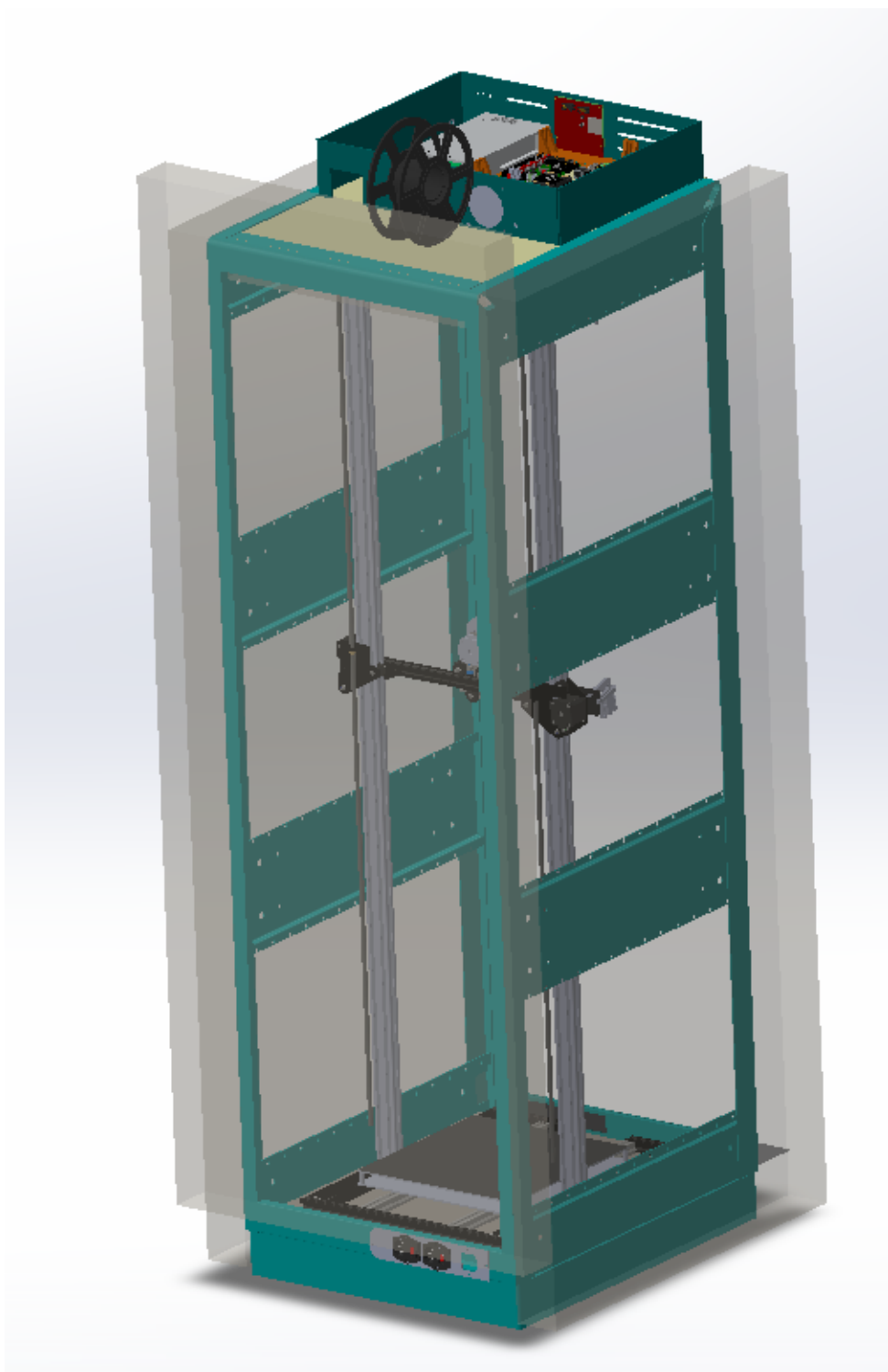


Figure 60. 3DPP CAD Model Back



Figure 61. 3DPP Front Without Door



Figure 62. 3DPP Front With Door



Figure 63. 3DPP Back



Figure 64. 3DPP Inside Bottom



Figure 65. 3DPP Inside Top

3.2 Design Alternatives

3.2.1 Belt/Counterweight Z-Axis Movement System

The first iteration of the Z-axis was a belt and pulley system, like those used on the X and Y axes. Since the Z-axis also had to counteract the force of gravity, a counterweight system was introduced so there would be a total of net zero force on the Z-motor at standstill. This would reduce the force the Z-motor needs to move the X-gantry up and down. Also, in the event of a power loss, the X-gantry would not enter free-fall; it would stay suspended since there is a net-zero force on the X-gantry. Unlike lead screws, a vertical belt and pulley system is not self-locking, so the counterweight stopped the X-gantry from crashing into the bed, damaging any components. As shown in section 3.1.4, Z-Axis Movement,

$$\Sigma M_L = 0 = F_{center}(l/2) + F_{right}(l) - F_{right\ support}(l)$$

$$F_{right\ support} = [8.201(0.416/2) + 2.099(0.416)] = 2.579/0.416 = 6.200N$$

$$\Sigma F_z = 0 = F_{left\ support} - F_{left} - F_{center} - F_{right} + F_{right\ support}$$

$$F_{left\ Support} = 6.151 + 8.201 + 2.099 - 6.200 = 10.251N$$

To suspend the X-gantry in air, there needed to be 10.251 N of force on the left side of the gantry, and 6.2 N of force on the right side. Due to the constraints of the chamber frame, a pulley design which wraps through the counterweight and connects again at the top, making the counterweight move through only half of the total height of the build volume was used. Otherwise, the counterweight would run into the top or bottom of the frame when the X-gantry is at the opposite extreme. The trade-off of this pulley system is the counterweight has to be twice

as heavy to counter the force of gravity. The following calculation will show the amount of weight that should be added to each counterweight to counteract the force of gravity.

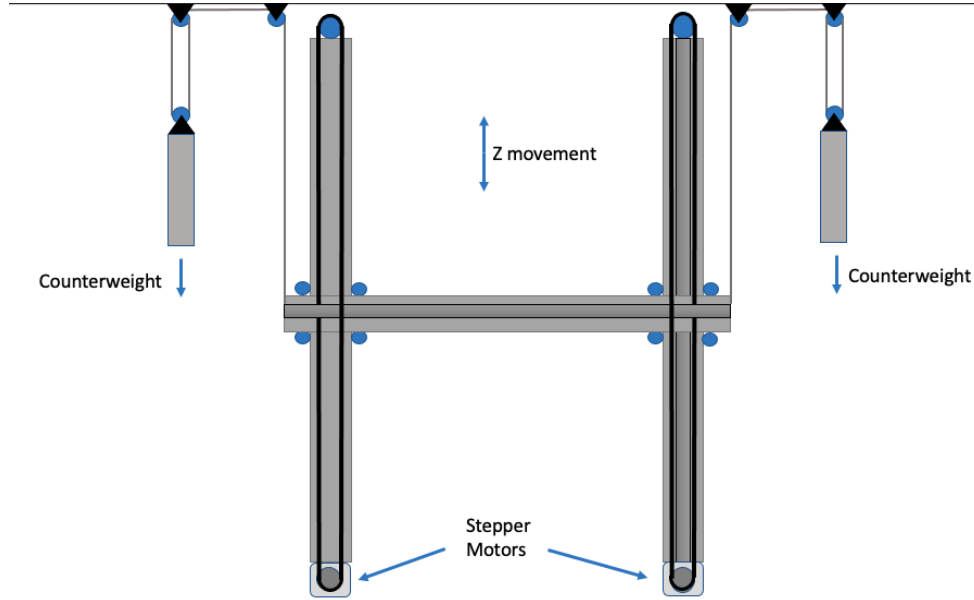


Figure 66. Counterweight System Design Concept

$$F_{left\ support} = \frac{F_{left\ counterweight}}{2} = \frac{m_{left\ counterweight}(g)}{2}$$

$$m_{left\ counterweight} = \frac{F_{left\ support}(2)}{g} = \frac{(10.251)(2)}{9.81} = 2.090\ kg$$

$$F_{right\ support} = \frac{F_{right\ counterweight}}{2} = \frac{m_{right\ counterweight}(g)}{2}$$

$$m_{right\ counterweight} = \frac{F_{right\ support}(2)}{g} = \frac{(6.200)(2)}{9.81} = 1.264\ kg$$

A dual stepper motor configuration was also used for this design so there would be more power available to move the X-gantry since the large weight of the system had a lot of inertia.

Construction of the system mainly failed due to poor group cohesion. Members of the group struggled to complete the necessary tasks, leading the counterweight system to not be constructed until four weeks past its scheduled finish. By the time the finished system was built, it worked, but very unreliably. The X-gantry was able to be suspended, but the motors were not able to move the X-gantry up and down consistently, even with 2A of driving current for each stepper motor. In most moves, the Z-axis stepper motors skipped steps, which would never be able to complete a successful print. Due to the delayed build time, corners were cut during the construction of the counterweight system, which ultimately led to its abandonment. There were so many moving parts in the counterweight system that it was replaced with the lead screw design, which had much fewer moving parts and ended up working successfully.

3.2.2 Top-Mounted Z-Axis Stepper Motors

Even when constructing the Z-axis lead screw system, multiple design iterations occurred. Originally, the stepper motors were to be mounted at the top of the chamber frame. This allowed them to be closer to the electronics, shortening their cable runs significantly. Also, it kept them out of the heated enclosure. Finding a way to mount the motors to the top proved difficult. The motor mount needed to have a small footprint, so a large hole wouldn't need to be drilled into the top of the enclosure. Minimizing the number and size of holes in the top of the heated chamber was important since the heat would try to escape primarily out of the top. To get the stepper motor perfectly square, attaching the motor mount to the vertical aluminum extrusions seemed to be the best solution. However, no matter how bulky the motor mount was, the Z-motor shaft

would not stay perfectly concentric to the lead screw, causing intermittent binding. Since the stepper motors could only be supported on one side due to their positioning, they would move around because the mount flexed while moving the lead screw. A spider coupler was installed to compensate for the mismatched rotational axes, but since gravity was pulling the lead screw down, the spider coupler fell apart. This led to the Z-axis stepper motors being moved to the bottom of the enclosure, which ended up working since the motors could be squared up with both the vertical aluminum extrusion and the nearby horizontal aluminum extrusions, supporting the stepper motors on both sides.

3.2.3 Heated Bed Belt Mount

Before a metal clamp was used to mount the belt to the Y-axis bed, a 3D printed design from Joakim on thiniverse.com titled “Anet A6/A8 Y Belt Holder Upgrade” was used [33]. In the design, the belt would wrap around itself, locking it in place. However, after operating the printer at maximum temperature, this part failed. There was no visible deformation from the print, but the belt slipped out during a print, disabling the Y-axis. Most likely, since the print is only supported on one side, the PC filament deformed slightly, allowing the belt to slip. This deformation was most likely caused by the bed’s 200°C temperature, and not the chamber’s 80°C. While the part would not have gotten close to 200°C, it is likely it got above 100°C due to its proximity to the heated bed. A quick, aluminum replacement part easily fixed this issue.

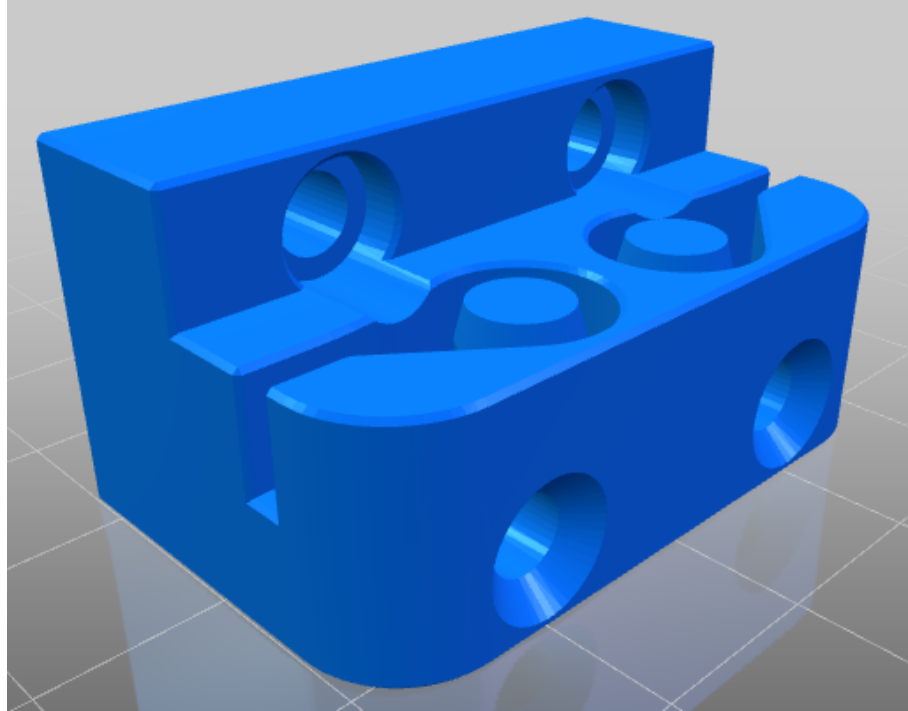


Figure 67. Y-Axis Belt Holder [33]

3.2.4 Alternative Power Cable Solution

Originally, regular 120V outlet sockets were used to take in AC power. This resulted in custom male-male cables needing to be made. This solution worked, but was not safe. If one end was plugged into the wall, the other end was a safety hazard since the exposed metal prongs were live. These were swapped out with male-female cables, causing the receptacles to be replaced with male ends as well.



Figure 68. Male-Male Power Cable

3.3 System Analysis and Optimization

3.3.1 Power Analysis

One of the design requirements was that the 3DPP was able to operate using 3 different 15A connections. That way, if it was used in a residential home, it would still be able to operate as long as the load was distributed between different breaker circuits. To make sure this requirement held true, a worst-case scenario power analysis was needed. This analysis took every component on each circuit and looked at the maximum power draw plus a liberal conversion inefficiency to calculate the total power draw of each circuit. In the United States, AC power operates between 110-120V [34]. For the worst-case scenario, 110V is assumed. On a 15A breaker, each circuit has $110V * 15W = 1650W$. For the 1500W space heaters, each has its own independent

circuit, meaning both can safely operate below the power requirement. The third AC circuit powers many different components. While it is unlikely they will all be operating at maximum power at the same time, they must be able to for the safety requirements.

Part	Voltage (V)	Amperage (A)	Wattage (W)
Peltier Plates x 2	5	1.5 [35]	7.5
Raspberry Pi	5	0.4 [36]	2
LED Strip	5	0.06 [37]	0.3
Space heater fans	12	0.66	7.92
Total wattage			17.72
Buck Converter Conversion efficiency:	80% [38]	Total wattage after efficiency conversion	21.264

Table 10. Power Draw for Components Powered by Buck Converters

Part	Voltage (V)	Amperage (A)	Wattage (W)
Z-axis stepper motor	24	2	48
Z2-axis stepper motor	24	2	48
X-axis stepper motor	24	0.8	19.2
Y-axis stepper motor	24	0.8	19.2
E-axis stepper motor	24	0.8	19.2
SKR 2	24	1	24
50W Heater Cartridge	24	2.083	50
Total wattage:			227.6

Table 11. Power Draw for Components Powered by an AC-DC Power Supply

All amperage values were set and controlled by hardware, except for the SKR 2 current draw, which was determined experimentally. The heated bed used AC power, drawing 10A, for 1100W [39]. Adding together the wattage from the buck converter-powered components and from other components listed in table 11, yields a wattage of 248.8W. Factoring in the AC-DC power supply efficiency of 92% [40], $248.864W + (248.864 * (1 - .92)) = 268.773W$. Adding this to the heated bed wattage yields 1368.773W for the last AC circuit, which is less than the 1650W requirement.

3.4 Simulation and/or Experimental Test

3.4.1 Fluid Velocity

One disadvantage of mounting the space heaters at the top of the build volume is fans are required at the top to force the hot air downward. This creates airflow in the chamber, which can disrupt a print if it is very tall and narrow. The print would act as a long lever arm, allowing the air to vibrate the print, or cause it to fail altogether. Gathering insight as to how this issue will affect prints will be helpful to the sponsor, in the event a tall narrow print is needed. Fluid flow simulations were performed to get an idea of where airflow will affect the print.

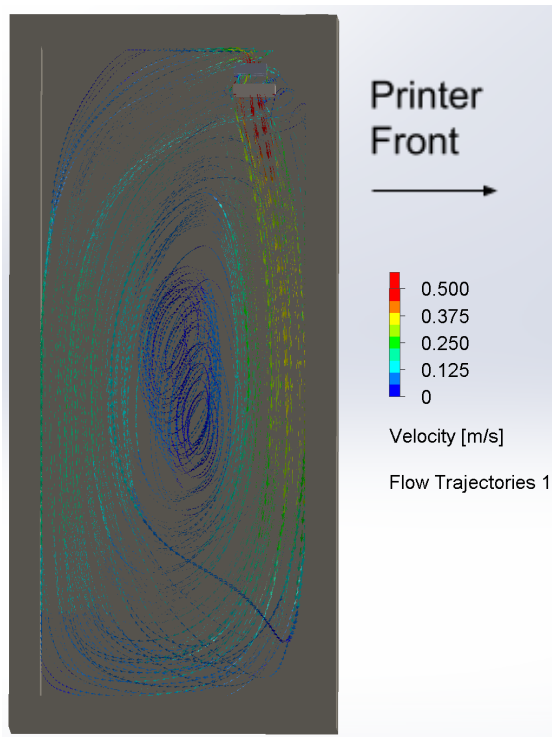


Figure 69. Air Velocity in the Heated Chamber

Figure 67 demonstrates the trajectory and velocity of the air in the chamber caused by the heating fans. The velocity of the air is the largest at the front of the printer. Large prints should be placed in the middle/back of the printing bed to reduce the effect that flowing air will have on the print quality.

3.4.2 Warm-Up Time Comparison

Thermal simulations can also help reveal other useful overlooked information. By creating a simplified version of the prototype including the fan, space heaters, and insulation, the time that it takes to heat the chamber to 80°C under ideal conditions can be studied. The results should give a rough estimate of the heating time, but the results are going to most likely be faster since the model has ideal run conditions, such as a perfectly sealed chamber. As shown in figure 68,

the simulation shows it should take approximately 7 minutes for the chamber to reach 80°C with 3-inch thick insulation.

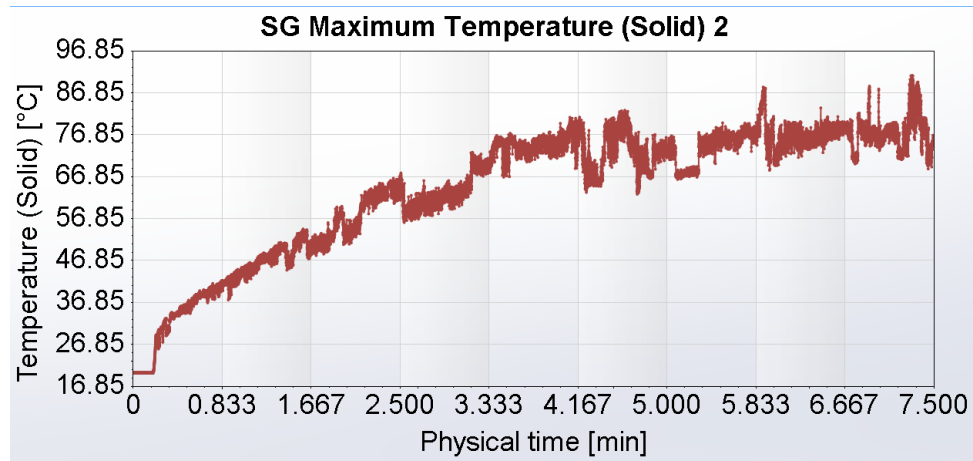


Figure 70. Average Fluid Temperature with 3-Inch Thick Insulation

3.4.3 *Surface Temperature Distribution*

While the average temperature of the fluid is important to simulate, it does not take into account that there are varying temperatures inside the chamber. Therefore, it is important to look at the temperature distribution in the chamber to ensure that the heat is being distributed properly. The chamber thermistor is on the X-gantry, which is near the floor at the start of a print when the printer is heating up. This simulation mimics that by setting the maximum temperature of the floor to 80°C. When this temperature is reached on the floor surface, the heat generation of the space heaters will turn off until the temperature decreases below 80°C, then turn on again. By simulating this heating system, the temperature distribution in the chamber can be analyzed.

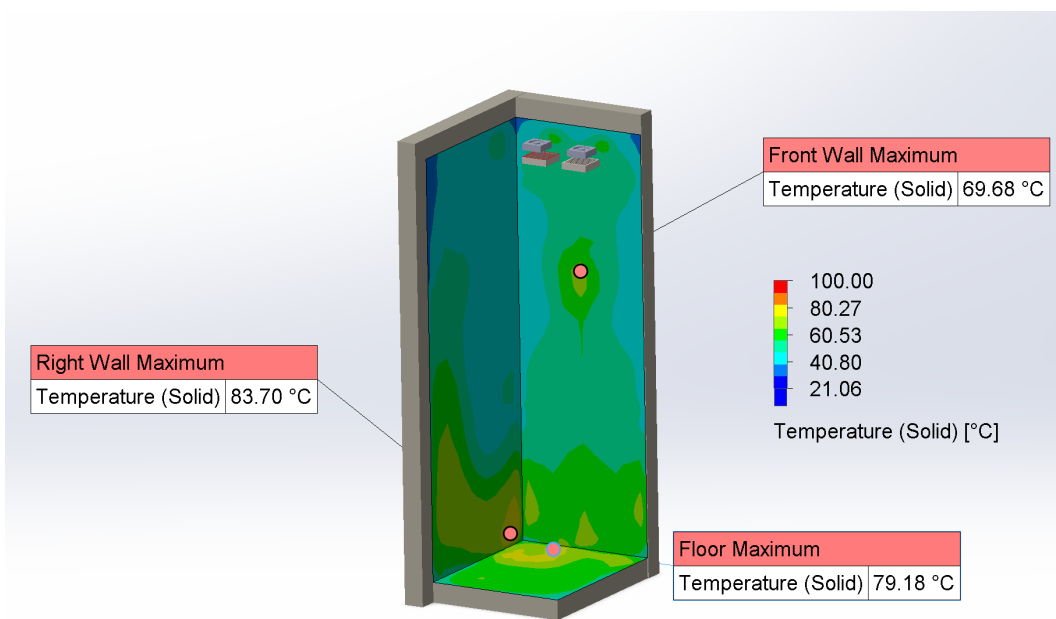


Figure 71. Floor, Right, and Front Wall Temperature Distribution

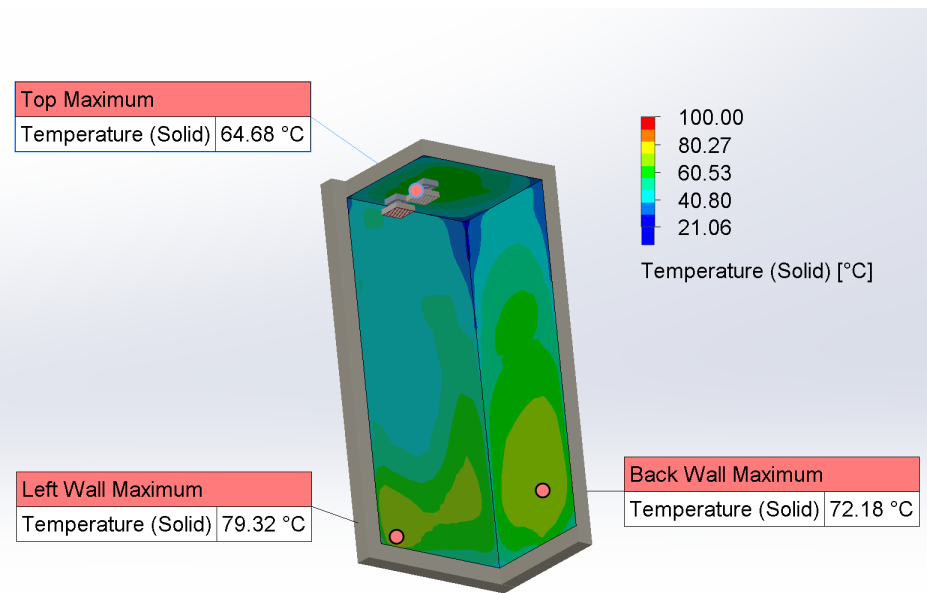


Figure 72. Top, Left, and Back Wall Temperature Distribution

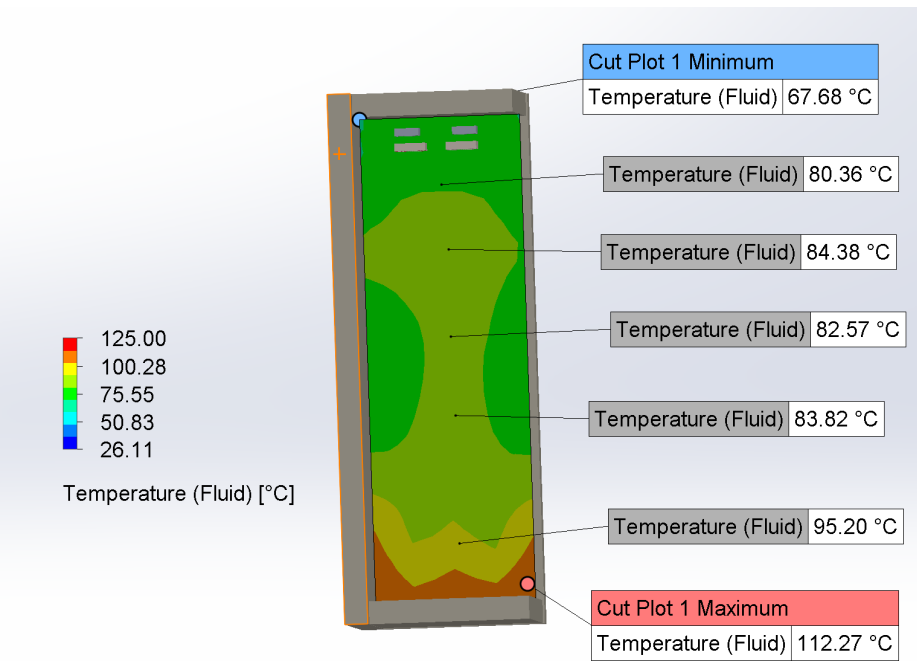


Figure 73. Temperature Distribution Cross Section

Figure 69 and 70 display the surface temperature on each face of insulation. It is worth noting that the temperature is distributed fairly evenly in the chamber when the printer is up to temperature. There is no concern for the insulation near the space heaters getting too hot, and almost every surface is kept below the constraint of 80°C. The cross-section in Figure 71 looks at the air temperature in the center of the printer, where the extruder moves in the X and Z directions. This is the most important section of the chamber to analyze because it is the plane that contains the majority of the temperature-sensitive components in the chamber. There is a steady temperature gradient that is the lowest on the ceiling and increases steadily to the floor. If there is any concern for melting parts in the movement system, it will occur near the floor of the chamber, where the maximum air temperature could reach up to 112.27°C. This simulation explains the failure of the original Y-Axis belt holder in section 3.2.3. Due to the floor reaching a

higher temperature than 80°C, this is most likely what caused the original belt mount to deform, causing the belt to slip.

4 CHAPTER 4: RESULTS AND DISCUSSIONS

4.1 Results



Figure 74. PLA Benchy Printed with the 3DPP



Figure 75. Minor Print Defects in the PLA Benchy



Figure 76. PPS Benchy Printed with the 3DPP



Figure 77. Print Defects in the PPS Benchy



Figure 78. PEEK Benchy Printed with the 3DPP



Figure 79. Tall PLA Static Mixer

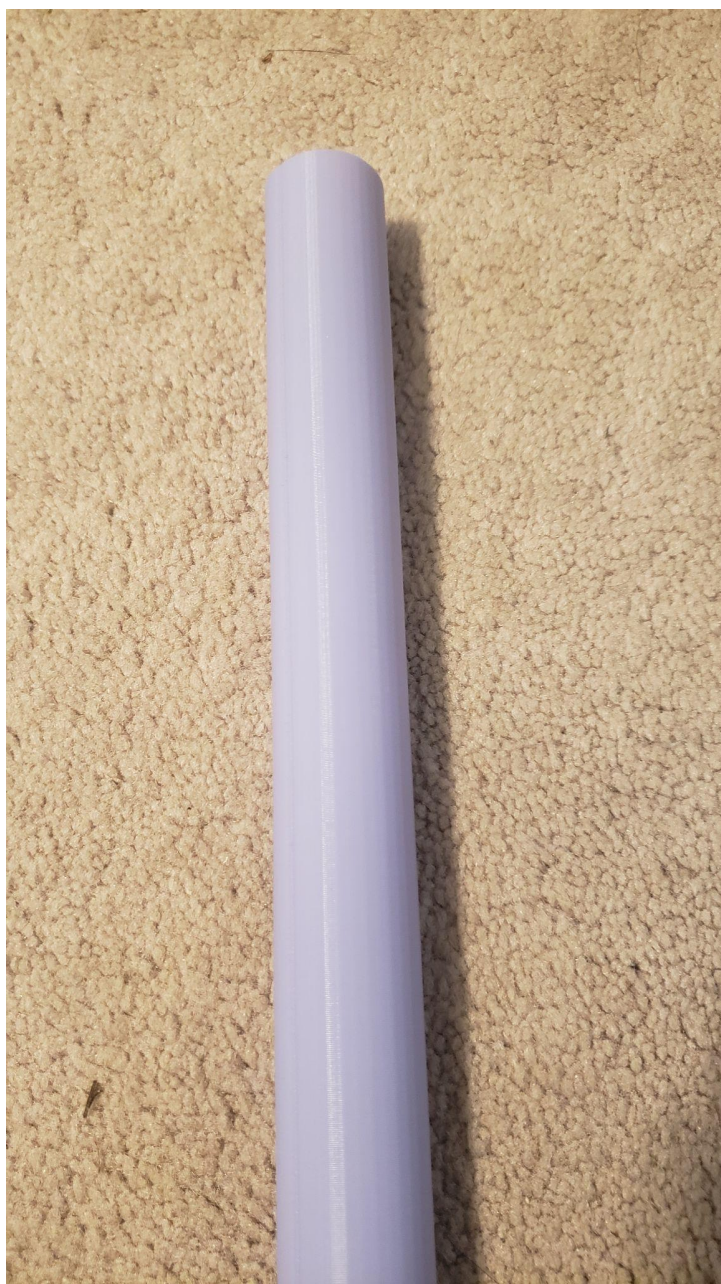


Figure 80. Surface Finish of the PLA Static Mixer

4.2 Discussions

The results from the 3DPP were fantastic, although not perfect. Figure 72 is a picture of a benchy printed out of PLA. A benchy is a test print that “is designed to offer a large array of challenging geometrical features for 3D printers” [41]. It serves as a good printing benchmark, especially when testing across printers. The PLA benchy printed nearly flawlessly, with only small blemishes, as seen in figure 73. If held in the right light, small ripples can be seen going up the front of the hull. This is most likely Z-axis ghosting due to the Z-axis moving too quickly, which can be remedied in software. Since this Z-axis ghosting does not cause any structural issue, the increase in speed is worth the minor cosmetic tradeoff.

The same model was printed out of PPS, a high-temperature engineering grade plastic with printing properties similar to that of PEEK. PPS is much cheaper, so it makes sense to do the initial testing out of PPS instead of PEEK. The benchy is still of very high quality with blemishes only appearing with close inspection. While the Z-axis ghosting does not appear here, most likely due to the decreased print speed of PPS, some layers seem to have poor adhesion. This could be attributed to either printing at too low of a temperature, or more likely, moisture in the filament. Since the spool of filament has been sitting out for many days, moisture has collected it. When the water gets to the 320°C print temperature, it instantly boils, creating an air gap in the print, resulting in a bubble, which causes the warp in the layer. This can be remedied by keeping the filament in a dry container before printing and dehydrating the currently moisture-saturated filament. After the successful results from the PPS benchy, a PEEK benchy was printed, as shown in figure 78. The

quality of the benchy is very high, with the main issue being stringing, which is usually caused by too high printing temperature or too low of retraction. These issues are easily remedied, but it was not worth the cost of printing another benchy for an issue that does not affect the structural integrity. When the sponsor has a practical print to use the PEEK for, the print temp and retraction setting will be changed, but he has stated at this time he does not have any jobs lined up. The next test print was a tall PLA static mixer to test the 3DPP's height capabilities, which came out very well. A close-up picture of the PLA static mixer is shown in figure 80 to show the lack of blemishes. Since the benchys showed only minor quality differences between the PLA and engineering-grade plastics, it stands to reason the same would hold true for tall prints. Tall engineering-grade tests prints were not performed due to filament cost, and, as mentioned, tall practical prints were not performed because the sponsor said he did not have any print jobs lined up he wanted to use his filament on yet.

5 CHAPTER 5: PROJECT MANAGEMENT

5.1 *Tasks, Schedule, and Milestones*

Designing this printer from scratch was no easy task, so effectively managing each group member's time and task allotment was critical. Initially, YouTrack was used to assign and manage tasks, Git to keep track of files and have a version history, and OneNote to share links, resources, etc. The first two weeks of the project were spent researching existing 3D printing solutions, learning about available 3D printers, coming up with aspects of a preliminary design, and getting comfortable with the chosen management software (YouTrack, Git, OneNote).

During this time, a member of the group, Caleb, was sick with COVID. He fell behind since he was not able to meet with the group due to his illness. When he was able to rejoin the group, there was so much to get caught up on, that he never took the time to learn our management software, which drastically reduced how we were able to manage tasks. Caleb spent most of his time catching up CADing the designed systems, that by the time he was caught up and had time to learn the management systems, the group had evolved to something more primitive, because it was easier to use. YouTrack was used extensively between Dillon and Josh to maximize task tracking and division so each of us knew exactly what needed to be done. However, as the semester progressed, we also got enveloped in the work and stopped updating the YouTrack. Part of the reason may have been from analysis paralysis, where too many sub-tasks were created for each main task, leading to too much overhead. Another reason was it became a headache to juggle tasks between YouTrack and how Caleb was manually tracking his tasks. Additionally, Caleb and Dillon were not well versed in Git, which caused Git to cause more problems than it

fixed. Since most of their work was done on a single computer owned by the Sponsor, Git was mainly used to keep track of reports and other documents sparingly. It did still prove useful if any type of analysis was being done on campus or remotely since it was a convenient way to gather most of the project's important information in one place. Eventually, OneNote became the primary source of information tracking. Weekly, to-do lists were created for each group member to complete their assigned tasks, and each week we would meet up and make sure all assigned tasks were completed to follow the defined schedule.

Week	Date	Timeline
Week 1	01/18 – 01/21	Capstone introduction
Week 2	01/24 – 01/28	Project selection
Week 3	01/31 – 02/04	Part selection for movement system CAD all parts for movement system for future analysis Setup project requirements Initial budget
Week 4	02/07 – 02/11	Continue CADing all parts for the movement system Design case for mounting electronics Determine a Z-axis mechanism for movement
Week 5	02/14 – 02/18	Design Y tensioning mechanism Build case Preliminary report/presentation
Week 6	02/21 – 02/25	Install movement system and wiring
Week 7	02/28 – 03/04	Debug movement system Design/replace parts that need it

Week 8	03/07 – 03/11	Calibrate printer w/o heated chamber Start thermal analysis
Week 9	03/14 – 03/18	Determine thermal materials and order it Critical design report/presentation
Week 10	03/21 – 03/25	Install thermal materials and get the printer up to temperature
Week 11	03/28 – 04/01	Run test prints at max temperatures
Week 12	04/04 – 04/08	Debug thermal/electrical issues
Week 13	04/11 – 04/15	Debug thermal/electrical issues Create final report
Week 14	04/18 – 04/22	Work on final report and presentation
Week 15	04/25 – 04/29	Finish final report/presentation and dry run presentation

Table 12. Project Schedule

The project schedule was designed so the 3DPP could be designed and the main important parts purchased. Then, while those parts were in the mail, the electronic case could be designed since it only used basic materials that were either 3D printed, or found at a local hardware store. The case was supposed to only take a week to design and a week to build but ended up taking an extra week. However, this also gave the ordered parts plenty of time to arrive. The schedule was followed strictly until week 7 when it was time to install the movement system. The X and Y axes were installed and ready, but the Z-axis (which was the counterweight system at the time) was not installed. Dillon was lead on installing the counterweight system but did not get it installed until week 10. By the time it was installed, there was no time for him to debug the system, as it was not working. The 3 spent waiting on the counterweight system were not completely lost, as while Dillon was working on the counterweight, Caleb was able to continue

CADing and Josh was able to work through the wiring and firmware/software. After week 10, the lead screw movement system was switched to. Thankfully, most of the design was done by this point, so over the next 3 weeks, assembly occurred non-stop until the printer was built, tested, and working. Given the time frame, if the design phase had been sloppy and the tests not performed so well, the 3DPP would most likely not have been finished in time. However, since meticulous planning and design occurred in the initial stages of the project, the lost time was able to be made up since the debugging time was reduced from about 3 weeks total to only taking slightly less than a week. The project has been consolidated and all relevant files have been uploaded to GitHub to be open-sourced at <https://github.com/jfcbooth/3dpp>

5.2 Resources and Cost Management

Table 13 lists the costs for the parts associated with the 3DPP. A couple of these items were for multiple or an assortment of parts, even if not all of the items in the assortment were used. If the 3DPP were mass-manufactured, this would bring the price down since the total price of the assortment would be split between multiple printers. Since a couple of pieces on the 3DPP had multiple iterations, there were some wasted costs that did not add to the overall unit cost listed in table 14. This includes parts for designs that were scrapped and components that were broken during assembly.

Part	Unit Cost	Number needed	Total cost
SKR 2	49.99	1	49.99
Rpi	34.99	1	34.99
Buck Converters x5	9.99	1	9.99
LCD	16.95	1	16.95

SSR x3	10.49	1	10.49
Fuses x5	8.47	1	8.47
Power Supply	35.99	1	35.99
Aluminum Extrusions	60	1	60
High power stepper motors	13.99	2	27.98
Low power stepper motors	10.99	2	21.98
Heat sinks	\$9.99	1	9.99
Peltier Plates	11.99	1	11.99
5015 fans x4	11.99	1	11.99
Camera	29.99	1	29.99
End stops x4	9.99	1	9.99
Mosquito hotend	149.99	1	149.99
PT1000 thermistor	33.97	1	33.97
50W heater cartridge	15.99	1	15.99
led strip	11.92	1	11.92
Threaded inserts	17.99	1	17.99
80mm fan x2	12.99	1	12.99
GT2 Idler Pulley x10	12.99	1	12.99
Belt terminating buckles	9.99	1	9.99
Outlets x3	19.99	1	19.99
Micro Swiss Direct Drive Extruder	61.22	1	61.22
Garolite print surface	15.95	2	31.9
Heated bed	159.99	1	159.99
Leadscrews	55	2	110

anti-backlash nuts	10.98	1	10.98
Insulation	150	1	150
Ceramic fiber insulation blanket	40	1	40
High temp belt	40	1	40
high temp V-wheels	21.99	1	21.99
switches	9.99	1	9.99
sheet metal	80	1	80
frame	75	1	75
printed parts (estimate)	100	1	100
wifi adapter	10.55	1	10.55
BLTouch	40.26	1	40.26
capacitors	11.65	1	11.65
Silicone wiring	58.31	1	58.31
X-axis mounting plates	29.99	1	29.99
Ball bearings	14.49	1	14.49
USB Cable	7.99	1	7.99
Magnets	9.99	1	9.99
GT2 pulley	7.99	1	7.99
Wires	80	1	80
Hardware	152.44	1	152.44
Weather strip	7.73	1	7.73
Bowden Setup	19.99	1	19.99
Total Overall Cost:			1979.05

Table 13. Total Unit Cost

Name	Cost
Counterweight material	10
Metal cable	8.99
Block pulleys	30.99
PVC pipe & caps	27.56
High-temperature belts for the counterweight system	94.48
Hardware	92.15
Mosquito Thermistor (broke)	67.99
Camera (broke)	29.99
SKR 2 (broke)	49.99
Total wasted cost	412.14

Table 14. Total Wasted Cost

5.3 *Lessons Learned*

When designing and building the 3DPP, both technical and non-technical lessons were learned.

From the non-technical side, we learned the importance of good group communication and trust.

If the members of a group do not feel comfortable sharing their opinions, that closes the door to collaboration. Being able to comfortably reach out to the team for help also falls under having good communication skills. When someone did not know how to solve a problem, it was helpful to talk with the group and explain where they were struggling. It takes vulnerability to be able to admit the inability to do something, so having a good channel of communication makes this much easier. This falls hand-in-hand with trusting the team. Without team trust, it is hard to open

up about not being able to solve a problem if we believed the group would not be supportive and would instead criticize. Also, without trust, task delegation becomes difficult, and progress stalls. We found if tasks were laid out for each group member at the beginning of the week and by the end of the week none of them were done, this not only lets the group down but brings hesitation in the future when assigning tasks because no one wants the same thing to happen again.

From a technical perspective, many design lessons were learned. The most important was, especially with prototyping, design with the intention of taking the part off again. Many times during the project, the original design did not work, so a solution was quickly engineered. However, this solution was often not elegant and would be buried under multiple other components. The phrase “we should never have to take this off again, so it will be fine” was uttered countless times, but never once held true. Engineering with the future in mind would alleviate this problem, saving time in the future even if a solution can not immediately be deployed. As the project progressed, the group got better at taking time to fix new issues properly instead of going with the easiest solution that would also cause more problems in the future because it was buried under another component. Another important lesson was designing with safety in mind. As is apparent with the original power cable designs (see figure 66.), safety was not always a priority. However, after getting repeatedly shocked and burned by the printer, some components were redesigned and a couple tweaked to prevent injury. Most of the technical lessons learned were to design for the worst-case scenario, even if they should never happen. Chances are, the worst-case scenario will happen, and often when it is least expected.

6 CHAPTER 6: IMPACT OF THE ENGINEERING SOLUTION

6.1 *Economical, Societal and Global*

3D printing is a revolutionary technology that enables decentralized manufacturing. Traditional, centralized manufacturing involves a central factory mass producing products, packaging them individually for transport, and then transporting them to the end user. Often, there are even multiple intermediaries involved. A produced item is transported to a store, then the end user has to still go to the store and get the product. There are logistical inefficiencies in this model in an attempt to distribute a product made in a single location across the world. Additionally, for each part made and sold, a broad net must be cast. The product made hopes to solve each end user's individual problem with the same part, making the end user adapt to fit the product's purpose, not the product adapting to fit the end user's purpose. With 3D printing, manufacturing is shifted away from a centralized factory, and into each user's home. The user is able to manufacture only the part they need, and can even adapt the part to fit their individual needs. This saves from the wastefulness of mass production, since only what is needed is produced and it does not need to be transported across a continent to be delivered. While this is an alternative solution to already existing logistical solutions in developed countries, it also offers a comparable solution to less developed countries without the massive logistical infrastructure.

3D printing has massively progressed in the past decade, but it is still viewed as a solution for hobbyists and tinkerers. Cheap 3D printers require tinkering and tweaking to get working because the cost to add sensors and equipment to automatically solve some of these problems

raises the printer cost out of most consumer budgets. However, the modern marvel of the car also started in a similar way. Early cars were only owned by those willing to work on them. As the technology progressed, cars became cheaper and cheaper until it was economical to put an array of problem-detecting sensors in the car so the end-user does not have to know anything about the car. This solution only came after years of development by tinkerers and manufacturers alike. Currently, 3D printing looks to be headed in the same direction. One of the main deficits is the limited size and strength of low-end 3D printers. As shown in the market analysis, 3D printers capable of printing engineering-grade plastics are in the 5-figures. The 3DPP is a unique solution that brings the price way down to a level affordable to zealous consumers. In future work, if the 3DPP was adapted for mass production, it serves as a viable solution to both the size and strength problems that holds 3D printing back from a solution to centralized manufacturing.

6.2 Environmental and Ethical

Decentralized manufacturing like 3D printing has a huge environmental impact. Even slightly reducing the carbon footprint of transportation trucks, planes, and boats greatly helps the environment. Semi-trucks alone account for 6% of the total U.S. carbon emissions [42]. Removing the transportation costs associated with small parts that can be made on a 3D printer reduces the number of trucks on the road, and thus carbon emissions. Also, by the consumer making their own part, waste is reduced since there are no extra parts produced that will be thrown away. Only exactly what is needed is made. This mindset complies with the IEEE Code of Ethics and “sustainable development practices.” [43].

7 CHAPTER 7: CONCLUSIONS AND RECOMMENDATIONS

7.1 *Summary of Achievements of the Project Objectives*

The 3DPP complies with all the design requirements and project objectives listed in section 1.3. It is able to print PLA, PPS, PEEK, and other common filaments in a very large build volume. It provides safety protection and usability in an average home. It also has multiple user-friendly ways to interact with the printer from an LCD on the printer to a web interface.

7.2 *New Skills and Experiences Learnt*

Each member of the group came with a different set of skills. Between all group members, some of the most used skills that were acquired and learned about during this project include:

- How to use metal shop tools including, but not limited to a sheet metal cutter, mill, vertical and horizontal band saw, and drill press
- Marlin firmware
- Linux
- G-code
- C
- Transient Fluid Flow in Solidworks/thermal analysis
- Assembling large models in Solidworks
- Forced convection thermal design
- 3D printing parts for the prototype

- Engineering design process for a real-world project
- Power Analysis
- Stepper Motor Kinematics
- YouTrack
- Git

7.3 Recommendations for Future Work

For improvements to the 3DPP itself, some of the wiring could be upgraded. As mentioned, most of the wiring was replaced with high-temperature resistant silicone wiring, and then wrapped in heat resistant cloth and aluminum tape. However, at the base of each connected part, some wire is exposed that is not wrapped nor is replaced with silicone wiring. This is because the parts were not made with high-temperature wiring. Most wiring is able to survive in 80°C-90°C. However, for the 3DPP, that is a very small safety factor, so finding a way to either cover the exposed wire to replace it with silicone wire would be beneficial. Another aspect of the 3DPP that could be improved on is the insulation's foil. The insulation is covered in foil, but during assembly, the insulation was taken on and off multiple times. This led to many small tears in the foil, letting the insulation flake, which could potentially disrupt a print. If the insulation was replaced or another 3DPP was built from scratch, this would most likely not be an issue. However, it is worth mentioning that this is one way the 3DPP could be improved. Another improvement to the 3DPP is to offer a moisture-lock box attachment. Most filaments should be stored in a humidity-controlled environment. The 3DPP simply uses a spool mount in the open air to hold the filament as it is fed into the printer. There is nothing inherently wrong with this, but if the filament is left on the spool, over many days this could cause the filament to absorb water,

reducing print quality. Having an attachment that stores the filament in a humidity-controlled box and fed directly into the printer from there would be useful.

The 3DPP is a very promising platform, as it is able to print nearly any material given to it. This lets it print even the most experimental of filaments, making it a unique printer that can be used to test and advanced filament technology. A great example of this is filaments by The Virtual Foundry. They offer a filament, similar to PLA, that has a high amount of metal embedded in the plastic. The filament is printed regularly, then the object is placed in a kiln. This melts away the plastic, leaving the now fused metal left. This effectively enabled the 3D printing of metal [44]. Other printers could use this filament, but the 3DPP makes it convenient to test new filament since it has nearly any functionality a filament maker could ask for. Testing some of these new filaments would be useful work for the 3DPP.

REFERENCES

- [1]. "The Complete History of 3D Printing: From 1980 to 2022", 3DSourced, 2022. [Online]. Available: <https://www.3dsourced.com/guides/history-of-3d-printing/>. [Accessed: 21- Apr- 2022]
- [2]. "CoreXZ | Principle of Operation", Corexz.com, 2022. [Online]. Available: <https://www.corexz.com/theory.html>. [Accessed: 21- Apr- 2022]
- [3]. T. Novicio, "10 Biggest Industries in the World 2021", Yahoo.com, 2022. [Online]. Available: <https://www.yahoo.com/video/10-biggest-industries-world-2021-150703784.html>. [Accessed: 21- Apr- 2022]
- [4]. "Technical Data Sheet: ECOMAX® PLA 3D Printing Filament", 3dxtech.com, 2022. [Online]. Available: <https://www.3dxtech.com/wp-content/uploads/2021/03/PLA-TDS-v03.pdf>. [Accessed: 21- Apr- 2022]
- [5]. "Technical Data Sheet: 3DXMAX™ PETG 3D Printing Filament", 3dxtech.com, 2022. [Online]. Available: <https://www.3dxtech.com/wp-content/uploads/2021/03/PETG-TDS-v03.pdf>. [Accessed: 21- Apr- 2022]
- [6]. "Technical Data Sheet: 3DXMAX® Polycarbonate 3D Printing Filament", 3dxtech.com, 2022. [Online]. Available:

- <https://www.3dxtech.com/wp-content/uploads/2021/03/PC-TDS-v03.pdf>. [Accessed: 21-Apr- 2022]
- [7]. "Technical Data Sheet: ThermaX™ PPS 3D Printing Filament", 3dxtech.com, 2022. [Online]. Available:
https://www.3dxtech.com/wp-content/uploads/2021/03/PPS_TDS_v03.pdf. [Accessed: 21-Apr- 2022]
- [8]. "Technical Data Sheet: ThermaX™ PEEK 3D Printing Filament", 3dxtech.com, 2022. [Online]. Available:
<https://www.3dxtech.com/wp-content/uploads/2021/03/PEEK-TDS-v03.pdf>. [Accessed: 21-Apr- 2022]
- [9]. C. Schwaar, "PEEK 3D Printers – The Ultimate Guide", All3dp.com, 2022. [Online]. Available: <https://all3dp.com/1/peek-3d-printer>. [Accessed: 21- Apr- 2022]
- [10]. Global 3D printing material market size 2026 | Statista", Statista, 2022. [Online]. Available: <https://www.statista.com/statistics/590113/worldwide-market-for-3d-printing/>. [Accessed: 14- Feb- 2022].
- [11]. M. Santora, "Bearing friction basics: A Primer", bearingtips.com, 2022. [Online]. Available: <https://www.bearingtips.com/bearing-friction-basics-primer/>. [Accessed: 21- Apr- 2022]
- [12]. "NEMA 17 Standard Hybrid Stepper Motors", MOONS, 2022. [Online]. Available:
<https://www.moonsindustries.com/series/nema-17-standard-hybrid-stepper-motors-b020105>. [Accessed: 21- Apr- 2022]

- [13]. "Application Note 015 - Microstepping", Faulhaber.com, 2022. [Online]. Available: https://www.faulhaber.com/fileadmin/user_upload_global/support/MC_Support/Motors/APPNotes/Faulhaber_AN015_EN.pdf. [Accessed: 21- Apr- 2022]
- [14]. S. Dufresne, "Peltier effect cooling efficiency test", Rimstar.org, 2022. [Online]. Available: https://rimstar.org/science_electronics_projects/peltier_effect_module_cooling_efficiency_test.htm. [Accessed: 21- Apr- 2022]
- [15]. "Gates 2GT Belts (High Temperature EPDM)", Filastruder.com, 2022. [Online]. Available: <https://www.filastruder.com/products/gates-2gt-belts-high-temperature-epdm>. [Accessed: 21- Apr- 2022]
- [16]. "Heat Deflection Temperature (HDT) at 0.46 MPA (67 psi)", Omnexus.specialchem.com, 2022. [Online]. Available: <https://omnexus.specialchem.com/polymer-properties/properties/hdt-0-46-mpa-67-psi>. [Accessed: 21- Apr- 2022]
- [17]. R. Cable, "CR10S Pro V2 Y axis tension by rkaneknight", Thingiverse.com, 2022. [Online]. Available: <https://www.thingiverse.com/thing:4628684/files>. [Accessed: 21- Apr- 2022]
- [18]. "High Temperature Heated Beds", E3D Online, 2022. [Online]. Available: <https://e3d-online.com/products/high-temperature-heated-beds>. [Accessed: 21- Apr- 2022]
- [19]. B. Dreger, "Ender 3 - Z Motor Mount by briandregeril", Thingiverse.com, 2022. [Online]. Available: <https://www.thingiverse.com/thing:5316673>. [Accessed: 21- Apr- 2022]

- [20]. F. Conrad, "CR-10 Dual Z timing belt sync brackets v2 by Kingofmonkeys", Thingiverse.com, 2022. [Online]. Available: <https://www.thingiverse.com/thing:3418165>. [Accessed: 21- Apr- 2022]
- [21]. "The Mosquito® Hotend", sliceengineering.com, 2022. [Online]. Available: <https://www.sliceengineering.com/products/the-mosquito-hotend>. [Accessed: 21- Apr- 2022]
- [22]. T. Hullette, "Direct Drive vs Bowden Extruder: The Differences", All3dp.com, 2022. [Online]. Available: <https://all3dp.com/2/direct-vs-bowden-extruder-technology-shootout/>. [Accessed: 21- Apr- 2022]
- [23]. D. Petsel, "Petfang Duct for CR10 MicroSwiss/Stock/E3Dv6/Volcano/TevoTornado /Tarantula Hot End/E3Dv6 CNC Mount & 5015 fan Bullseye Blokhead by dpetsel", Thingiverse.com, 2022. [Online]. Available: <https://www.thingiverse.com/thing:2759439>. [Accessed: 21- Apr- 2022]
- [24]. Y.S. Touloukian, P. E. Liley, S. C. Saxena, "Thermophysical Properties of Matter. Vol. 3: Thermal Conductivity," NY, 1970, ISBN 0-306067020-8 [Accessed: 15- April2022]
- [25]. "RTD Pt1000", sliceengineering.com, 2022. [Online]. Available: <https://www.sliceengineering.com/products/rtd-pt1000>. [Accessed: 21- Apr- 2022]
- [26]. "Thermistor Cartridge", E3D Online, 2022. [Online]. Available: <https://e3d-online.com/products/thermistor-cartridge>. [Accessed: 21- Apr- 2022]
- [27]. "ETC Thermistor for Temperature Measurment", Mouser.com, 2022. [Online]. Available: <https://www.mouser.com/catalog/specsheets/tdkc-s-a0001076622-1.pdf>. [Accessed: 21- Apr- 2022]

- [28]. "Marlin Firmware", marlinfw.com, 2022. [Online]. Available: <https://marlinfw.org/>. [Accessed: 21- Apr- 2022]
- [29]. "Tuning Stepper Motor Drivers", duet3d.dozuki.com, 2022. [Online]. Available: https://duet3d.dozuki.com/Wiki/Tuning_Stepper_Motor_Drivers. [Accessed: 21- Apr- 2022]
- [30]. G. Häußge, "OctoPrint.org", OctoPrint.org, 2022. [Online]. Available: <https://octoprint.org/>. [Accessed: 21- Apr- 2022]
- [31]. E. Soha, "OctoPrint-PrintTimeGenius", OctoPrint Plugin Repository, 2022. [Online]. Available: <https://plugins.octoprint.org/plugins/PrintTimeGenius/>. [Accessed: 21- Apr- 2022]
- [32]. "OctoPrint-BetterHeaterTimeout", OctoPrint Plugin Repository, 2022. [Online]. Available: <https://plugins.octoprint.org/plugins/BetterHeaterTimeout/>. [Accessed: 21- Apr- 2022]
- [33]. N. Nhu Tuan, "Creality CR-10S Pro Basic Frame", Grabcad.com, 2022. [Online]. Available: <https://grabcad.com/library/creality-cr-10s-pro-basic-frame-1>. [Accessed: 21- Apr- 2022]
- [34]. R. Kolle, "CR10 Extruder Bracket", Grabcad.com, 2022. [Online]. Available: <https://grabcad.com/library/cr10-extruder-bracket-1>. [Accessed: 21- Apr- 2022]
- [35]. "Power Supply Meanwell RSP500-48", Grabcad.com, 2022. [Online]. Available: <https://grabcad.com/library/power-supply-meanwell-rsp500-48-1>. [Accessed: 21- Apr- 2022]

2022]

- [36]. M. Pouria, "SSR Crydom H1 Series", Grabcad.com, 2022. [Online]. Available: <https://grabcad.com/library/ssr-crydom-h1-series-1>. [Accessed: 21- Apr- 2022]
- [37]. C. Martins, "LCD Full Graphic Smart Controller", Grabcad.com, 2022. [Online]. Available: <https://grabcad.com/library/lcd-full-graphic-smart-controller-1>. [Accessed: 21- Apr- 2022]
- [38]. R. Akopov, "Raspberry Pi 2 model B, 3D CAD assembly model", Grabcad.com, 2022. [Online]. Available: <https://grabcad.com/library/raspberry-pi-2-model-b-3d-cad-assembly-model-2>. [Accessed: 21- Apr- 2022]
- [39]. "BIGTREETECH SKR 2 control board", Grabcad.com, 2022. [Online]. Available: <https://grabcad.com/library/bigtreeetech-skr-2-control-board-1>. [Accessed: 21- Apr- 2022]
- [40]. "Flex coupler 5mm 8mm", Grabcad.com, 2022. [Online]. Available: <https://grabcad.com/library/flex-coupler-5mm-8mm-1>. [Accessed: 21- Apr- 2022]
- [41]. H. Kashima, "Toggle Switch SPDT 0.1in pitch", Grabcad.com, 2022. [Online]. Available: <https://grabcad.com/library/toggle-switch-spdt-0-1in-pitch-1>. [Accessed: 21- Apr- 2022]
- [42]. J. Davis, "E3D High Torque Nema 17 Stepper Motor", Grabcad.com, 2022. [Online]. Available: <https://grabcad.com/library/e3d-high-torque-nema-17-stepper-motor-mt-1704hsm168re-1>.

[Accessed: 21- Apr- 2022]

[43]. A. Lin, "Filament Spool", Grabcad.com, 2022. [Online]. Available:
<https://grabcad.com/library/filament-spool-5>. [Accessed: 21- Apr- 2022]

[44]. F. Ort, "BLTouch V3.1", Grabcad.com, 2022. [Online]. Available:
<https://grabcad.com/library/bltouch-v3-1-2>. [Accessed: 21- Apr- 2022]

[45]. T. Walters, "Nema 17 Pancake Stepper Motor", Grabcad.com, 2022. [Online]. Available: <https://grabcad.com/library/nema-17-pancake-stepper-motor-bondtech-lgx-1>.
[Accessed: 21- Apr- 2022]

[46]. M. Nabil, "IEC Power Cable Socket", Grabcad.com, 2022. [Online]. Available:
<https://grabcad.com/library/iec-power-cable-socket-1>. [Accessed: 21- Apr- 2022]

[47]. J. Karue Wa Wanjohi, "AC Power Outlet Socket", Grabcad.com, 2022. [Online]. Available: <https://grabcad.com/library/ac-power-outlet-socket-1>. [Accessed: 21- Apr- 2022]

[48]. "Anet A6/A8 Y Belt Holder Upgrade by Area51", Thingiverse.com, 2022. [Online]. Available: <https://www.thingiverse.com/thing:2347849>. [Accessed: 21- Apr- 2022]

[49]. "Electricity 101", Energy.gov, 2022. [Online]. Available:
<https://www.energy.gov/oe/information-center/educational-resources/electricity-101>.
[Accessed: 21- Apr- 2022]

[50]. "Product Specifications Of Thermoelectric Cooling Module", Cdn-reichelt.de, 2022.

[Online]. Available: <https://cdn-reichelt.de/documents/datenblatt/C800/TECB1.pdf>.

[Accessed: 21- Apr- 2022]

[51]. S. Shovon, "Raspberry Pi 3 Power Requirements", Linuxhint.com, 2022. [Online].

Available: https://linuxhint.com/raspberry_pi_3_power_requirements/. [Accessed: 21-

Apr- 2022]

[52]. L. Ada, "RGB LED Strips", adafruit.com, 2022. [Online]. Available:

<https://learn.adafruit.com/rgb-led-strips/current-draw>. [Accessed: 21- Apr- 2022]

[53]. J. Farr, "Review of DC to DC buck converter based on LM2596",

hobbyelectronics.net, 2022. [Online]. Available:

https://www.hobbyelectronics.net/review_dctodcmodule.html. [Accessed: 21- Apr- 2022]

[54]. D. Rock, "High Temperature Heated Bed Datasheet", e3d-online.zendesk.com, 2022.

[Online]. Available:

<https://e3d-online.zendesk.com/hc/en-us/articles/360017251138-High-Temperature-Heate>

d-Bed-Datasheet. [Accessed: 21- Apr- 2022]

[55]. "Overview of Mean Well DC power supplies | Electronic components. Distributor,

online shop – Transfer Multisort Elektronik", Tme.eu, 2022. [Online]. Available:

<https://www.tme.eu/en/news/library-articles/page/43762/overview-of-mean-well-dc-power>

-supplies. [Accessed: 21- Apr- 2022]

- [56]. "About #3DBenchy", 3dbenchy.com, 2022. [Online]. Available:
<https://www.3dbenchy.com/about/>. [Accessed: 21- Apr- 2022]
- [57]. "Diesel Trucks Are A Major Cause of Pollution", corovan.com, 2022. [Online]. Available: <https://corovan.com/diesel-trucks-are-a-major-cause-of-pollution>. [Accessed: 21- Apr- 2022]
- [58]. "IEEE Code of Ethics", Ieee.org, 2022. [Online]. Available:
<https://www.ieee.org/about/corporate/governance/p7-8.html>. [Accessed: 21- Apr- 2022]
- [59]. "The Virtual Foundry, inc. - Metal 3D Printing", The Virtual Foundry, inc., 2022. [Online]. Available: <https://thevirtualfoundry.com/>. [Accessed: 21- Apr- 2022]